PB 183797

Radiation Bio-Effects

Summary Report
January - December 1968

[illegible]

Reproduced by the
CLEARINGHOUSE
for Federal Scientific & Technical
Information Springfield Va. 22151

RADIATION BIO-EFFECTS

Summary Report January-December 1968

William A. Mills, Ph.D., Chief
Radiation Bio-Effects Program
Rockville, Maryland 20852

Compiled and Edited by
Donald M. Hodge

U. S. DEPARTMENT OF HEALTH, EDUCATION, AND WELFARE
Public Health Service
Consumer Protection and Environmental Health Service
Environmental Control Administration
Bureau of Radiological Health

NOTICES

This report contains preliminary data and was prepared primarily to record the year's work, and is not intended as a substitute for publication in the open literature. It is subject to revision and does not represent a final report. Please do not quote from or refer to this work in open literature without permission from individual authors to reference the material as a personal communication.

The use of commercial preparations or products specified in this report in no way constitutes endorsement by the U.S. Public Health Service.

FOREWORD

During a recent reorganization of the Bureau of Radiological Health (formerly National Center for Radiological Health), the research associated with the Radiation Bio-Effects Program was integrated into an expanded biological research group named the Division of Biological Effects. The studies summarized in this report are representative of the biological investigations conducted by the Program during 1968.

Following the enactment of the Radiation Control for Health and Safety Act of 1968 in October, the Bureau of Radiological Health was authorized to administer, with some exceptions, the day-to-day functions implementing the Act. The responsibility for conducting biological research in areas covered by the Act has been delegated to the Division of Biological Effects. Future investigations by the Division may therefore consider not only those areas included in this summary, but also the biological effects of radiations from virtually the entire frequency spectrum. As in the past, results of this research will appear in Government reports and in appropriate scientific journals.

Raymond T. Moore

Raymond T. Moore, M.D.
Acting Bureau Director
Bureau of Radiological Health

BLANK PAGE

PREFACE

This report summarizes the research activities of the Radiation Bio-Effects Program during 1968. The first part of the report outlines the administrative organization of the Program and the Laboratories that comprise it. In day-to-day laboratory operations, however, the administrative divisions are rather indistinct, and communications and information exchanges are unrestricted throughout the laboratory. (the main work concerns)

Until this year, the prime emphasis in this Program has involved research identifying the effects of low levels of ionizing radiation on animals or animal systems. In October 1968, the Public Health Service Act was amended "to provide for the protection of the public health from radiation emissions from electronic products." This Radiation Control for Health and Safety Act of 1968, gave the Secretary of Health, Education, and Welfare the responsibility for developing and administering performance standards to control the emission of radiation from electronic products and to undertake research and investigation into the effects and control of such radiation emissions.

Enactment of this legislation has altered the scope of responsibility of the Radiation Bio-Effects Program. We are now interested in examining the biological effects of much broader spectra of mechanical and electromagnetic emissions. Although the source of energy impinging on the biological specimen is no longer restricted to that of ionizing radiation, our interest in the result--biological alterations induced by the energy received--remains unchanged.

Dr. Arthur H. Wolff, former Chief of the Radiation Bio-Effects Program, is now associated with the Office of Research and Development in the newly established Consumer Protection and Environmental Health Service. Through the foresight and efforts of Dr. Wolff and men like him, the Radiation Bio-Effects Program was conceived and has evolved into its present form. The guidance and leadership practiced by Dr. Wolff established the competence of the Program in the field of ionizing radiation. It is in the spirit of his foresight that the Program shall develop its widened scope of responsibility.

As has been the policy in the past, the results of our findings will, for the most part, be published in the open literature. Publications and presentations by Program investigators during 1968 are listed in the appendix of this report.

William A. Mills

William A. Mills, Ph.D., Chief
Radiation Bio-Effects Program
Bureau of Radiological Health

CONTENTS

Radiation Bio-Effects Program 1
  - Biometrics Unit 3
  - Animal Care Unit 3

Radiation Cytology Laboratory 5
  - Human Studies 5
  - Animal Studies 12

Radiation Physics Laboratory 21
  - Laboratory Services 21
  - Dosimetry and Radiation Physics 27
  - Lipid Analysis of Brains of Beagles Exposed to X Radiation 43

Radiation Oncology and Pathology Laboratory 45
  - Thyroid Age Sensitivity Study in Young Rats 45
  - Spontaneous Lesions in a Colony of Chinese Hamsters 49
  - Studies of Radiation-Virus Interactions 51
  - Radiation-Ethionine Ultrastructure Studies - A Serial Section Evaluation 54

Radionuclide Toxicology Laboratory 59
  - Status and Production of the Cat Colony 60
  - Qualitative Evaluation of the Embryonic Skeleton in Cats 62
  - Placental Transfer of Strontium and Calcium in the *Felis Domestica* 63
  - Metabolism of ^{85}Sr in Cats 66
  - Dosimetry of Radiostrontium in Skeletal Tissues of Cats 73
  - Lethal Effects of ^{89}Sr in Cats 79
  - Localization of ^{131}I-Labeled Tetracycline in Tumors Using Scinti-Scanning 82
  - Experimental Myxedema in Cats Produced by ^{131}I 84
  - Maternal-Fetal ^{131}I Relationships in the Guinea Pig 85
  - Distribution of Carrier Free and ^{99}Mo-Labeled Milk in Cats 86
  - Carcinogenic Effects of Deposited Radioactive Particles in the Lung 87
  - Investigation of Alpha Particle and Tobacco Smoke Synergism 88

Physiology and Biophysics Laboratory 89
  - Effects of Microwave Radiation on Chinese Hamster 89
  - Hematopoietic Changes Associated with *In Utero* Irradiation 94
  - *In Utero* Irradiation with High- and Low-Energy X Rays at Various Dose Rates 97
  - Effect of X-Ray Radiation and Microwave Radiation In Vitro and In Vivo on Human and Rat Gamma Globulins 98
  - The Isolation of Kupffer Cells from Rat Liver and Studies of Cellular Respiration During Phagocytosis 100

Collaborative Radiological Health Laboratory.................... 105
The Barrier-Maintained Colony.................................. 105
The Long-Term Experiment: Current Status and Feasibility Studies.. 107
Irradiation of the Embryo, Fetus, and Neonate................. 109
Data Processing.. 111

APPENDIXES

Publications January - December 1968......................... 113
Presentations January - December 1968........................ 116
Advisory Committees.. 118
Radiation Bio-Effects Program Staff........................... 120

FIGURES

1. Tasmanian Rat Kangaroos and Chromosomes of Male.............. 4
2. Satellite Association between Acrocentric Chromosomes of a Cultured Human Lymphocyte........................... 8
3. Relation between Nucleolar Diameter and the Number of Chromosomes Adhering to the Nucleolus..................... 9
4. Electron Micrograph of a Whole-Mounted Chromosome............ 11
5. Marker Chromosome in Cultured Chinese Hamster Thyroid Cells.. 12
6. Two Chinese Hamsters with Gray Hair after 1,200 Rads of X Rays... 16
7. Mitosis in Spermatogonia Cultured from Chinese Hamsters...... 19
8. The Sertoli Cell-Spermatogonium Side-by-Side Orientation at the beginning of In Vitro Culture of Testicular Tissue of the Chinese Hamster.......................... 19
9. Circuit Diagram of Decade Circuit Board...................... 23
10. Milliampere Stabilizer Developed for Use with Low-Energy X-Ray Machine.. 26
11. Attenuation Properties of Three X-Ray Beams.................. 28
12. One of the Positions Used in Irradiating Skull Phantoms to Obtain Dose Distributions in Brain....................... 29
13. Mean Absorbed Dose in Brain as a Function of Half Value Thickness and X-Ray Tube Potential....................... 32
14. Emission Spectra of the RCA 25AP22A Picture Tube with and without Its Safety Panel.................................. 35
15. Spatial Distribution of X-Ray Flux at Various Angles About a Point on the Picture Tube Face......................... 35

16. Narrow Beam Attenuation Coefficients of Various Glasses and Bonding Resins.. 36
17. Relative Transmission of 25 keV X-Ray Photons as a Function of Glass and Resin Thickness.................... 36
18. Encapsulated LiF Dosimeters Imbedded in Rat Cadavers Used to Determine X-Ray Dose to the Pituitary and Thyroid..... 38
19. LiF Thin Discs and Micro-Rods Used to Obtain Radiation Doses in Trabecular Regions of Cat Bones................ 39
20. Spectra with and without Sample........................... 41
21. Portable Scintillation Detector and Water Phantom Used to Measure Pentrability of Multiply Scattered Gamma Rays from Natural Thoria Deposits in North Carolina........... 42
22. Portable Multichannel Analyzer used to Process and Record Radiations from Natural Thoria Deposits................. 42
23. Brass and Lead Collimators Used in Narrow-Beam Irradiation of Rat Thyroid Glands...................... 47
24. Position of Anesthetized Rat During Thyroid Irradiation..... 48
25. Microscopic View of Anterior Cerebral Artery in the Brain of a Hamster with Acute Massive Cerebral Hemorrhage...... 50
26. Liver.. 50
27. Uterus... 50
28. Data from Three Experiments Show the Enhancement of Cell Transformation after Irradiation and Infection with SV40. 52
29. Artistic Representation of the Structure of Nuclear Cytoplasmic Invaginations................................ 55
30. Invagination of Nuclear Membrane Showing Channel-Like Pore which Provides Continuity between the Cytoplasm and the Invaginated Material............................ 56
31. Apparent Opening or Break in the Wall of the Invaginated Nuclear Membrane...................................... 57
32. Hepatoma Nucleus Showing Nuclear Cytoplasmic Inclusions as Well as Cytoplasmic Remnants........................ 58
33. Weight and Radioisotope Content in Embryos................. 64
34. Weight and Radioisotope Content of Placenta................ 64
35. Radioisotope and Phosphorus Content and Weights of Embryos.. 65
36. Excretion Curves of Cats Given a Single Oral Dose of ^{85}Sr... 68
37. Retention Values Generated from Excretion Equations of Chronically Dosed Cats.................................. 68
38. Feces and Urine Values for Cats on Chronic Uptake and on Chronic Excretion Regimens............................. 69
39. Strontium Levels in Three Types of Skeletal Tissue as a Function of Age... 72
40. Cross Section of an Adult Cat Femur Showing Associated Autoradiograph, X Ray, and Absorbed Dose Rates in Rads per Day.. 75
41. Photomicrographs Showing Cellular Detail of Adult Cat Femur Shown in Figure 40............................... 76

42. Longitudinal Section of Weanling Cat Femur Labeled with $^{90}Sr + ^{90}Y$ 77
43. Blood Element Responses of Four Animals That Received ^{89}Sr Doses at Rates of 250 and 50 μCi per Day 80
44. Effect of X Rays at Various Gestation Times on White Cell Count Taken at 24 Hours of Age 95
45. Effect of Irradiation at Day 15 of Gestation on White Cell Count at Various Ages After Birth 95
46. Effect of Various Doses Given at Day 15 of Gestation on the White Cell Count Taken at 24 Hours 95
47. Effect of Various Doses Given at Day 15 of Gestation on Total Red Blood Cells and Nucleated RBC at 24 Hours 96
48. Effect of Various Doses Given at Day 15 of Gestation on Body Weight and Hematocrit at 24 Hours 96
49. Phase Photomicrograph of Unstained Kupffer Cells 100
50. Oxygen Uptake Curves for Various Types of Liver Cell Preparations 102
51. Phase Photomicrograph of Unstained Kupffer Cells that Had Been Incubated with Polystyrene Particles In Vitro 102
52. Electron Photomicrograph of Kupffer Cells That Had Been Incubated with Polystyrene Particles In Vitro 103
53. Oxygen Uptake Curves for Liver Mince 103

TABLES

1. Aberrations in Blood Cultures from Radionuclide Workers 6
2. Tumors in Chinese Hamsters Two Years after Intraperitoneal Injection of ^{131}I 13
3. Survival of Mice and Chinese Hamsters after 1,200 Rads of 250 KVP X-Rays 15
4. Chinese Hamster Hair Type, Distribution, and Average Measurements before and after Epilation 17
5. Nuclear Rotation from Time-Lapse Cinemicrographic Analysis 18
6. Irradiations at the Twinbrook Laboratory, 1968 22
7. Dimensions of Head Phantoms 28
8. Mean Dose to the Brain 31
9. Dose to the Thyroid, Eye, and the Pituitary 33
10. Thyroid and Pituitary Doses for Four Age Groups 38
11. Lithium Fluoride Exposure Determinations in Cat Bones 39
12. Significance of Lipid Formation in Irradiated and Unirradiated Dog Brain 44
13. Deaths of Rats Irradiated at Various Ages 48
14. Incidence of Lesions in Relation to Dose of ^{131}I 49
15. Kitten Production During 1963-1968 61
16. ^{85}Sr Distribution and Weights of Organ Systems of Adult Cats Following Chronic Dosage 70

17. Weight and ^{85}Sr Distribution in Cat Skeleton................ 71
18. Predicted and Observed ^{89}Sr in Kittens from Conception to 1 Year.. 80
19. Relative Activity of Amino Acid Incorporation at Various Times after Microwave Irradiation........................ 92
20. Effect of Irradiation Dose at 15 Days Gestation on Litter Size and Survival of Pups Born........................... 94
21. Rate of Oxygen Uptake of Kupffer Cells...................... 104

RADIATION BIO-EFFECTS PROGRAM

The Radiation Bio-Effects Program, Bureau of Radiological Health, conducts an multidisciplinary research program aimed at defining the long-term effects of low-level radiation exposures in man. These studies, of public health significance, include an examination of the biological effects of non-ionizing radiations such as microwaves and radiowaves as well as the effects of X and γ rays and other emanations that are of high enough energy to produce ionization.

Greater knowledge of the relationships between radiation exposure and biological effects has become imperative as our population is confronted with potentially increasing exposure levels. The projected increases in population exposure will accrue through increasing use of radiation in medicine, industry and in consumer products, and the projected commercial use for nuclear energy.

Animal studies, conducted in our laboratories and elsewhere, provide evidence to support the hypothesis that the unborn and the young may be uniquely sensitive to the deleterious effects of radiation. Using a variety of mammalian species, these experimental findings have shown that radiation exposure of adult animals inhibits the production of certain proteins and enzymes. The experimental results suggest that these effects may be the result of radiation-induced alteration of DNA, the molecule which carries genetic information that exercises control over all phases of cellular activity.

Studies of cellular genetic material--chromosomes--have shown that radiation doses as low as 10 rads can produce visible damage in chromosomes. Cultured cells from different organs appear to be equally sensitive to radiation. The age of a person at the time of irradiation does not appear to affect the extent of chromosome damage; such radiation damage may persist for a number of years.

The interactions between environmental factors and ionizing radiation are being examined extensively. Studies of cultured cells treated with radiation and viruses have shown that radiation markedly predisposes the cells to malignant transformation by the viruses. It has been shown that a chemical agent, ethionine, which is not specifically carcinogenic to mammary tissue, will increase mammary tumors when combined with radiation.

In the field of radiation dosimetry, the type of radiation emitted by some faulty color television receivers has been evaluated, making possible calculations of the radiation exposure to humans. Through various experimental techniques, X-ray doses to the brain, eye, and thyroid gland have been calculated to provide a laboratory basis for evaluating the results of an epidemiological study of 20,000 children in Israel whose hair was removed by soft X rays as part of a treatment for ringworm of the scalp.

To examine the lifelong effects of single, low doses of radiation, a large dog colony has been established in collaboration with Colorado State University. Other studies have focused on the uptake metabolism, internal distribution, and secretion of certain radionuclides of such elements as iodine, strontium, and lead. These investigations examine the dose distribution and biological effects of such internal emitters on the organs and blood forming systems of several species, principally the cat.

To conduct these investigations, the Radiation Bio-Effects Program is organized as outlined below. Biological research conducted by each of the six laboratories and discussed in the later sections of this publication is ably supported by the Biometrics and Animal Care Units.

RADIATION BIO-EFFECTS PROGRAM

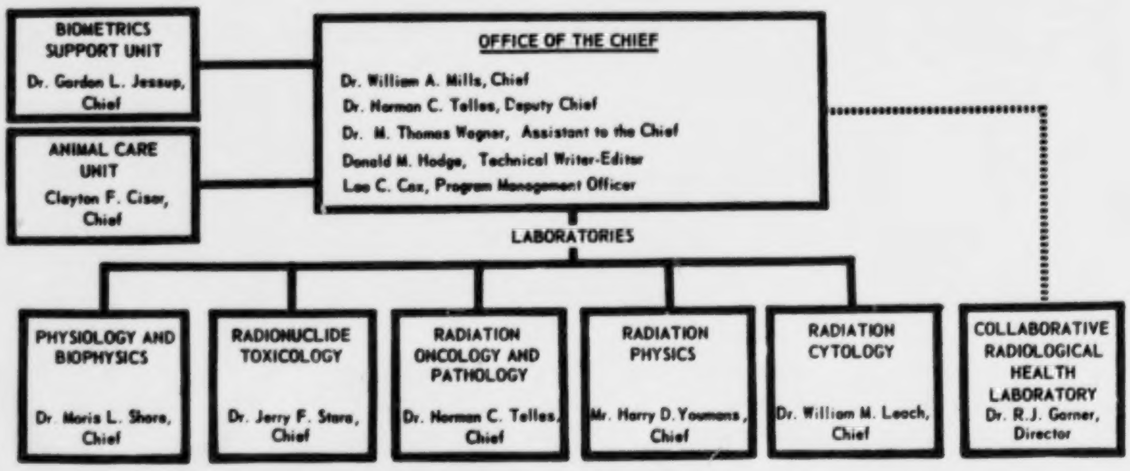
BIOMETRICS SUPPORT UNIT
Dr. Gordon L. Jessup, Chief
ANIMAL CARE UNIT
Clayton F. Cisar, Chief
OFFICE OF THE CHIEF
Dr. William A. Mills, Chief
Dr. Norman C. Telles, Deputy Chief
Dr. M. Thomas Wagner, Assistant to the Chief
Donald M. Hodge, Technical Writer-Editor
Lee C. Cox, Program Management Officer
LABORATORIES
PHYSIOLOGY AND BIOPHYSICS
Dr. Moris L. Shore, Chief
RADIONUCLIDE TOXICOLOGY
Dr. Jerry F. Stara, Chief
RADIATION ONCOLOGY AND PATHOLOGY
Dr. Norman C. Telles, Chief
RADIATION PHYSICS
Mr. Harry D. Youmans, Chief
RADIATION CYTOLOGY
Dr. William M. Leach, Chief
COLLABORATIVE RADIOLOGICAL HEALTH LABORATORY
Dr. R.J. Garner, Director

BIOMETRICS SUPPORT UNIT

Dr. Gordon L. Jessup, Chief

The Biometrics Support Unit provides statistical design and data analysis services to the Radiation Bio-Effects Program laboratories for a variety of radiobiological investigations. The results of these services are lucidly and concisely summarized in a newly adopted "Biometrics Analysis" report that is proving to be an invaluable source of information. The standard format for these reports includes statements of the objective, experimental procedure, analysis, and conclusions.

The Unit also develops mathematical models to characterize physical or biological systems, coordinates the design of experiments, and conducts research in mathematical and statistical methodology. The Unit cooperates with the investigators to define experimental objectives and variables, formulate mathematical functions, define and estimate the components of variance, and synthesize number systems to characterize, compare, and evaluate individual factors and their interactions.

ANIMAL CARE UNIT

Mr. Clayton F. Cisar, Chief

The Animal Care Unit provides animals and animal care for the studies conducted by the Radiation Bio-Effects Program at the Rockville, Maryland, laboratory. The Unit plans with the investigators the space, the most suitable species or strain, and the special breeding or handling required for a particular study.

One part of the Animal Care Unit provides animals for relatively short-term studies; the other part, operated by contract, provides care for animals in long-term experiments. During the year the two facilities handled approximately 7,200 rats, 280 mice, 37 dogs, 8 monkeys, and odd lots of guinea pigs, rabbits, Syrian hamsters, swine, and cats. Approximately 2,000 Chinese hamsters were produced during the year. This number is expected to increase as the species becomes more popular.

The general health of the animal colony has been excellent and must be rigidly maintained. The subtle effects displayed by animals exposed to radiation might otherwise be overshadowed by symptoms of ill health. The strict hygienic discipline maintained by the caretakers is mainly responsible for the absence of disease outbreaks.

Methods of handling animals exposed to radiation and radioisotopes have been studied in the Animal Care Unit. Also, animal production methods and genetic traits of selected species have been examined.

The four pairs of rat kangaroos (Potorous tridactylis) have been particularly useful to the Radiation Cytology Laboratory because their chromosomes are relatively large, few in number (13 in the male, 12 in the female), and are easy to identify (Figure 1). Leukocytes separated from blood are easily grown in culture, and cell strains derived from the kidney, cornea, thyroid, and testicle have been maintained for more than a year. However, the four pairs of rat kangaroos maintained in this laboratory have produced only two offspring in the four years since they were obtained from Tasmania. One of these died soon after birth but the other has been raised to maturity. Breeding difficulties might be overcome if these animals were maintained in large outside enclosures during the summer months. The slow reproduction rate is probably one factor that limits the popularity of this species for scientific research.

Congenital cataracts associated with skull malformations were noted in a strain of Sprague-Dawley rats obtained from the National Institutes of Health. Through a cooperative study with NIH the cataracts were found to be inherited through a fully-expressed simple autosomal recessive gene. Histopathologic study revealed a distinctive overproduction of the lens capsule and proliferation of lens epithelium. This is a unique finding in animals and resembles changes seen in some human syndromes associated with congenital cataract.

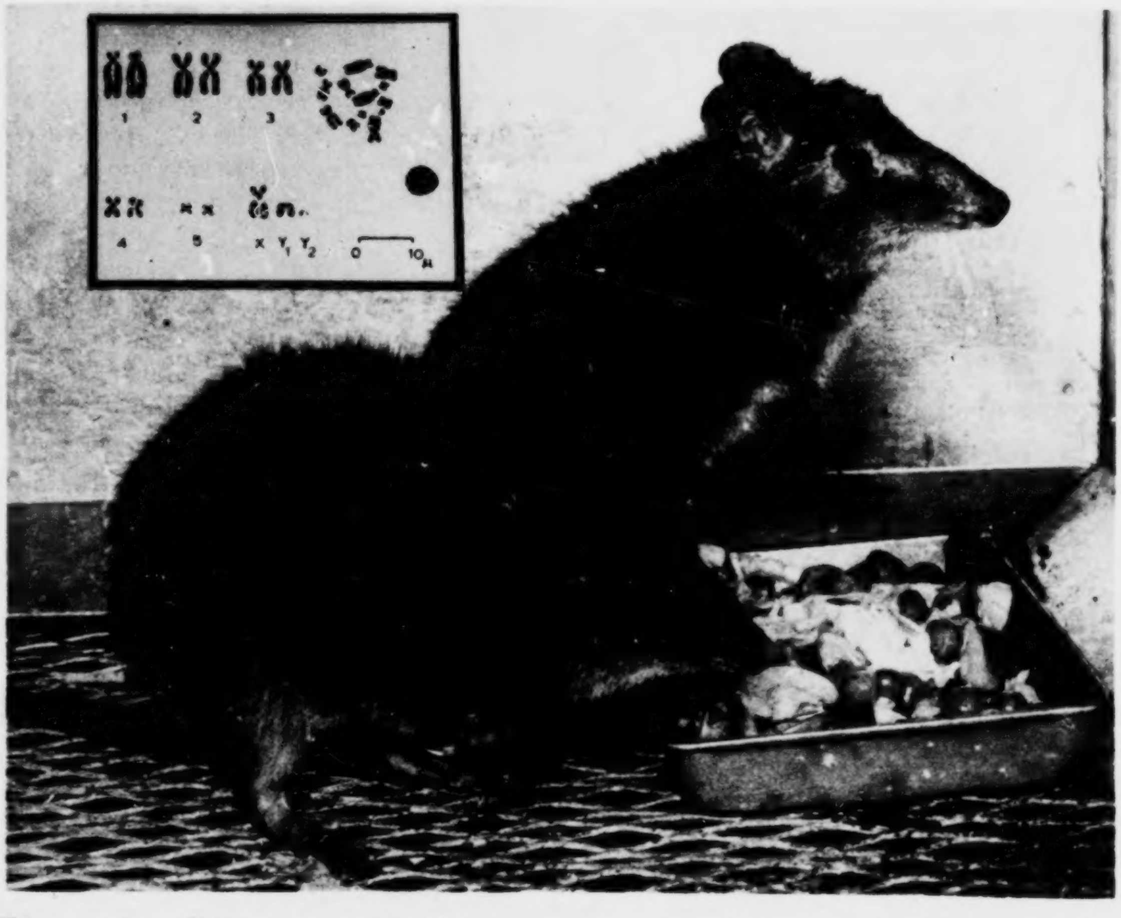

Figure 1. Tasmanian Rat Kangaroos and Chromosomes (inset) of Male.

RADIATION CYTOLOGY LABORATORY

Dr. William M. Leach, Chief

The Radiation Cytology Laboratory examines cellular responses to radiation. Primarily, morphological studies relate the extent of an effect to the radiation exposure. Cells are irradiated while growing in vitro or are cultured from irradiated animals. Humans, rat kangaroos, and Chinese hamsters are used for the major part of the studies.

A. HUMAN STUDIES

1. Radiation Effects on Human Peripheral Leukocytes

Little information is available in the area of chromosomal response of human peripheral leukocytes irradiated in situ. As discrete and relatively available human populations are identified with known radiation exposure histories, the Radiation Cytology Laboratory has attempted to ascertain changes in their chromosomes. Two groups have been examined: One, a small group undergoing experimental X-ray and drug therapy for chronic lymphocytic leukemia; and the other, a group occupationally exposed to beta- and gamma-emitting mixed isotopes.

a. Chromosomal Analysis of Patients During Treatment for Chronic Lymphocytic Leukemia

E. C. Beyer, W. M. Leach

A study of chromosomal changes in persons treated with whole-body X radiation for chronic lymphocytic leukemia (CLL) was initiated collaboratively with the Radiation Branch, National Cancer Institute, National Institutes of Health. Thirteen patients were followed serially for various periods of time to observe chromosomal damage in cultures derived from peripherally circulating leukocytes. For clinical reasons, the treatment of CLL patients was expanded to include chemotherapy. Patients are now receiving the chemotherapy as an adjunct to X-ray therapy. Inasmuch as the drugs being used are radiomimetic, the use of chromosomal changes as an index of in situ damage has become impossible.

It is possible that the leukocytes which grew in cultures were normal, not leukemic. The possibility has been examined initially by the staining of Periodic Acid-Schiff (PAS) bodies in lymphocytes. The staining of cultured cells derived from normal volunteers has been successful, but is not quantitatively reliable enough to invite direct comparisons of the stainabilities of cultured cells derived from normal and CLL patients.

b. Chromosomal Analysis of Persons with Body Burdens of Mixed Radioisotopes

E. C. Beyer

In 1967 spectrometric analysis of body burdens of persons occupationally in contact with a variety of radioisotopes was initiated at the Northeastern Radiological Health Laboratory, National Center for Radiological Health. Although the body burden was well below established limits for each isotope, the persistence of the body burden made chromosomal analysis of the workers an attractive possibility.

A total of ten exposed persons were entered on the study. Peripheral blood was obtained and leukocyte cultures were established with standard culture techniques. Cells were harvested after 48 hours of growth at 38°C and 72 hours of growth at 37°C.

The results of the chromosome analysis from the first contact with the group are shown in Table 1. On the basis of the results, additional contacts with the group are planned.

TABLE 1. ABERRATIONS IN BLOOD CULTURES FROM RADIONUCLIDE WORKERS

Body Burden, μCi[a]	Cumulative Rem During Employment[b]	No. of Cells Scored	Calculated Yields per 100 Cells: Chromatid Aberrations	Chromosome Aberrations	Aneuploidy
0.73	19.7	61	4.9	1.6	4.9
0.63	8.4	47	4.2	0	14.9
0.62	4.9	47	0	2.1	6.4
0.46	7.3	41	2.4	2.4	9.8
0.23	4.7	58	8.6	0	15.5
0.14	1.3	100	12.0	2.0	5.0
0.13	3.5	25	4.0	0	16.0
0.12	0.7	77	10.4	0	11.7
0.08	1.8	100	16.0	0	11.0
0.02	5.5	75	6.8	4.0	6.8
-[c]	-	25	4.0	0	4.0

a. Determined from whole-body counting techniques by Northeastern Radiological Health Laboratory, Winchester, Mass., within 3 months of the cell culturing.

b. From employer's records of film badge readings.

c. Not a radionuclide worker.

2. Studies on Possible Etiologies of Congenitally Defective Aneuploid Humans

H. R. Nankin, S. Brecher

Aneuploidy in congenitally defective humans is thought to result from unequal distribution of chromosomes by nondisjunction during gametogenesis. In mitotic cells acrocentric chromosomes may be grouped together nonrandomly in colchicine-blocked cells. The clustering of acrocentric chromosomes has been termed satellite association, and is shown in Figure 2A. The possibility that causes of satellite association in mitotic cells may also operate in cases of nondisjunction in meiotic cells has led to a study of satellite association in leukocyte cultures from normal human female volunteers.

Satellite association was found to decrease with increasing time of culture, e.g., from an average of 89.9 percent of metaphase cells in 48-hour cultures to 66.1 percent in 96-hour cultures. Because from 2 to 10 acrocentric chromosomes may participate in satellite association, an association index, the percent of acrocentric chromosomes in satellite association, was determined. The association index paralleled the satellite association curve for time in culture.

The appearance of nucleoli in cells in prophase and prometaphase was examined. In azure B bromide stained cells, nucleoli were observed in 26.8 percent of prophase/prometaphase cells cultured for 48 hours, in 31.6 percent of cells cultured for 72 hours, and 13.1 percent of cells cultured for 96 hours. At each culture time over half of nucleolar-containing cells showed one nucleolus. As many as 20-30 chromosomes were apposed to the stained nucleolar mass (Figure 2B). However, the identification of the chromosomes was not possible.

3. X-Ray Effects on the Nucleolus and on its Role in Chromosome Distribution

S. Brecher

The possible connection between nucleolar material and satellite association, implied in the above study, led to the development of a technique to examine nucleoli in colchicine-arrested metaphase cells in cultures of human peripheral blood. Nucleoli can be caused to persist into metaphase by addition of cobalt ions to the culture for an interval before fixation. Nucleoli in over 50 percent of metaphase cells in cobalt-treated cultures have been observed. The persistent nucleoli are surrounded by chromosomes. The relationship between the nucleolar size and the number of adhering chromosomes is shown in Figure 3. Fixation procedures to allow visualization of the nucleoli preclude positive identification of adhering chromosomes.

Persistent nucleoli, after exposure of 50 to 300 rads of X rays, break apart. The range of the number of nucleolar fragments has not been determined.

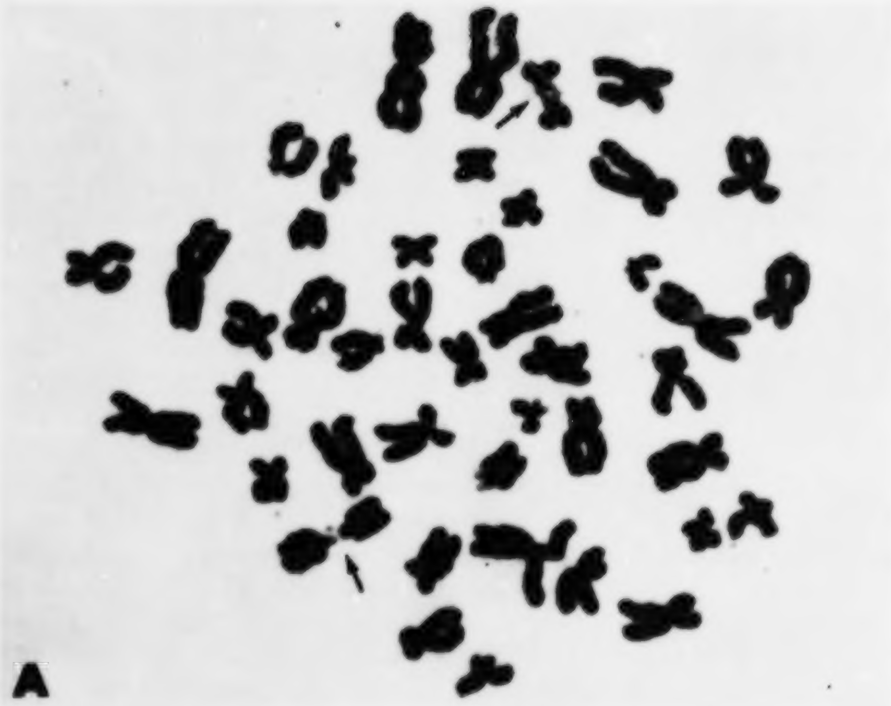

Figure 2A. Satellite Association between Acrocentric Chromosomes of a Cultured Human Lymphocyte. Short satellited arms of acrocentric chromosomes are closely apposed to similar arms of other acrocentric chromosomes (arrows).

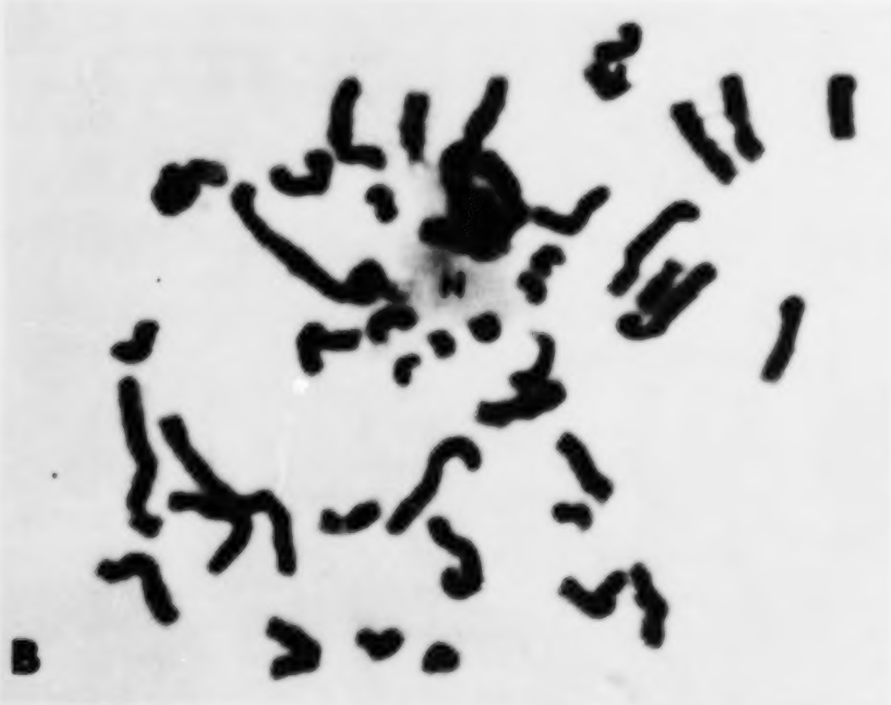

Figure 2B. Nucleolar-Chromosomal Association. Some chromosomes of cultured human lymphocytes are oriented around nucleolar material (N). Similar orientation is observed during a part of prophase and in Colcemid-blocked metaphase cells with visible nucleolar material.

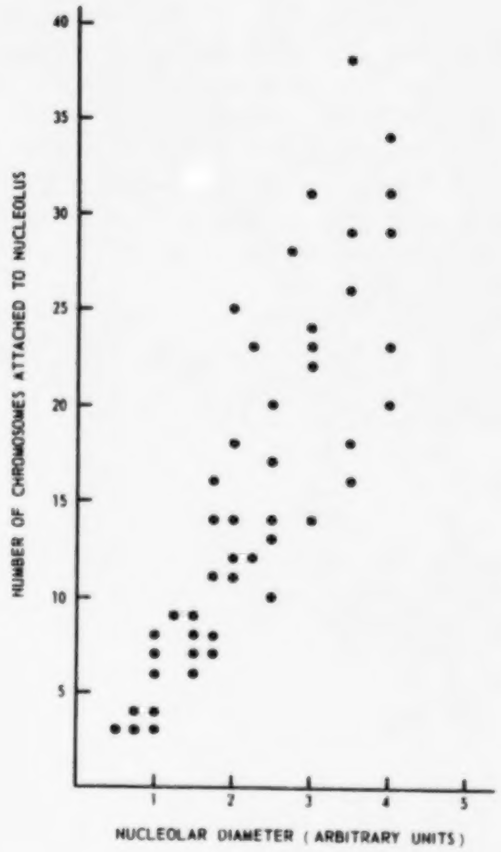

Figure 3. Relation between Nucleolar Diameter and the Number of Chromosomes Adhering to the Nucleolus. Measurements of the longest diameter of the nucleolar mass (N) were made on photographs of metaphase cells of cobalt-treated lymphocyte cultures.

4. Ultrastructure of X-Irradiated Chromosomes

J. G. Abuelo, D. E. Moore, S. Brecher

Resolution of the problem of strandedness of chromosomes is critically required for the accurate interpretation of X-ray-induced chromosome aberrations. Ultrastructural studies of chromosomes were therefore initiated. For electron microscopic examination, chromosomes were spread on the surface of a Langmuir trough and dried on grids in CO_2 at the critical point.

Colchicine-blocked metaphase chromosomes showed a bipartite, or chromatid, organization. Specific sub-chromatid organization was not observed. In extended areas 8-16 parallel fibers were oriented with the longitude of the chromosome. Fiber loops were observed along the periphery of chromosomes. Other fibers extended beyond the main chromatin mass, as well as between the arms of sister chromatids. In the kinetochore region fibers crossed from one chromatid to the other. The diameter of the fibers ranged between 190 and 290 Å. The diameter of the fibers was reduced by limited digestion with trypsin and Pronase. The digestion also loosened the packing of fibers so that the chromosomes appeared less compact than before digestion. In the loosened chromosomes a sort of banding appeared along their length, shown in Figure 4A. Limited digestion with DNAase resulted in breakage of the fibers, as shown in Figure 4B. Prolonged digestions with either the proteases or the DNAase removed chromosomes from the grid.

Chromosome fragments, dicentrics, and chromatid gaps have been observed. No ultrastructural changes have been associated to date with the regions of chromosome damage.

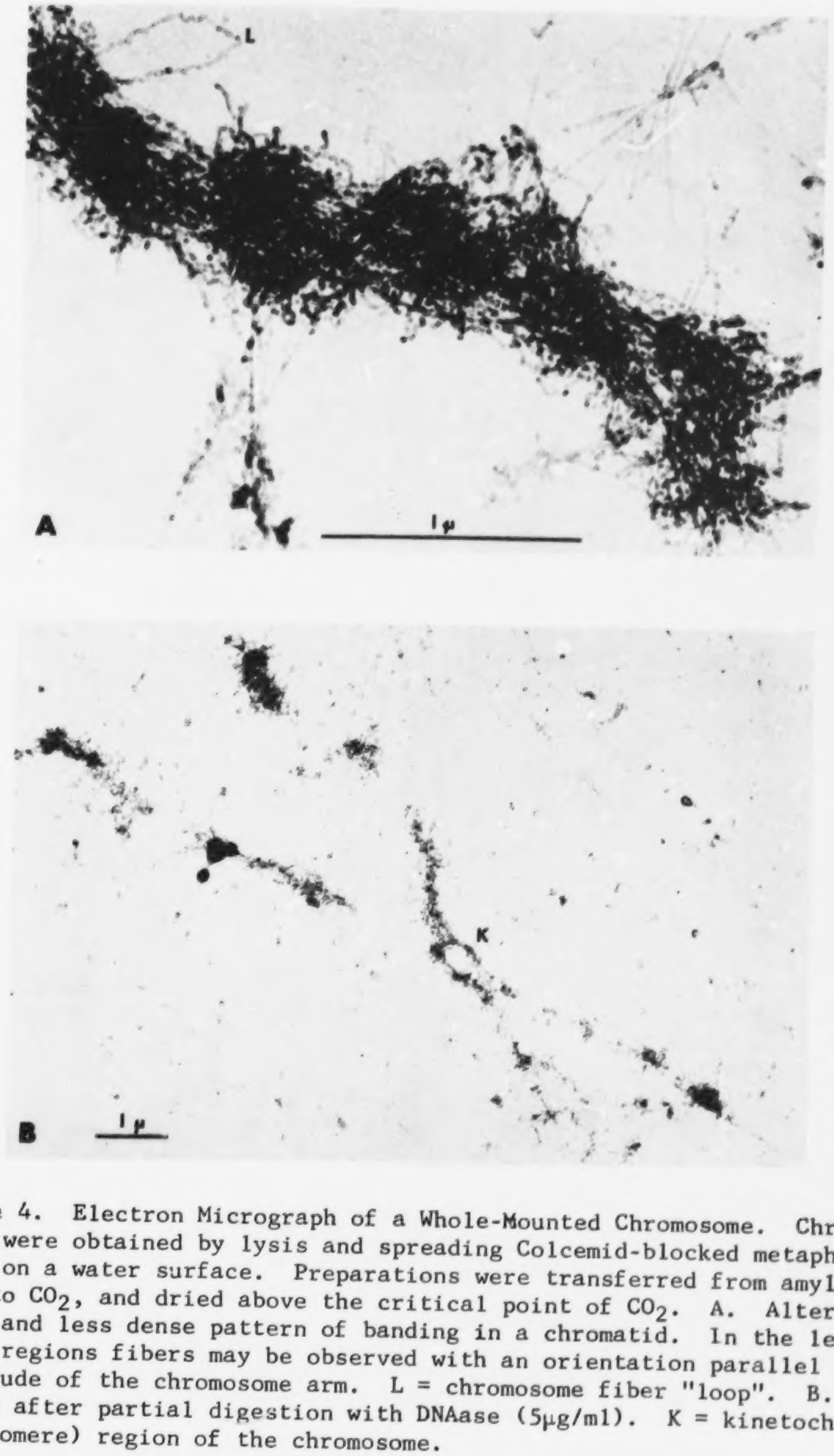

Figure 4. Electron Micrograph of a Whole-Mounted Chromosome. Chromosomes were obtained by lysis and spreading Colcemid-blocked metaphase cells on a water surface. Preparations were transferred from amyl acetate to CO_2, and dried above the critical point of CO_2. A. Alternating dense and less dense pattern of banding in a chromatid. In the less dense regions fibers may be observed with an orientation parallel to the longitude of the chromosome arm. L = chromosome fiber "loop". B. Chromosome after partial digestion with DNAase (5µg/ml). K = kinetochore (centromere) region of the chromosome.

B. ANIMAL STUDIES

1. Influence of Age on the Incidence of Chromosomal Aberrations in the Thyroid

W. M. Leach

If X-ray-induced tumorigenesis in thyroid glands depends, in part, on the age of the animals at the time of irradiation, the age variation in sensitivity may be reflected in the incidence of chromosomal aberrations. To examine this effect, Chinese hamsters were irradiated at one week or one year of age, and thyroid glands were prepared for tissue culture. Available data showed no difference in the yields of chromosome aberrations in the two age groups.

In the course of sub-culturing thyroid cells, three or four marker chromosomes have been identified. Two of the markers have been observed in other laboratories in long-term cultures of cells derived from other tissues of Chinese hamsters. A third marker has been observed in more than 95 percent of cells in division. The marker appears in cells after about the fourth in vitro passage. In Colcemid-blocked cells the marker is located near the periphery of the chromosome group (Figure 5). Observations of the fourth marker chromosome are not extensive. Its frequency in cells is about the same as the third marker.

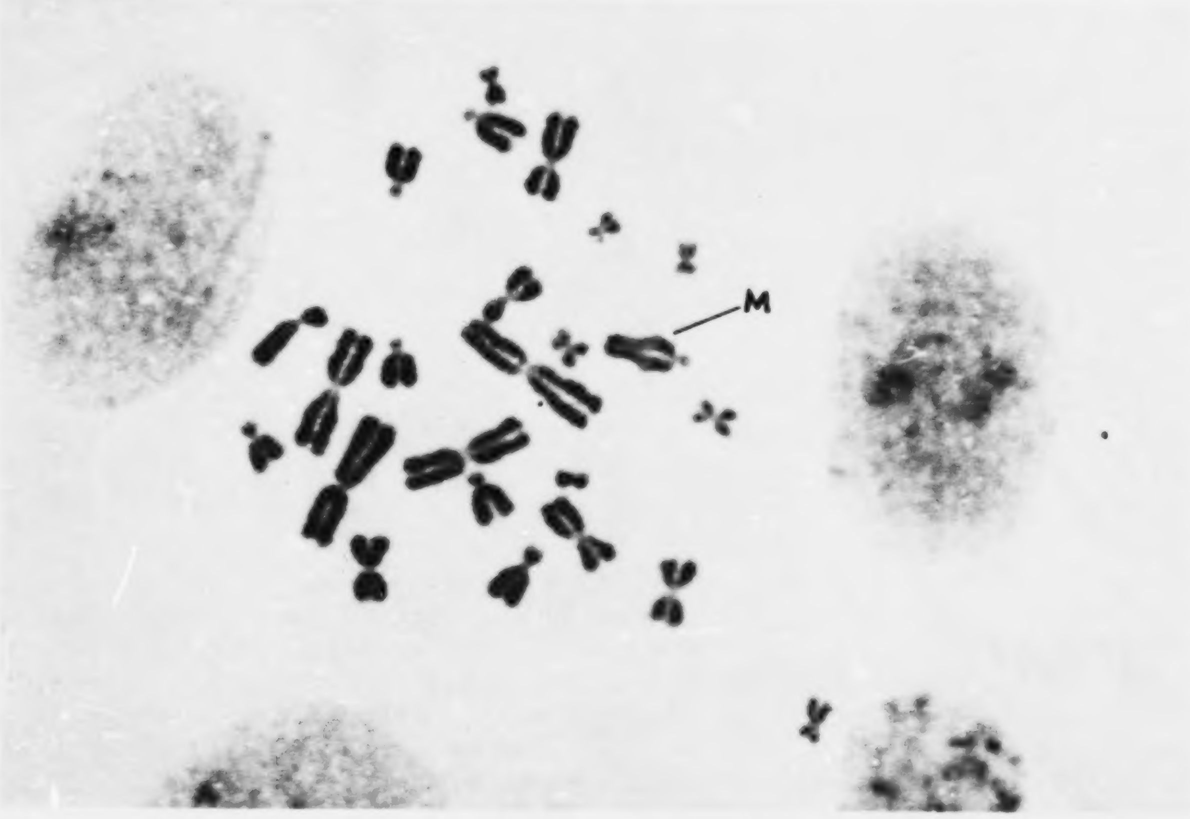

Figure 5. Marker Chromosome (M) in Cultured Chinese Hamster Thyroid Cells.

2. Effect of ^{131}I on the Incidence of Thyroid Tumors

B. C. Ward, W. Moore, Jr., W. M. Leach

In order to determine the incidence of thyroid tumors in Chinese hamsters after ^{131}I exposure, 7-10 day old animals were injected with 0.001-0.1 μCi of ^{131}I (the approximate dose to the thyroid is estimated to be 10 to 1000 rads). Hamsters were sacrificed about two years after injection, and examined for tumors.

Tumors were found in the thyroid gland, liver, and uterus. In addition brain vascular changes were found which resulted in massive cerebral hemorrhage. The hemorrhage was the greatest single cause of death to hamsters during the experiment. The number of tumors is summarized in Table 2. Incidence of lesions in the uterus, liver, and brain appeared to be unrelated to ^{131}I exposure. In the thyroid two of the 20 tumors were carcinomas and the other 18 were adenomas. In view of the small number of animals in the study, the dose-effect relationship for thyroid tumorigenesis remains unclear.

TABLE 2. TUMORS IN CHINESE HAMSTERS TWO YEARS AFTER INTRAPERITONEAL INJECTION OF ^{131}I

Injected ^{131}I, μCi/animal	No. of Animals	Tumors in			Animals with Brain Vascular Changes
		Thyroid	Uterus	Liver	
0.1	49	3	8	14	12
0.05	53	6	5	12	11
0.01	51	4	5	11	11
0.001	50	7	6	11	10
none	50	0	6	18	7
Totals (Frequency)					
^{131}I	203	20(0.10)	24(0.12)	48(0.24)	46(0.23)
Control	50	0(0)	6(0.12)	18(0.36)	7(0.14)

3. Chromosome Stickiness and Division Delay in Irradiated Cultured Cells

W. M. Leach, E. C. Beyer

Chromosome stickiness may be observed in dividing cells that were near division at the time of exposure to heat, X-rays, or hypertonic medium. Data obtained in this laboratory indicate that stickiness effects are mitigated through RNA on the chromosomes of dividing cells.

The possibility that chromosomal changes, induced by microwaves, result from stickiness effects is being explored. Chinese hamsters are exposed to microwaves from microwave ovens at various intervals after injection of Colcemid to arrest bone marrow cells at metaphase. Direct smears of bone marrow cells are made after 4-5 hours of Colcemid exposure.

In preliminary studies no chromosome aberrations have been observed. Chromosomes from irradiated animals appear not as well spread after hypotonic treatment as chromosomes from unirradiated controls. Both intrachromosomal and interchromosomal stickiness phenomena are observed in irradiated cells.

4. The Effects of X-ray Quality on Chromosome Aberration Yields

K. T. S. Yao, E. C. Beyer, W. M. Leach

Bureau interest in public health hazards of X rays produced by color television receivers has prompted comparative studies of X-ray quality on the yield of chromosome aberrations in animals and in cells cultured in vitro. Three X-ray sources operating at a 25 kVp, 250 kVp, and 3.6 MVp, are to be used. The latter source delivers X rays in a pulse lasting 10^{-3} second.

To date 14 Chinese hamsters have been flash irradiated at nominal exposures of 10, 50, or 100 R, each delivered as a single pulse of 3.6 MVp X rays. Animals were sacrificed 1, 6, 13, and 27 days post-irradiation, and kidneys and hearts were removed for tissue culture. Preliminary analysis of the slides of cultured cells reveals small differences in the aberration yields when either X-ray exposure levels or organs of the same animals are compared. The frequency of aberrations for each exposure level and for each tissue is higher than the frequency in unirradiated control animals.

5. Effects of Rat Kangaroo Hematopoietic Cell Lines on the Survival of X-Irradiated Animals.

K. T. S. Yao

Injection of normal bone marrow or spleen cells either freshly obtained or from short-term cell cultures may prolong the survival of animals which have received X-ray doses greater than the species LD 50/30. The technique has been used effectively with accidentally exposed humans. The purpose of this study was to investigate the effectiveness of long term heterologous cells on prolonging animal survival.

Chinese hamsters and mice were given 800, 1,200 or 1,600 rads of X rays (250 kVp, 15 mA, HVL 1.82 mm Cu plus 1 mm Cu and 1 mm Al added filtration, 60 cm air distance, dose rate approximately 52 rads per minute). Within 4 hours after irradiation the animals (68 hamsters, 52 mice) were injected with cells derived from either the bone marrow or spleen of the rat kangaroo. Chinese hamsters were injected intraperitoneally with about 10^7 cells in 1 ml; mice were injected intravenously with approximately 2.5 x 10^6 cells in 0.5 ml. Unirradiated control animals were injected with saline. The rat kangaroo cell lines were initiated in August 1966, and had 32 subculture passages when the experiments were started.

Animals that received 800 rads showed no radiation death, with or without cell injections. All of the animals that received 1,600 rads died within 7 days after irradiation. In the Chinese hamsters receiving 1,200 rads, 12.5 percent survived at least 30 days with cell injections and 10.5 percent survived at least 30 days without the injections. In the mice receiving 1,200 rads, 35.1 percent survived at least 30 days with cell injections, but no mice survived to 30 days without cell injections.

Mice given 1,200 rads showed 31.5 percent survival after spleen cell injections and 38.8 percent survival after bone marrow cell injections. In the hamsters 5.5 percent survival followed spleen cell injections and 18.1 percent followed bone marrow injections. The data are summarized in Table 3.

TABLE 3. SURVIVAL OF MICE AND CHINESE HAMSTERS
AFTER 1,200 RADS OF 250 KVP X-RAYS

	Rat Kangaroo Cell Injections						Saline Injections		
	Spleen			Bone Marrow					
Animal Species	No. of Animals	Average Survival Time, Days[a]	No. of 30-day Survivors	No. of Animals	Average Survival Time, Days[a]	No. of 30-day Survivors	No. of Animals	Average Survival Time, Days[a]	No. of 30-day Survivors
Mouse	19	15.7	6	18	18.9	7	15	10.1	0
Chinese Hamster	18	9.7	1	22	14.2	4	19	10.7	2

a. The average survival calculations included animals surviving at least 30 days. For the calculation 30 days was used, regardless of the actual duration of survival.

A relatively specific pattern of epilation and hair graying was observed in seven irradiated Chinese hamsters. Two of the seven died at 19 and 24 days postirradiation, one was sacrificed at 30 days and two others at 60 days postirradiation. The other two survived more than one year. By the 14th day postirradiation, shedding of hair started at the top of the head. Shedding extended progressively toward the posterior, but stopped at the waistline. At about 30 days white hair appeared in the shed areas. By 60 days the white hair covered the shed areas except the top of the head. Graying of the normal agouti hair began behind the waistline about 90 days and extended progressively toward the tail. By 250 days animals were gray-white except for agouti ears, tail, a small posterior spot, and black upper lip whiskers. Two grayed and one unirradiated animal are shown in Figure 6.

Hair samples were taken from the two surviving irradiated animals and from one unirradiated animal, and were prepared for microscopic examination. Four hair types were found: Type A has a single row of medullary cells; type B has a proximal "stalk" section with a single row of cells and a distal "blade" section with 2-5 rows of cells; type C is similar to B, except that a constriction occurs between the stalk and blade sections; and type D, otherwise similar to A, has a constriction close to the tip and 2-4 bends in the hair. The degree of pigmentation of the hairs was graded as follows: Grade 1, less than 15 percent lack of pigmentation; grade 2, 15-50 percent unpigmented; grade 3, 50-85 percent unpigmented; and grade 4, 85-100 percent unpigmented. Table 4 summarizes the results of the hair measurements, with standard deviations of average values shown.

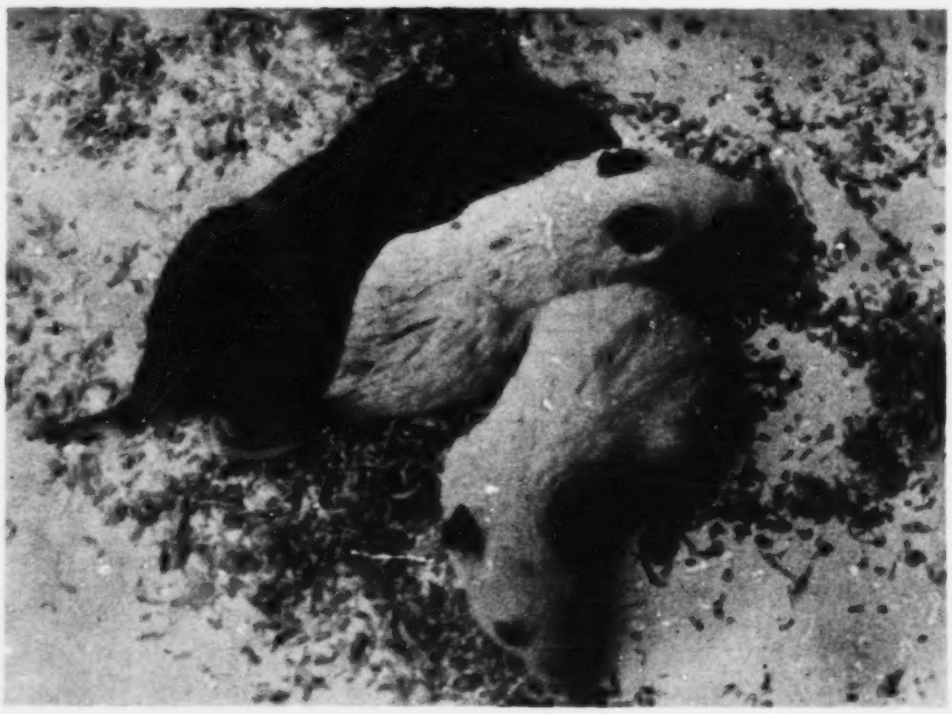

Figure 6. Two Chinese Hamsters with Gray Hair after 1,200 Rads of X Rays. After irradiation, animals were injected with cultured cell lines originally derived from the rat kangaroo. Back to about the waistline, the gray hair grew in after marked epilation. One normal agouti animal is also shown.

TABLE 4. CHINESE HAMSTER HAIR TYPE, DISTRIBUTION, AND AVERAGE MEASUREMENTS BEFORE AND AFTER EPILATION

X-Ray Dose, Rads	Body Region	Hair Type	Number of Hairs	Length[a]	Number of Constrictions[a]	Pigment Grade[a]	Frequency of White Tips, Percent
0	Shoulder	A	6	6.8 ± 0.72	0	1.3 ± 0.40	0
		B	28	7.9 ± 0.77	0	1.9 ± 0.49	0
		C	11	7.6 ± 0.76	1.1 ± 0.90	1.6 ± 0.45	0
		D	75	6.5 ± 0.70	1.6 ± 1.09	1.7 ± 0.46	0
	Haunch	A	9	8.3 ± 0.88	0	1.3 ± 0.45	0
		B	46	9.2 ± 0.97	0	1.9 ± 0.55	0
		C	13	8.9 ± 0.96	1.1 ± 0.99	1.7 ± 0.52	0
		D	52	7.8 ± 0.90	1.4 ± 1.11	1.3 ± 0.45	0
1200	Shoulder	A	10	4.9 ± 0.84	0	3.3 ± 0.65	90.0
		B	39	6.1 ± 0.93	0	3.7 ± 0.68	94.9
		C	18	6.3 ± 0.95	1.0 ± 0.85	3.8 ± 0.70	94.4
		D	53	5.5 ± 0.89	1.3 ± 0.97	3.2 ± 0.64	98.1
	Haunch	A	20	6.8 ± 1.08	0	1.6 ± 0.85	30.0
		B	27	8.5 ± 1.21	0	2.3 ± 1.02	14.8
		C	11	8.5 ± 1.21	1.1 ± 1.06	2.3 ± 1.02	9.9
		D	62	6.9 ± 1.09	1.6 ± 1.27	1.7 ± 0.88	14.5

a. Average ± one standard deviation is shown.

6. In Vitro Cultivation of the Seminiferous Epithelium of Chinese Hamsters

D. J. Ellingson, K. T. S. Yao

In order to examine directly radiation effects on spermatogenesis, we have attempted to culture germinal cells. Rose chambers have been used to contain portions of seminiferous tubules under a dialysis membrane. Eagle's minimum essential medium supplemented with 1.0 mM sodium pyruvate, 1.0 mM non-essential amino acids and 20 percent calf serum, was used. L-Glutamine (2-4 mM) plus 100 units of penicillin and 100 μg equivalents of streptomycin per ml were added. The cultures were maintained at 31°C at a pH between 6.8 and 7.0.

Tubules were flattened by the dialysis membrane. Some of virtually each cell type, and most of the spermatocytes developing spermatids and spermatozoa were pressed out from the cut ends. Most spermatogonia, Sertoli cells, and some spermatocytes remained inside the tubule. Expressed spermatocytes, as well as developing spermatids, survived 3-4 days in vitro. Spermatocytes in metaphase I or II completed one meiotic division. Spermatogonia lived 2-3 weeks in culture and underwent mitosis (Figure 7). Sertoli cells began migration out of the tubule in about 24 hours. Sertoli cells divided actively, and overgrew cultures by 3-6 weeks of age. The Sertoli cells at culture initiation were associated rather specifically with spermatogonia (Figure 8).

Oscillation and/or rotation of nuclei and metaphase plate were observed in spermatogonia and spermatocytes. In the spermatocytes nuclear rotational movement was seen during the first 3-4 days of culture; in spermatogonia movement persisted after three weeks of culture. Movements were sporadic, uncoordinated, and either clockwise or counterclockwise. Occasionally a cell reversed its direction.

Time-lapse cinemicrographic observations of 14 cells with rotating nuclei were analyzed, and the results are shown in Table 5.

TABLE 5. NUCLEAR ROTATION FROM TIME-LAPSE CINEMICROGRAPHIC ANALYSIS

Cell Number	Number of Observed Rotations	Range of Speed of Rotation, seconds	Average Speed of Rotation, seconds
1	5	118 - 591	362 ± 181
2	16	46 - 192	96 ± 44
3	8	71 - 412	202 ± 108
4	8	108 - 342	180 ± 78
5	3	285 - 690	429 ± 226
6	3	288 - 642	450 ± 179
7	13	48 - 303	110 ± 70
8	15	48 - 288	101 ± 83
9	23	34 - 201	70 ± 25
10	13	46 - 281	117 ± 72
11	20	43 - 186	80 ± 43
12	16	51 - 184	99 ± 39
13	6	149 - 347	271 ± 63
14	23	46 - 109	68 ± 16
Total	172	34 - 690	---

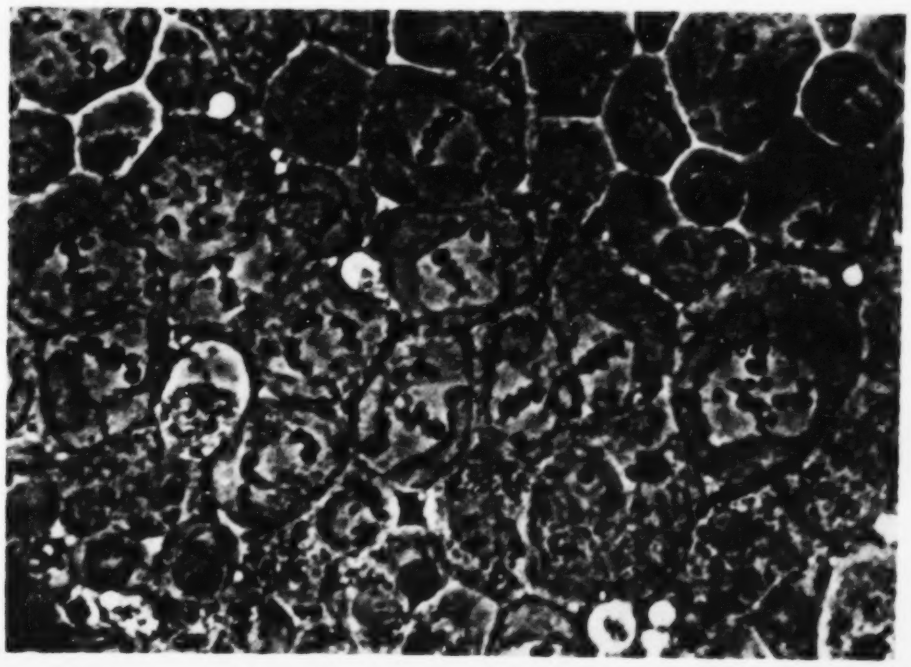

Figure 7. Mitosis in Spermatogonia Cultured from Chinese Hamsters. Cultures were in Rose chambers, where spermatogonia were recognized for 2-3 weeks after initiation of the culture.

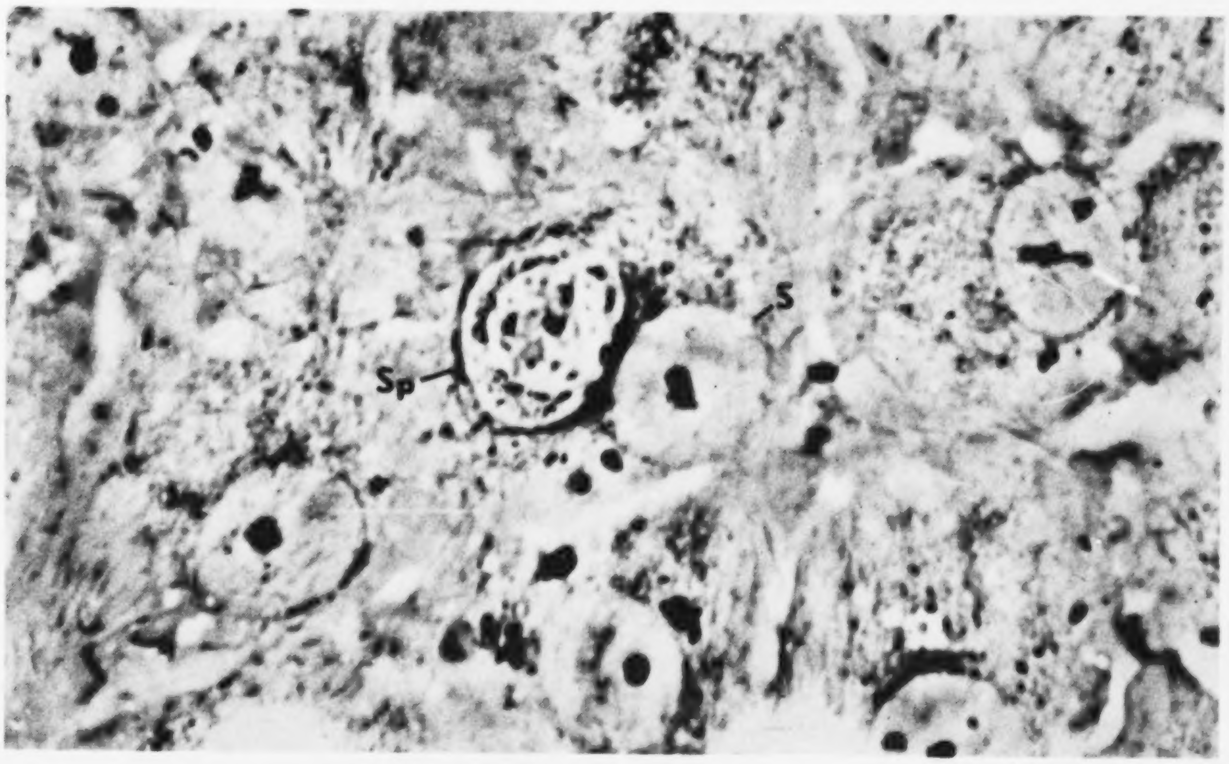

Figure 8. The Sertoli Cell-Spermatogonium Side-by-Side Orientation at the Beginning of In Vitro Culture of Testicular Tissue of the Chinese Hamster. During culture in Rose chambers, the Sertoli cells (S) may become less closely associated with some spermatogonia (Sp).

BLANK PAGE

RADIATION PHYSICS LABORATORY

Mr. Harry D. Youmans, Chief

The responsibilities of the Radiation Physics Laboratory are twofold: to provide the Radiation Bio-Effects Program with irradiation, dosimetry, and related supportive services, and to conduct research studies with primary emphasis on dosimetry. During most of 1968 the Radiation Physics Laboratory has been concerned with the generation and measurement of ionizing radiations, the accurate exposure of biological specimens, and the application of results of its research studies which are primarily directed at spectral measurements and determinations of absorbed dose.

The passage of the Radiation Control for Health and Safety Act of 1968 has increased the demands upon the Radiation Physics Laboratory for detailed firsthand knowledge concerning the interaction of nonionizing radiations with biological systems, their characteristics, and their measurement. A new microwave exposure facility has been installed. New investigations germain to nonionizing radiation dosimetry will provide information on the distribution of energy absorbed in non-homogeneous tissue and molecular systems in a wide range of wavelengths, the characteristics of tissue equivalent systems at various wavelengths, and the identification of the molecules and tissues that undergo primary beam energy absorption, as well as the molecules and tissues that respond to the energy absorption.

A. LABORATORY SERVICES

1. Irradiations

W. Lee, L. Kramer, V. Yancik

The Radiation Physics Laboratory provides X and gamma irradiation of biological specimens and the dosimetry of exposures both external and internal to biological or phantom systems. The irradiation facility consists of a 1,000 curie cesium-137 irradiator, a 250 kilovolt constant potential (kVcp) X-ray generator, and a 120 kilovolt-peak (kVp) superficial therapy X-ray unit. In addition, a specially designed, high-output, low-energy (0-75 kVp) X-ray source was installed in December. The primary dosimetry for this unit is now being done.

Specimens include a variety of animal species, cultured cells, and various tissue equivalent materials and phantoms. Because of this variety, only the outlines of dosimetric procedures can be standardized.

Although dosimetry is based upon National Bureau of Standards calibrated R-meters, dosimetry is usually performed with tissue equivalent phantoms and thermoluminescent dosimeters with energy corrections based upon measured spectra. The irradiations for the year are summarized in Table 6.

TABLE 6. IRRADIATIONS AT THE TWINBROOK LABORATORY, 1968

Specimen	Number	Beam On-Time, Hours
	X Irradiations	
Rats	3,626	259.5
Biological Specimens	486	34.0
Hamsters and Mice	283	8.0
Swine	2	1.1
	Cesium 137	
TLD Calibration		4
TLD Capsules		0.1
Biological Specimens	2	0.08

2. Instrumentation and Electronics

G. E. Anderson, R. A. Tell

In providing irradiation and dosimetry services to the Radiation Bio-Effects Program, the Radiation Physics Laboratory is occasionally confronted with the problem of developing instrumentation for the dosimetry work. One such device developed this year, a six-decade scaler, was developed as the readout display for a charge digitizer. The display and the digitizer are two units that will be used as part of a thermoluminescent dosimeter (TLD) system for studying the glow-curve response of lithium fluoride (LiF), a thermoluminescent material commonly used in dosimetric studies.

Each decade circuit board consists of a decade counter, a buffer-storage element, and a decimal decoder - display driver. These are all integrated circuit devices. The use of integrated circuits decreased the design time and resulted in a compact unit with dimensions of 9 by 9 by 3 inches. The circuit diagram is shown in Figure 9.

The entire unit consists of six decade boards with Nixie tube readout, two regulated power supplies, and an input gate circuit.

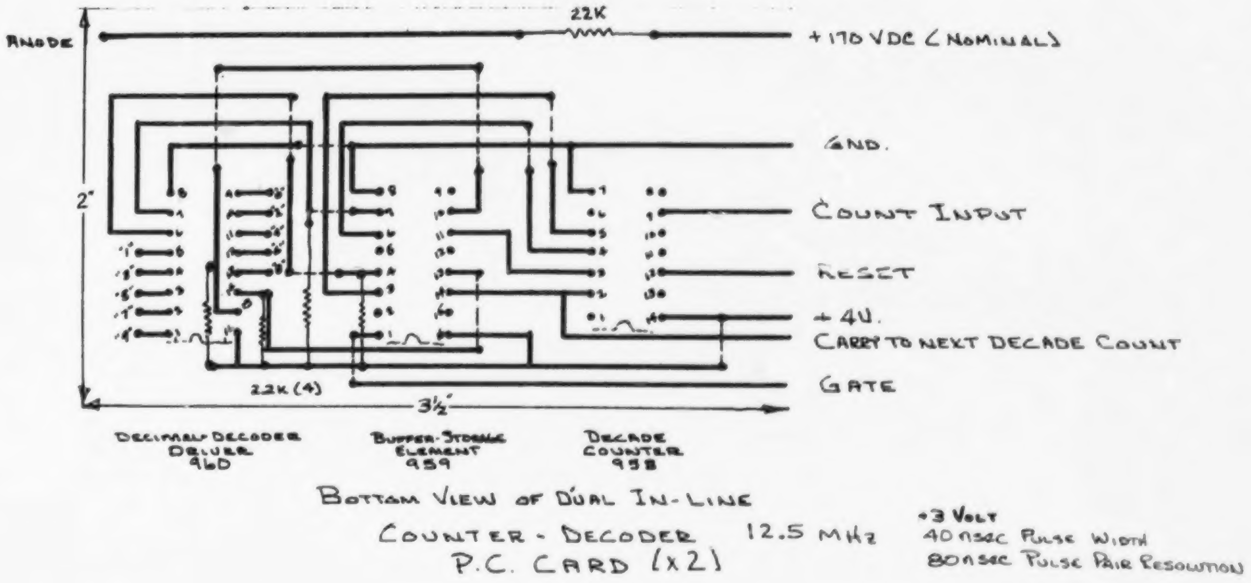

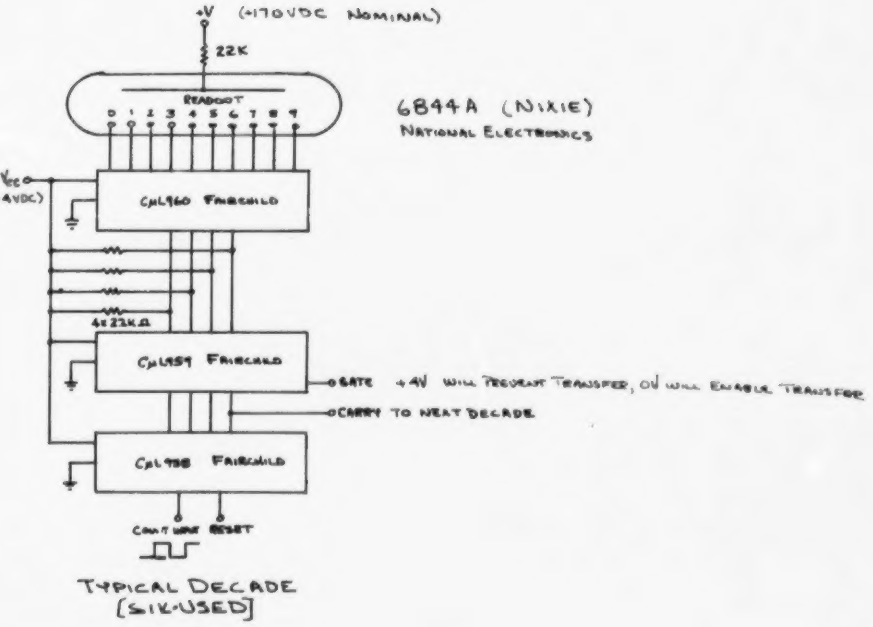

Figure 9. Circuit Diagram of Decade Circuit Board.

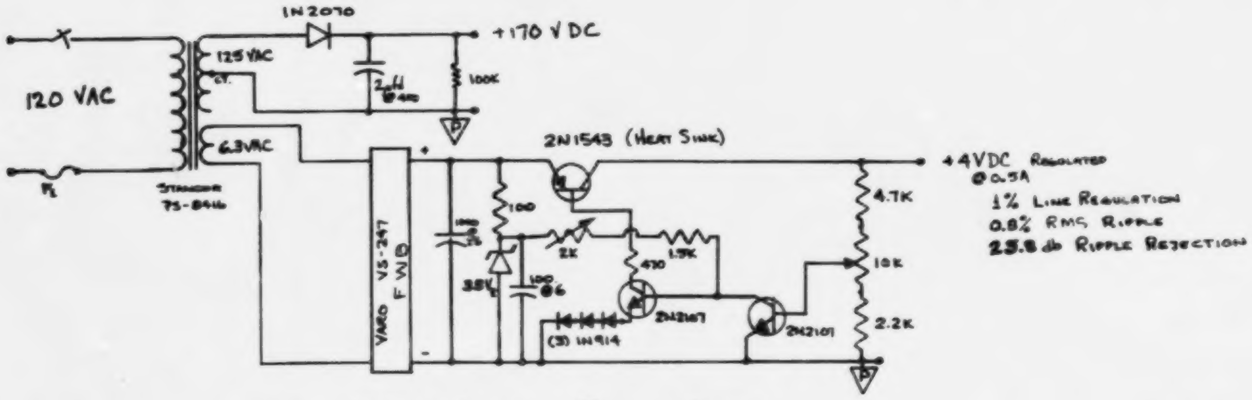

LOW & HIGH VOLTAGE POWER SUPPLY

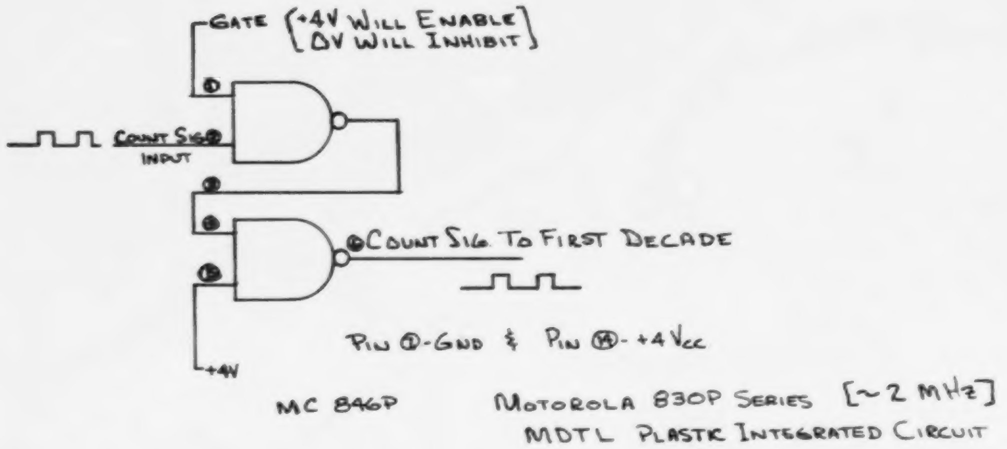
GATE [+4V WILL ENABLE
0V WILL INHIBIT]
①
②
COUNT SIG INPUT
③
④
⑤
⑥ COUNT SIG. TO FIRST DECADE
+4V
PIN ⑦-GND & PIN ⑭- +4 Vcc
MC 846P
MOTOROLA 830P SERIES [~2 MHz]
MDTL PLASTIC INTEGRATED CIRCUIT

INPUT GATE FOR COINCIDENCE COUNTING
OR
USE WITH AN EXTERNAL TIMER

Figure 9. Circuit Diagram of Decade Circuit Board (continued).

3. Installation of Low-Energy X-Ray Machine

G. E. Anderson, R. A. Tell

During the year the Radiation Physics Laboratory installed a low energy (0-75 kVp) X-ray machine, which, with proper filtration, will be capable of simulating the X rays emitted by color television receivers. The X-ray tube employed has a 5-mil beryllium window, a platinum target, and is capable of continuous operation at 30 kV and 100 mA.

Preliminary investigations of the X-ray emission indicate that the unfiltered exposure rate is of the order of 8.6×10^6 R/min at the window under operating conditions of 40 kVp and 75 mA. Higher exposure rates are expected at the maximum tube voltage rating of 75 kV.

The high voltage power supply also produces 0 to 75 kV dc at a rated current of 100 mA dc. An overall accuracy of 1% of the desired output voltage allows precisely controlled condtions of irradiation.

To obtain constant and reproducible exposure rates from the machine, an improved milliampere stabilizer and filament power supply were developed in this laboratory. The stabilizer employs the theory of closed loop stabilization. The basic loop consists of an amplifier, bias control circuit, filament drive circuit, detector, and a summing network. These are connected so that the bias control circuit will adjust the filament drive circuit and increase or decrease the X-ray tube current until the detector produces a feedback signal that cancels the input command (the desired current flow).

In general, the performance of the loop is related to its "stiffness." If it has high gain, then only a small error signal is needed to drive the controller; the output follows the input and any perturbations are then compensated.

The mathematical analysis of this kind of mechanism is rather complex but can be reduced to an algebraic manipulation of the coefficients of a system of differential equations. It will suffice to say the loop gain is adjusted so that the frequency response crosses the zero dB axis just prior to the second pole (180 degree phase shift). The circuit diagram for the mA stabilizer is shown in Figure 10. Short term stability tests indicate a drift of 0.02% from a mean value of current over a half-hour exposure time (after a 5 minute warm up).

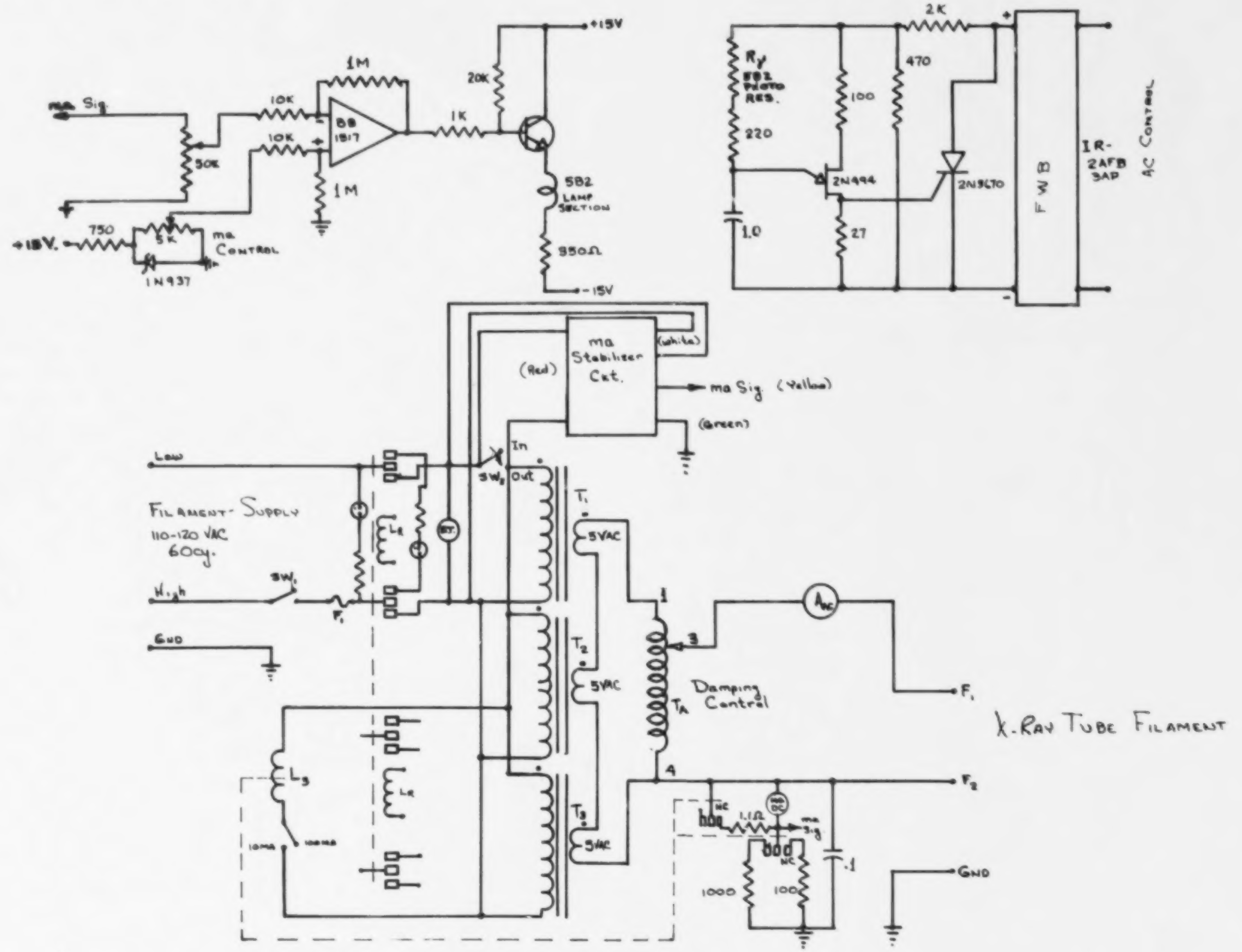

Figure 10. Milliampere Stabilizer Developed for Use with Low-Energy X-Ray Machine.

B. DOSIMETRY AND RADIATION PHYSICS

1. Doses in the Brain, Eye and Thyroid of Children from 63-112 kVp X-Ray Epilation for Tinea Capitis

W. Lee, H. D. Youmans

Tinea capitis is a fungal infection of the scalp which has occurred in epidemics among prepubescent children. X-ray epilation of the scalp was commonly used in treatment prior to the availability of griseofulvin in 1958. Recent studies indicate a relationship between X-ray epilation of the scalp and increased incidences of neurological disorders and malignancies. A collateral study by this laboratory has shown by thin layer chromatography that the lipid composition of in vivo irradiated beagle pup brain is altered by doses in this range (see page

This study was conducted to determine the distribution of dose in the brain, eye, and thyroid of children. Lithium fluoride dosimeters were used in phantoms made from mix-D and human skulls of ages 3 years, 6 years, and 12 years for exposure to 60 kVp, 90 kVp and 110 kVp X-irradiations. X-ray beam qualities were determined in air and in the phantom brain by both absorption methods and Ge(Li) spectrometry. The data were fully corrected for spectral dependence which results from heavy filtration of the incident beam by the scalp and skull. The doses ranged from 17 rad to 656 rad in brain, 11 rad to 92 rad in eye, and 3 rad to 23 rad in thyroid.

In general, the radiation treatments for "ringworm of the scalp" depended on the age of the patient (which was a reflection of brain size and cranium thickness) and the place of treatment. The radiation treatments varied from 60-120 kVp with HVT's of 0.4-4.0 mm Al, but the beams most commonly used were 75-100 kVp with 1.0 mm Al HVT. The radiation exposure ranged from 300 R to 500 R per field. Five such fields were used to obtain a uniform scalp dose (the Adamson-Kienböck technique).

In our study, three beams were used to cover the range of irradiation conditions. The qualities of the three beams were: (1) 63 kVp, HVT = 0.67 mm Al; (2) 88 kVp, HVT = 1.00 mm Al; and (3) 112 kVp, HVT = 3.90 mm Al. The X-ray tube current was 10 mA. Half-value thicknesses were determined with 99.99% aluminum foils and sheets. The attenuation curves of the three beams are presented in Figure 11.

Three children's skull phantoms (ages 3, 6, and 12 years) were selected for the dose distribution measurements. Variations in cranium thickness and skull dimensions are presented in Table 7. The brain phantoms of the three skulls were cast of Mix-D, a mixture of paraffin, polyethylene, MgO, and TiO_2. Its tissue equivalence was established theoretically and experimentally.

To gain access into the brain for dosimeter locations, the skulls and Mix-D brains were cut horizontally, dividing them in half. Two

TABLE 7. DIMENSIONS OF HEAD PHANTOMS[a]

Skull Phantom	Maximum Diameter		Cranium Thickness	
Age, Years	AP, cm	Lat, cm	Mean, mm	Range, mm
3	15.5	12.0	2.4	1.5-3.0
6	16.0	12.5	2.9	2.5-4.0
12	16.5	13.0	3.3	2.5-4.0

a. All measurements include a Mix-D scalp thickness of 3 ± 1 mm.

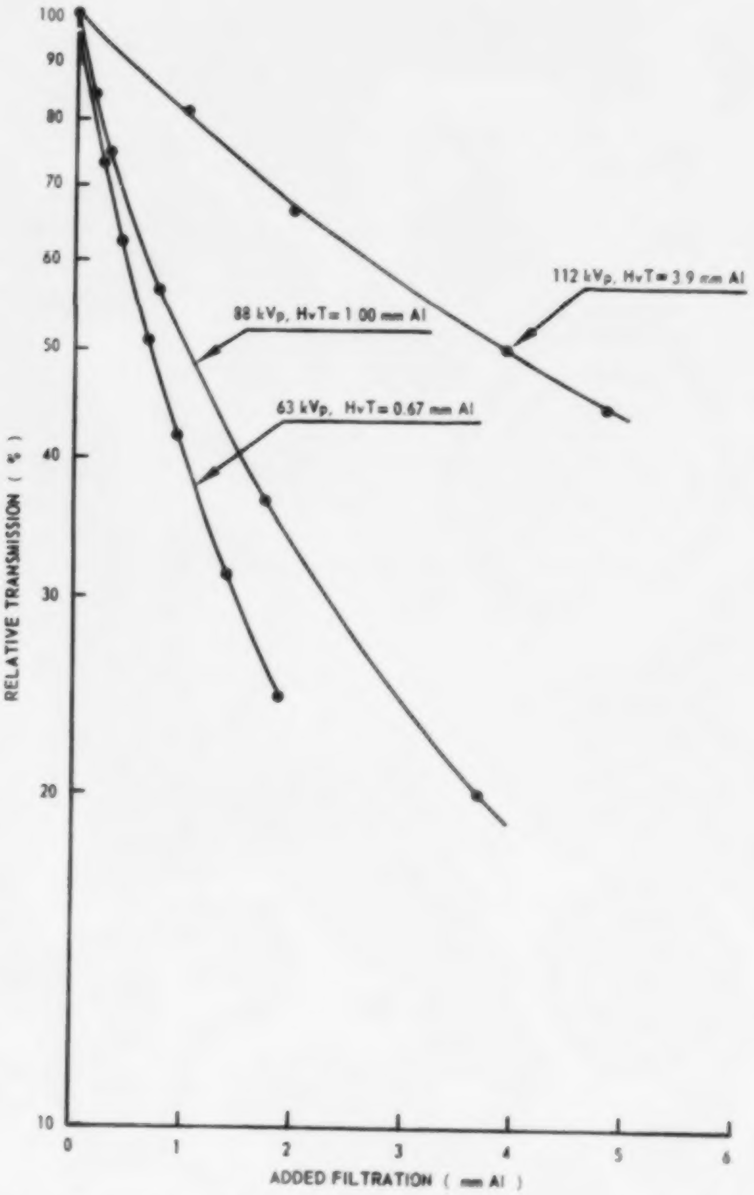

Figure 11. Attenuation Properties of the Three X-Ray Beams Used for This Study.

additional vertical cuts divided the brain into six sections. Forty-nine dosimeter locations were selected and dosimeter holes 5 mm in diameter and 12 mm deep were drilled into the six sections (Figure 12).

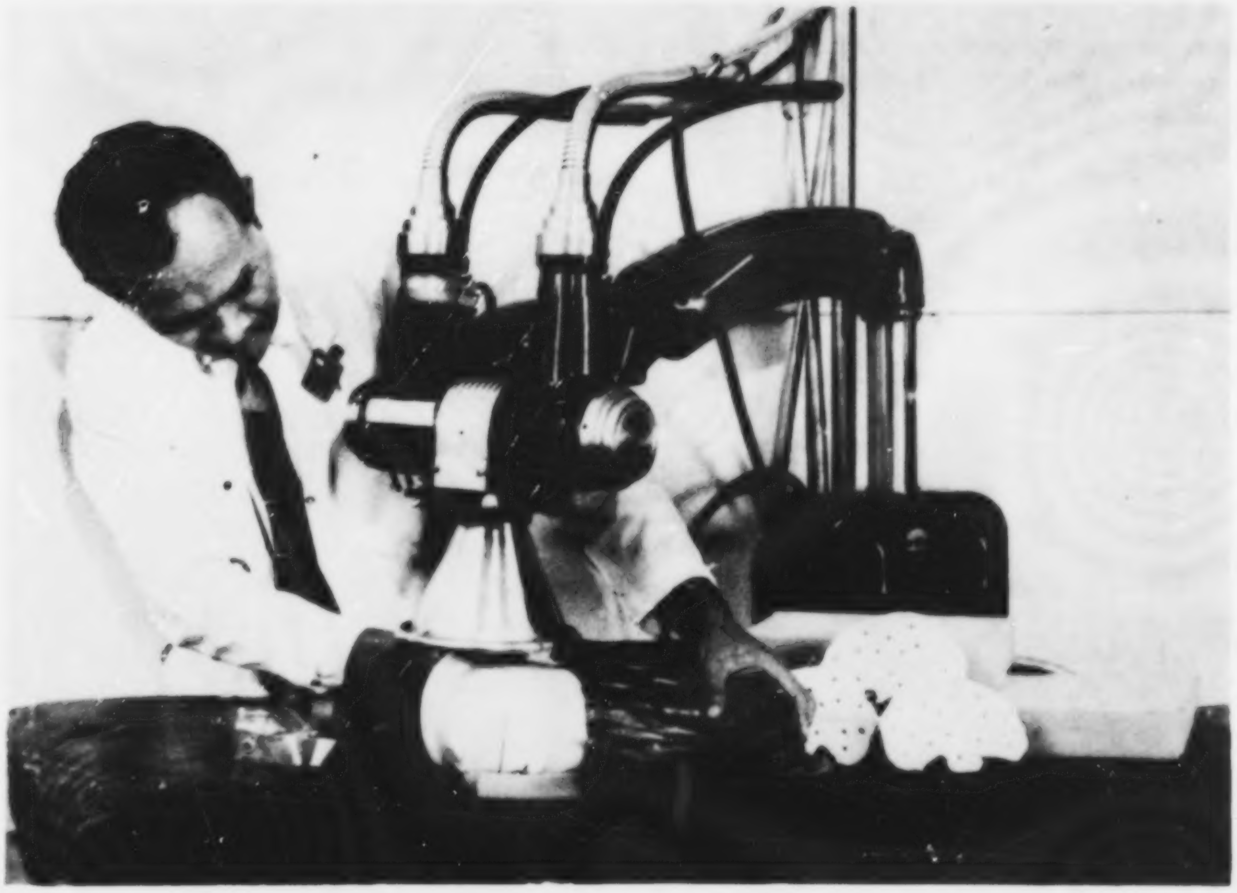

Figure 12. One of the Positions Used in Irradiating Skull Phantoms to Obtain Dose Distributions in Brain. Brain phantoms with holes for thermoluminescent dosimeters are shown at right.

Lithium fluoride (TLD-100) powder in thin gelatin capsules was employed for the dose measurements. The dosimeters were appropriately calibrated and their response as a function of exposure was determined. Since the response was linear up to 600 R, and the exposures rarely exceeded 600 R, 100 R (100 kVp, 3.5 mm Al HVT) was used for calibration.

The effective energies in the brain phantom for the three beams employed were measured with the "cap on -- cap off" method in the 3-year-old skull phantom. This method enables the quality of a beam to be estimated in any material simply by finding the ratio of exposures with an appropriate dosimeter at a point in the material when it is encapsulated in metal and when it is not encapsulated. If a set of ratios has been previously determined in air for a corresponding set of HVT's, any measurement of the ratio is equivalent to a determination of a HVT. Because two parameters are necessary to specify X-ray beam quality, such sets are not theoretically unique, but they are usually adequate when thoughtfully employed.

The qualities of the three beams in the middle of the 3-year-old head phantom were 2.1, 2.6, and 4.3 mm Al HTV for the 63 kVp, 0.67 mm HVT; 88 kVp, 1.00 mm Al HVT; and 112 kVp, 3.90 mm Al HVT, respectively. The energy responses of the dosimeters were within the experimental error.

The ratio of absorbed dose (in soft tissue) to exposure ($\bar{f}$) was relatively constant over the energy range of interest. The estimated HVT's of 2.1, 2.6, and 4.3 mm Al in brain corresponded to effective energies of 28, 30, and 38 keV. Therefore, the value of 0.88 rad/Roentgen (water) was used for all calculations of dose from exposure response.

The Adamson-Kienbock five-field treatment technique was used to irradiate the phantoms. The central axis of the X-ray beam was positioned at five points: frontal, vertex, occipital, and the left and right temporal areas. Each skull phantom was irradiated with the three beams described previously. During irradiation, a lead sheet 0.4-0.5 mm thick shielded the areas below the hair line of the phantom (Figure 12). Most lead-rubber used for patient shielding had lead equivalent thicknesses of 0.25 to 0.5 mm.

A Picker Zephyr Model NR-2 X-ray machine with an oil-cooled type CX-B X-ray tube and a 3.8 mm effective focal spot size was used. A vacuum-tube-controlled constant voltage transformer stabilized the electrical supply to the X-ray machine and the X-ray tube current was stabilized by a silicon-controlled rectifier circuit of our own design. This machine produced a field size 18 cm in diameter at a source-to-skin distance of 21.5 cm; the exposure was 400 R per field.

In general, the upper 2/3 of the brain, representing most of the cerebral cortex but excluding the lower frontal and temporal lobes of the cortex, received the highest doses. The lower 1/3 of the brain received a dose of only 60% of that received by the upper 2/3. This lower third included the cerebellum, brain stem, the lower half of the mid-brain, and the lower frontal and temporal lobes of the cortex. Considering the whole brain, the superior lobe of the frontal cerebrum received the highest dose; the brain stem and the lower half of the cerebellum received the lowest doses.

Since additional shielding was never present over the upper portion, and the frontal lobe of the cerebrum is at right angles to four of the five irradiation fields, the dose distribution to the upper 2/3 was somewhat higher than to the rest of the brain. Dose to the upper 2/3 of the brain was quite uniform relative to the average for the whole brain.

The mean absorbed doses in the brain as functions of HVT's of the irradiating beams and the ages of the skull phantoms are shown in Figure 13 and Table 8. As expected, an increase of the HVT of a beam increased the depth dose distribution in the brain. The dose-HVT relationship in Figure 13 is a strong function. An increase in cranium thickness of only 1 mm can reduce the dose by as much as 30% in the brain, depending on the quality of the irradiating beam.

TABLE 8. MEAN DOSE TO THE BRAIN

Beam Qualities		Dose,	Brain Phantom		
mm Al HVT	kVp	Rads	3-year	6-year	12-year
0.67	63	Average Dose	80.1	76.5	67.3
		Dose Range	23-139	31-118	17-119
1.00	88	Average Dose	147	131	112
		Dose Range	50-238	61-190	33-184
3.90	112	Average Dose	432	422	416
		Dose Range	164-656	211-562	139-611

When the mean absorbed dose was used as a common denominator, our calculations showed that the upper 2/3 of the brain absorbed about 120% of the mean dose, whereas the cerebellum and the lower 1/3 of the brain received only 50% and 75%. This relationship is fairly independent of the quality of the irradiating beam and the age of the skull phantom. Therefore, once a mean dose is estimated from Figure 13 the brain dose distribution can be approximated.

Doses to the eye, pituitary, and thyroid gland are presented in Table 8. Pituitary doses in the 6-year-old skull phantom were not determined because an additional vertical cut in the skull parallel to the face of the phantom was directly over the pituitary. For vertex and the temporal exposures, the cut provided radiation leakage to the pituitary and measured values would have reflected this defect. Doses to the pituitary in the 6-year-old phantom should be very similar to those of the 12-year-old because of their similarities in cranium thickness and brain size (Table 7). The thyroid dose in the 12-year-old phantom is higher than that of the 6-year-old. This might be due to the longer face and neck of the 6-year-old phantom; consequently a longer source-to-

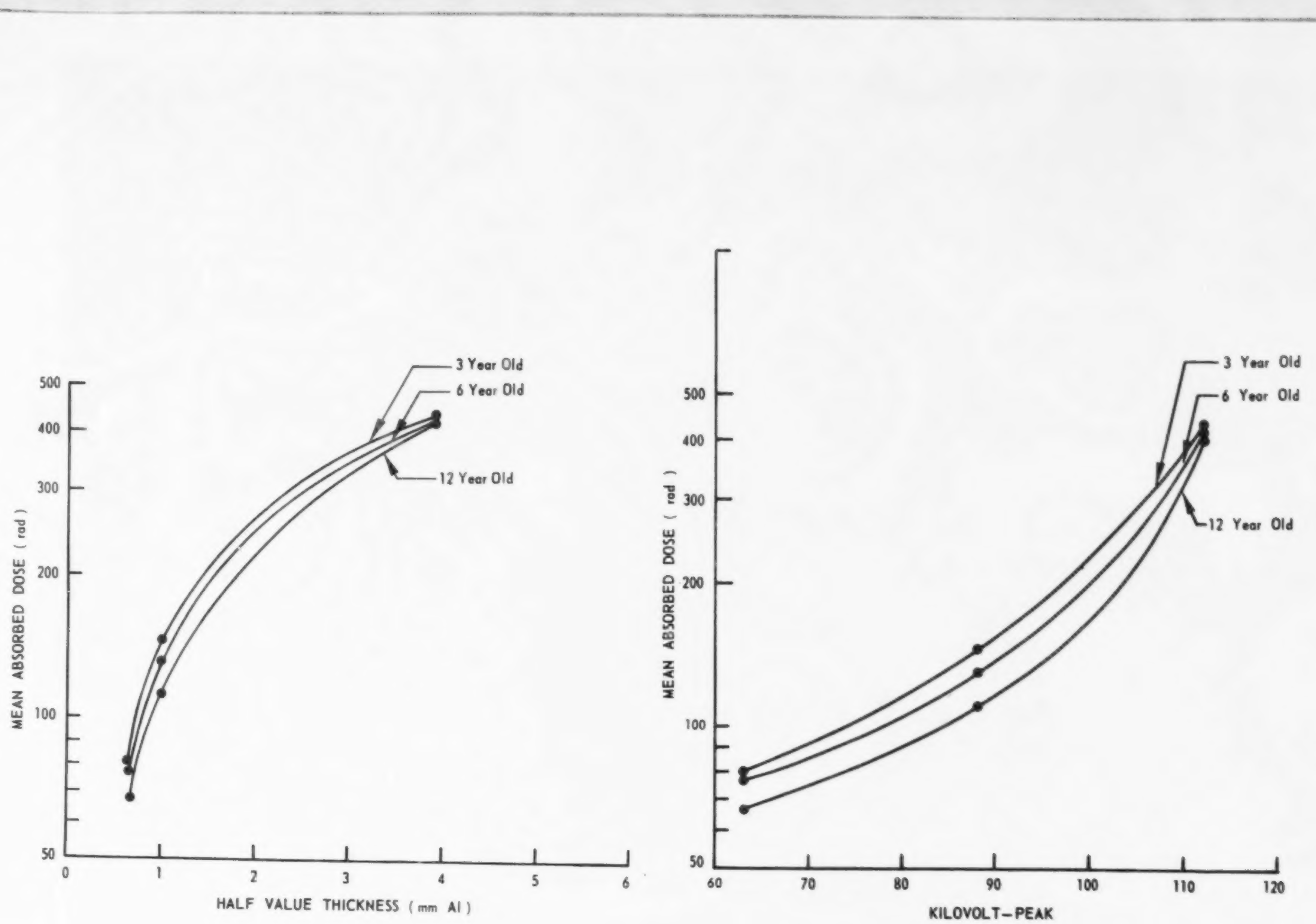

Figure 13. Mean Absorbed Dose in Brain as a Function of Half Value Thickness (left) and X-Ray Tube Potential (right).

thyroid distance. We do not know whether or not to consider this phenomenon to be unfortunate because just these variations exist in the population.

TABLE 9. DOSE TO THE THYROID, EYE, AND THE PITUITARY

Age of Phantom, Years	Beam Qualities		Dose, Rads		
	kVp	mm Al HVT	Thyroid	Eye	Pituitary
3	63	0.66	2.94	11.2	14.6
	88	1.00	5.04	23.6	34.6
	112	3.90	23.1	92.2	128
6	63	0.66	1.10	8.18	--
	88	1.00	2.40	18.4	--
	112	3.90	10.3	75.4	--
12	63	0.66	1.62	8.48	13.9
	88	1.00	3.60	17.6	29.7
	112	3.90	14.6	73.4	121

2. Spectral Transmission and Attenuation of X Radiation by Glasses and Resins used in Color Television Picture Tubes

R. A. Tell, G. E. Anderson, H. D. Youmans

A cooperative study between the Radiation Physics Laboratory, the Bureau's Electronic Products Radiation Laboratory, and Pittsburgh Plate Glass Industries was begun to evaluate the X-ray attenuation properties of certain glasses and resins used to construct color television receiver picture tubes. The attenuation coefficients of common and experimental glasses and resins and fully constructed face plates were evaluated. The results of this study will be used as a basis for selecting scientifically valid methods for assessing the attenuation effectiveness on a quality control basis.

The picture tube emission spectra of two different tubes were measured by using a NaI(Tl) detector and multichannel analyzer. Supportive data were taken with a Ge(Li) detector system. Figure 14 shows the emission spectra from the RCA 25AP22A picture tube with and without its safety panel. The bandwidth is narrow, on the order of 25 percent FWHM, and is comparable to that obtained with monochromatic X rays.

Photon intensity depends upon high voltage, and was found to vary typically from the 19th to the 30th power of the high voltage given by the empirical relation, $R = AV^k$

where R = detector response
A = constant of proportionality
V = picture tube high voltage
$19 < k < 30$

The anisotropic emission of X-ray flux was measured and is shown in Figure 15. The highest relative flux, measured 50 cm from the screen, occurred at an angle normal to the picture tube face.

After determining typical spectra from the picture tubes, an X-ray machine was adjusted so that its spectrum was similar to that of the television tubes. Using appropriate collimation, narrow beam attenuation coefficients were determined for various glasses and bonding resins. Figure 16 shows the results of these measurements. Using these values, Figure 17 was developed showing percent transmission of 25 keV X-ray photons as a function of material thickness. These data are in good agreement with the calculated values of the attenuation coefficients.

3. Dosimetry and Narrow Beam Irradiation of the Young Rat Thyroid

W. Lee, J. R. Childress, T. R. Horton

In cooperation with the Radiation Oncology and Pathology Laboratory, the Radiation Physics Laboratory has been providing radiation exposure and dosimetry services for a study examining the relative incidence of thyroid tumors in irradiated rats of different ages (see p. To examine age sensitivity, groups of 120 Long-Evans female rats, ages

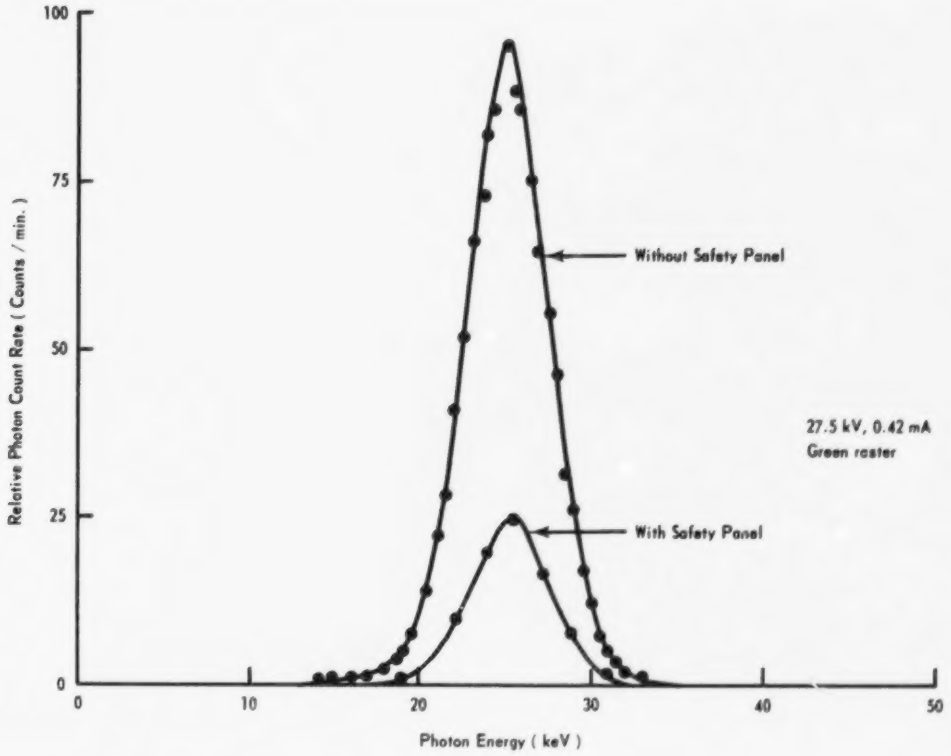

Figure 14. Emission Spectra of the RCA 25AP22A Picture Tube With and Without Its Safety Panel.

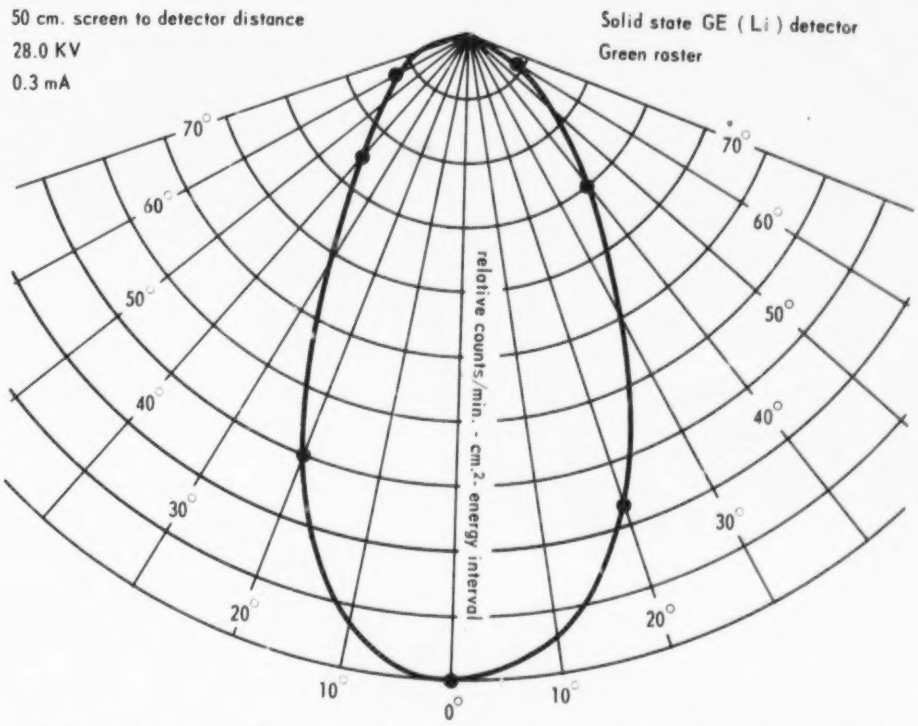

Figure 15. Spatial Distribution of X-Ray Flux at Various Angles About a Point on the Picture Tube Face.

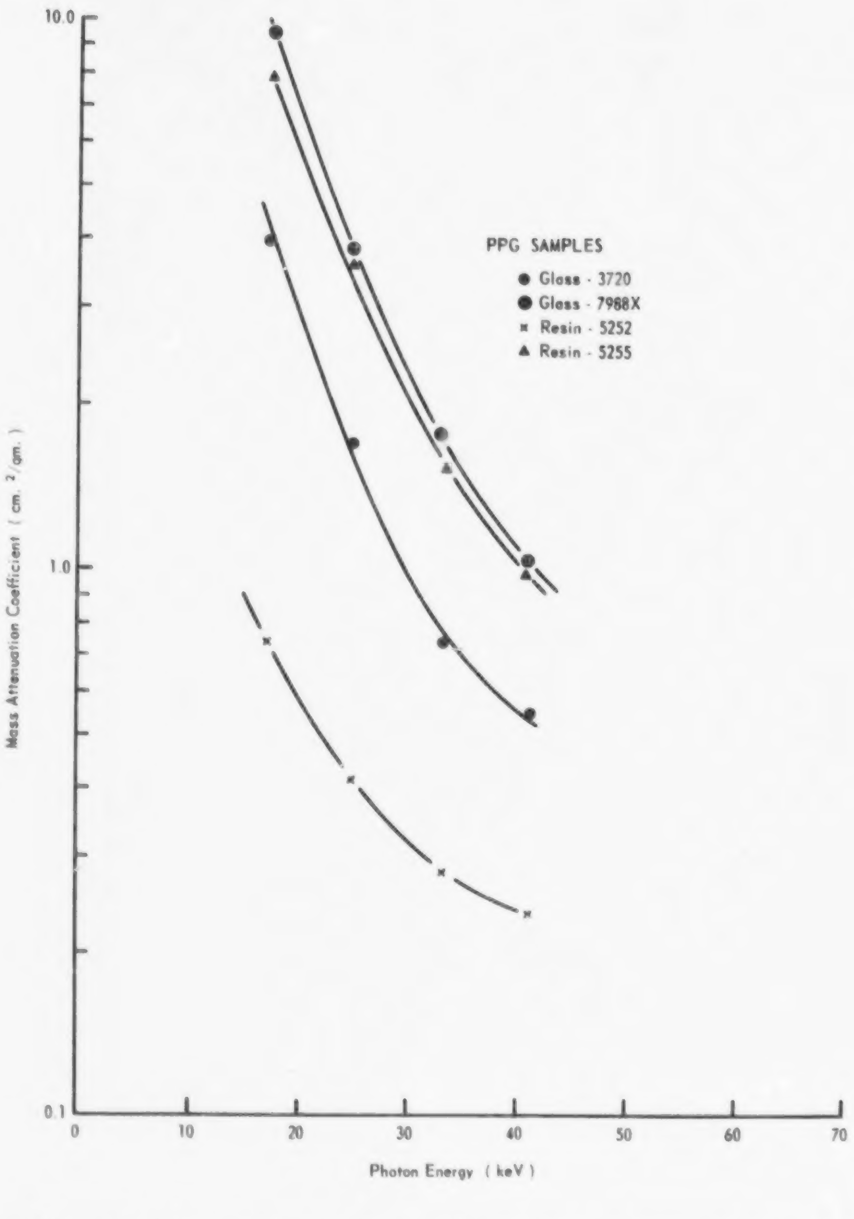

Figure 16. Narrow Beam Attenuation Coefficients of Various Glasses and Bonding Resins.

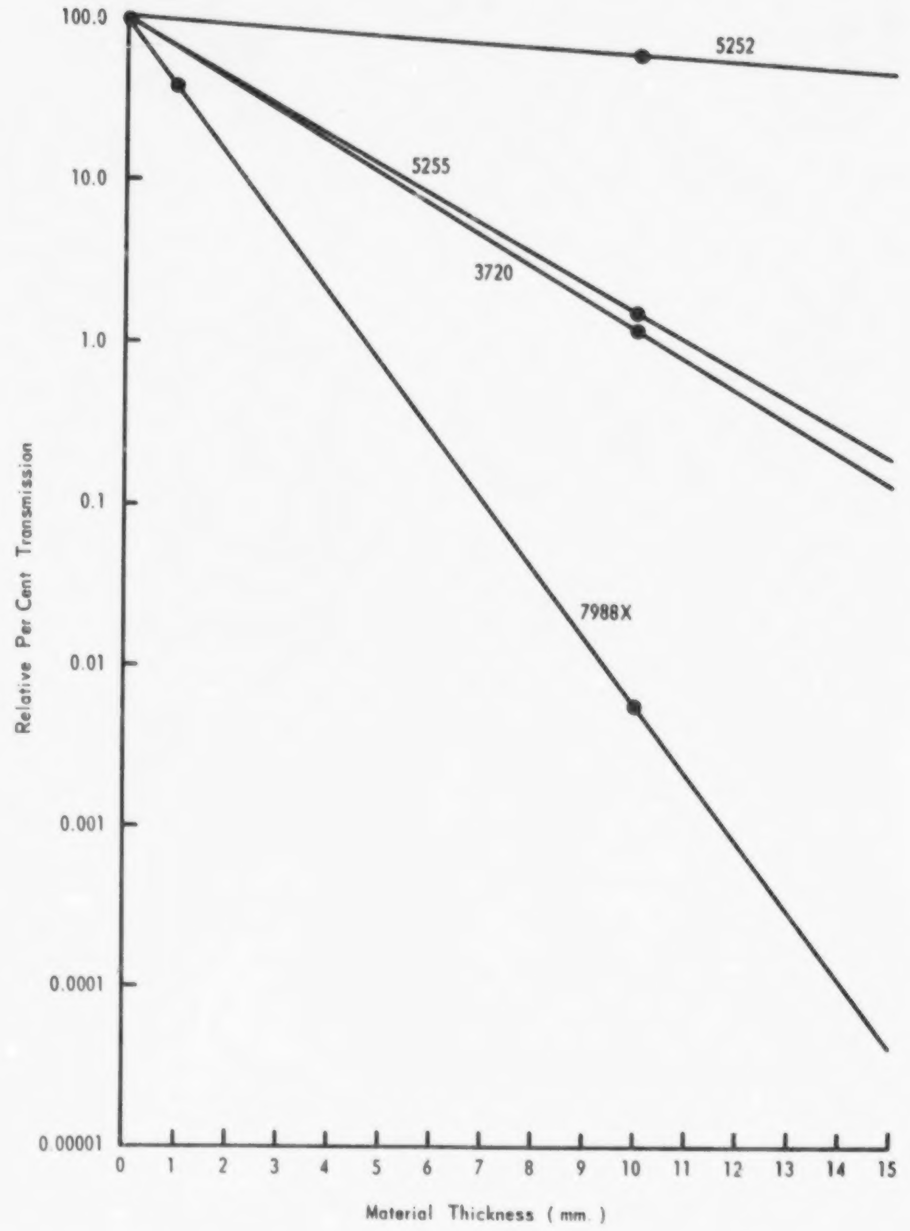

Figure 17. Relative Transmission of 25 keV X-Ray Photons as a Function of Glass and Resin Thickness.

10 days, and 1, 3, and 6 months were exposed to 1,000 rads of X radiation to the thyroid.

Because the thyroid and pituitary are functionally interdependent through hormonal biochemical mechanisms, care was taken not to expose the pituitary to the primary X-ray beam. This requirement, plus the small size of the young rat placed stringent restrictions upon exposure rate, dose uniformity, and dosimetry.

The X ray source was a 250 kVcp X-ray generator; the beam was collimated through specially designed and fabricated lead and brass collimators. Cross sectional uniformity of the beam and the positioning of the thyroid in the beam were evaluated radiographically. Depth dose, uniformity of dose, and the ratio of pituitary dose to thyroid dose were determined with encapsulated LiF rods imbedded in several sizes of rat cadavers (Figure 18).

As shown in Table 10 the absorbed dose rates varied from 1,754 rads to 1,931 rads per minute. The scattered radiation to the pituitary was only 2 to 3 percent of the thyroid dose. Thyroid dose rates of 1,900 rads per minute were achieved permitting the Class-A (NBS Handbook 88) irradiation of 240 rats in less than 2.5 hours of exposure time.

4. Dose Rate Determination in Bone Using LiF Thin Discs and Micro-Rods

U. H. Behling

A study was begun to investigate the use of LiF to determine the bone dose in cats that had been fed a steady diet of strontium 90 in equilibrium with its daughter yttrium 90. The high response, compactness, and relatively low energy dependence are characteristics of LiF that make it a desirable dosimeter. Thin discs of LiF-Teflon, 50 microns thick and 0.25 inch in diameter, and LiF extruded rods, 5.5 mm long and 0.8 mm in diameter were used.

Calibrated thin discs were taped to the exterior and to the longitudinally cut surfaces of bones; similarly calibrated LiF micro-rods were implanted in the trabecular regions of the bone (Figure 19).

As shown in Table 11 empirical exposure values of the discs ranged from 2.42 to 3.83 R/day which are in close agreement to theoretical values derived from β-fluence determination. Exposure rates for the microrods ranged from 2.44 to 3.53 R/day as determined from the response measured by the Conrad TLD Model 4 and quantitized from the calibration curve.

The exposure rates obtained from the micro-rods are not twice that of the thin discs as might be expected if the isotope were

TABLE 10. THYROID AND PITUITARY DOSES FOR FOUR AGE GROUPS

	10 days	1 month	3 months	6 months
Average weight, g	15.2	90	215	260
Anesthetic dose[a], mg	0.4	3.5	11.0	15.0
Thyroid Dose, rads	1000	1000	1000	1000
Pituitary Dose, rads	23.4	22.2	25	27
Thyroid Dose Rate, rads/min	1791	1754	1931	1869
Uncertainty, ± 1 S.D. %	3.2	5.7	2.5	3.8

a. Sodium pentothal administered per animal.

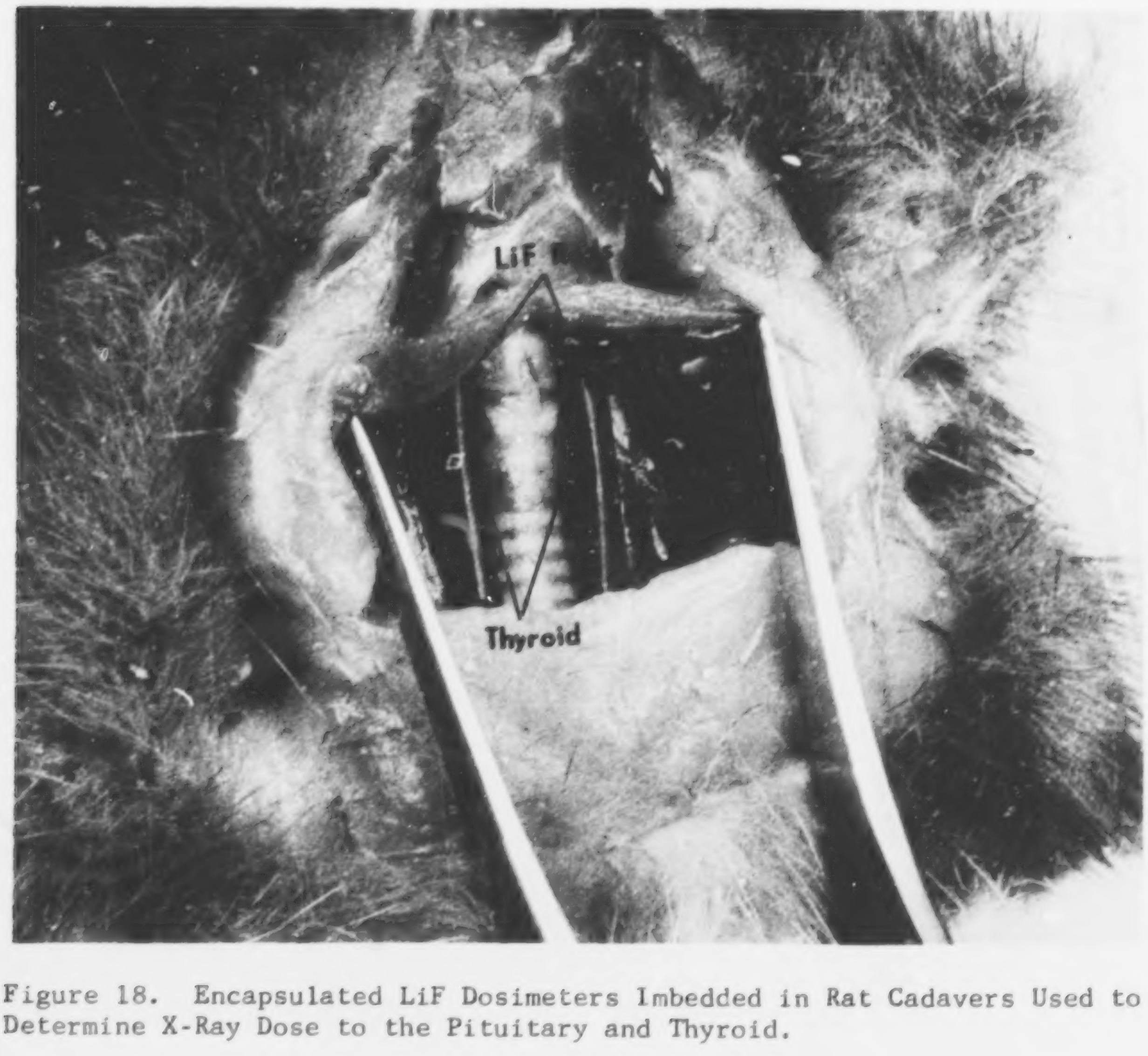

Figure 18. Encapsulated LiF Dosimeters Imbedded in Rat Cadavers Used to Determine X-Ray Dose to the Pituitary and Thyroid.

TABLE 11. LITHIUM FLUORIDE EXPOSURE DETERMINATIONS IN CAT BONES

	LiF Thin Discs			LiF Micro-Rods[a]	
Bone No.	Measured Exp. (R)	Measured Exp. Rate (R/day)	Calculated Exp. Rate (R/day)	Measured Exp. (R)	Measured Exp. Rate (R/day)
A					
Interior	9.94	2.48	3.38	20.8	3.53
Exterior	9.75	2.44	3.28	-	-
B					
Interior	11.60	2.90	3.34	14.4	2.44
Exterior	12.8	3.20	2.83	18.4	2.78
C					
Interior	-	-	-	15.8	2.54
Exterior	9.70	2.42	2.33	15.4	2.57
D					
Interior	9.70	2.42	3.29	21.7	3.51
Exterior	8.60	2.15	2.63	21.5	3.42
E					
Interior	-	3.38	3.33	16.8	2.77
Exterior	-	3.83	3.30	-	-

a. Except for the four spaces indicated, two internal measurements were made on each bone.

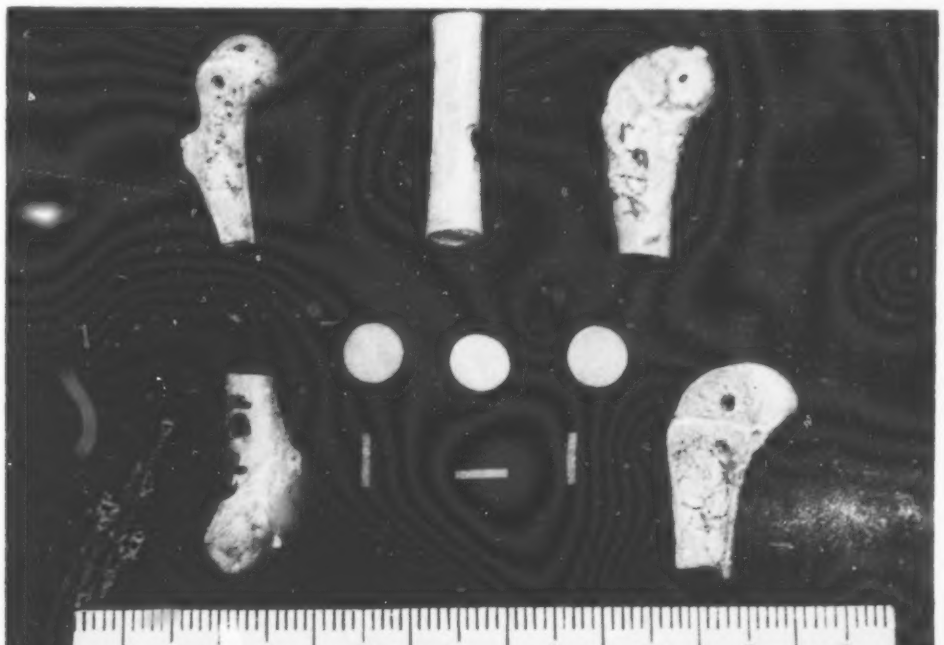

Figure 19. LiF Thin Discs and Micro-Rods Used to Obtain Radiation Doses in Trabecular Regions of Cat Bones.

uniformly distributed in a medium of homogeneous density.[1] The observed differences are probably influenced by a lower density (g/cm^3) toward the center portion of the bone and by differences in concentrations of the isotope (μCi/g).

5. Shielding Properties of Lead-Impregnated Rubber Gloves

U. H. Behling

The increasing use of radioisotopes in research and medicine intensifies the potential radiation hazard to the users. Those who wear rubber or plastic gloves are protected somewhat from a spilled solution, but gloves offer little protection to gamma-emitting nuclides.

Commercially available, lead-impregnated rubber gloves were evaluated by the Radiation Physics Laboratory to determine their effectiveness in shielding a wearer from the 0.035 MeV emission of iodine 125.

The 0.035 MeV gamma produced by iodine 125 was simulated through narrow beam collimation of an X-ray tube (Picker type PX 6-C) driven by a Westinghouse style 980228 generator. A variac was used between the output of the autotransformer and the primary of the high voltage transformer in order to produce very low energy X rays. Beam collimators for the X-ray tube measured 0.101 inch. In addition to the inherent filtration, 0.0900 inch of Cu and 0.110 inch of Al were used to "harden" the beam of the X-ray tube operating at 35 kVp and 10 mA.

The detector was a Harshaw one inch by one inch NaI(Tl) scintillation crystal with a 0.005-inch beryllium window, optically coupled to a photomultiplier tube (RCA model 8575). The beam collimator for the NaI(Tl) detector measured 0.052 inch. The output of the photomultiplier tube was fed into a pre-amplifier (Victoreen model SPA-M). All counting data were collected with a Victoreen model SCIPP 1600 multichannel analyzer equipped with a paper tape punch readout (Teletype model BRPE).

Discs 1 inch in diameter were cut from the tips of the five fingers and four places on the palm of the glove and placed in a specially designed holder for a counting time of three minutes. The effective shielding of the sample was measured in terms of its percent transmission of integral counts in a spectrum with no sample in place for the same time period (Figure 20).

The values indicate that more than 90 percent of the photons are absorbed by the glove, which gives an equivalent thickness of about four half value layers.[2] Monoenergetic photons (gamma and X radiation) are attenuated exponentially, which means that additional increments in absorber thickness yield minimal changes in effectiveness; i.e., the first HVL attenuates 50% of the primary beam in comparison to 25% of the second, 12 1/2% of the third, etc. Therefore, a further increase in glove thickness would change its shielding properties very little at the expense of flexibility, and limit the use of the gloves for laboratory operations.

---

[1] For a medium to meet this condition it has to be an "infinite slab of infinite thickness." The lower limit of the "infinite" dimension is twice the range of R_β-max energy, which is based on the theoretical beta-energy spectrum and changes for an infinitely thick source.

[2] HVL is defined as that thickness of a given material that will attenuate 50% of the incident photons of a given energy.

6. Background Gamma Spectrometry in North Carolina

G. E. Anderson, R. A. Tell, H. D. Youmans

Our study of population exposure to high natural radiation in Kerala, India, has provided estimates of mR/day ranges for different occupations, locations, ages, and sexes. The usefulness of these data is limited, however, by a lack of available accurate information on the effective photon energy of thoria background radiation. Estimates of organ dose as a fraction of an ambient field of omnidirectional gamma radiation for a range of photon energies have been published. Estimates of the average photon energy vary from 0.075 MeV to 1.25 MeV. Knowledge of the average and/or effective energy can also be used to provide a better design for the calibration of thermoluminescent personal dosimeters, such as those used in India.

To obtain knowledge of the photon energy from thoria, the attenuation characteristics of a thoria deposit in North Carolina were measured in water and in copper using a portable scintillation spectrometer. The principal deposit of thoria was exposed in a narrow vein above which the detectors and water phantoms were suspended from a wooden tripod (Figures 21, 22).

Forty-four 100-channel spectra were obtained. These data, which will provide information on the pentration of thorium gammas in water phantoms and copper sheets of various thicknesses, are presently undergoing computer analysis.

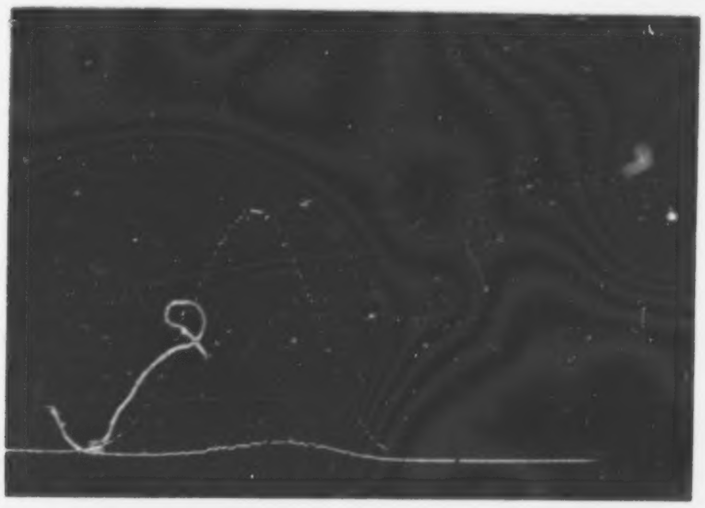

Figure 20. Spectra With and Without Sample.
Counting time 3 min; counts full scale 8 x 10^3.

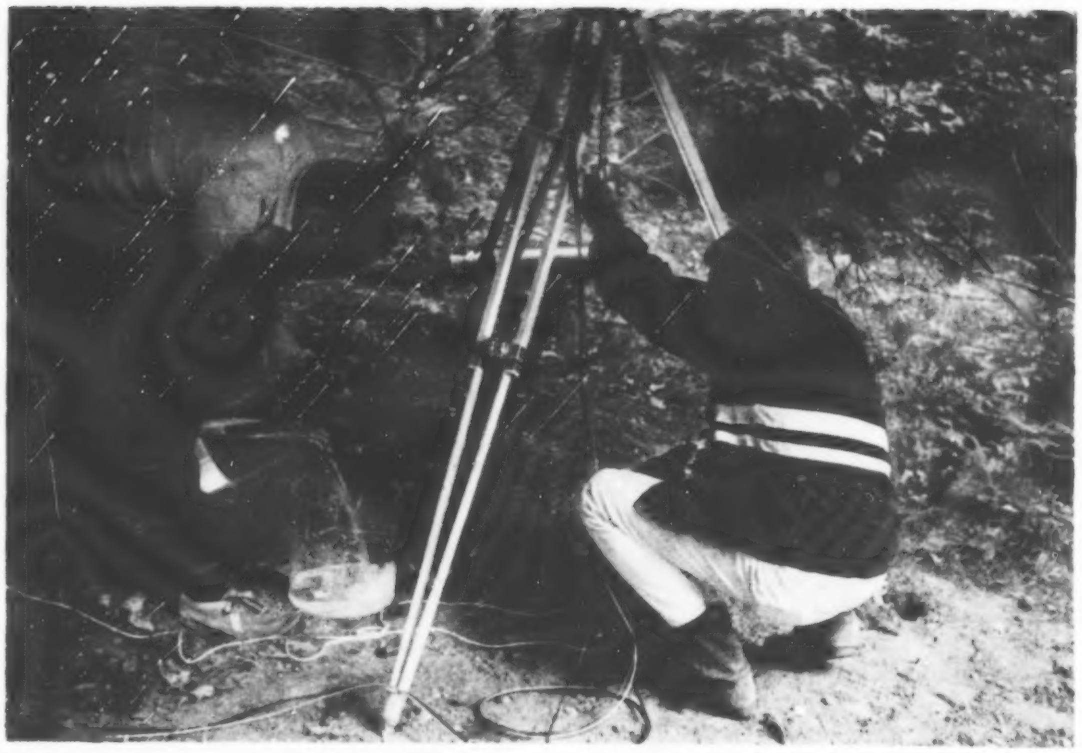

Figure 21. Portable Scintillation Detector and Water Phantom Used to Measure Pentrability of Multiply Scattered Gamma Rays from Natural Thoria Deposits in North Carolina.

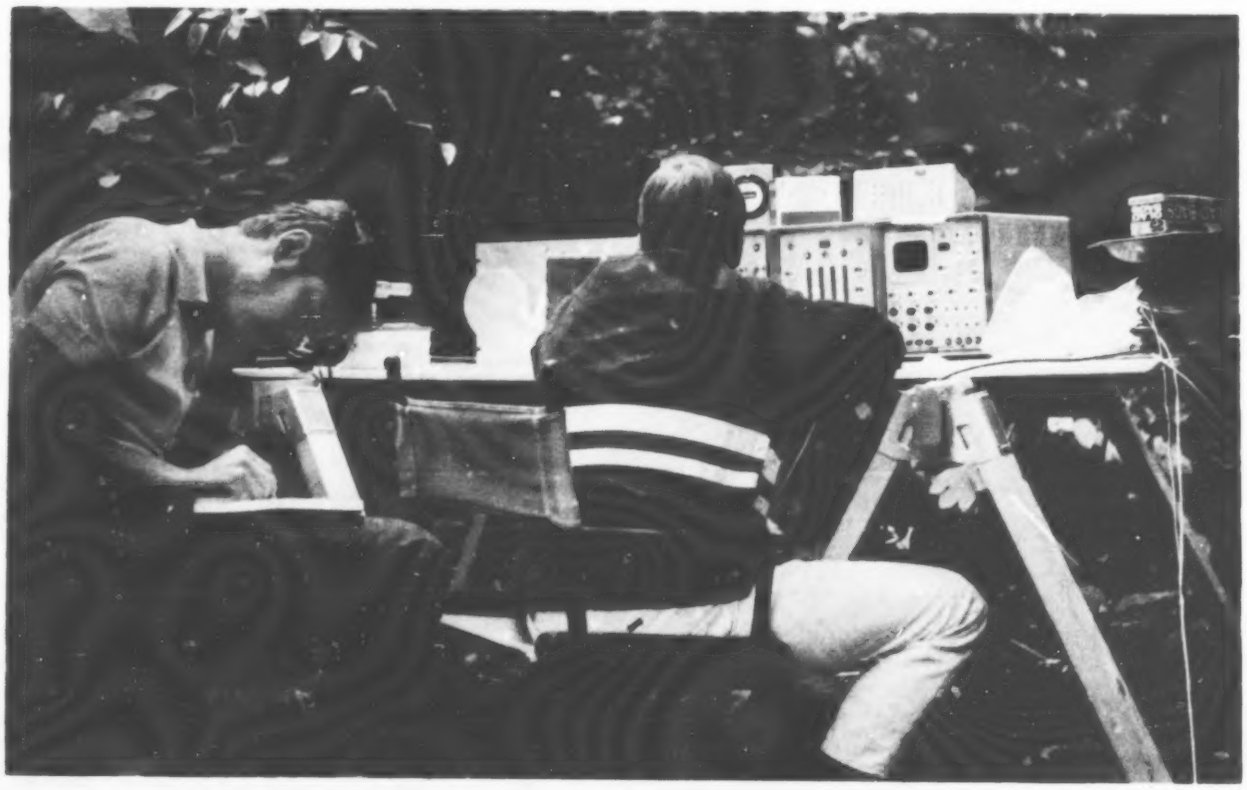

Figure 22. Portable Multichannel Analyzer used to Process and Record Radiations from Natural Thoria Deposits.

C. LIPID ANALYSIS OF BRAINS OF BEAGLES EXPOSED TO X RADIATION

J. D. Manes, R. P. Chiacchierini, H. D. Youmans

Prior to 1958, a large number of children were X-ray epilated as part of the treatment for tinea capitis, a fungal infection of the scalp. Subsequently, it was reported that a substantial proportion of the treated patients suffer from mental disorder, cancer, and permanent damage to the scalp. A previous pilot study in this laboratory with 1-year-old beagles indicated that both lipid and morphological changes might occur at the 200-rad level. The present study was conducted to measure changes in brain lipid fractions that might result from tineal X-ray exposures.

Thirteen beagle pups from four litters were included in the study. At 6 weeks of age, eight pups were irradiated with 500 R to the head only; five served as controls. At 1, 30, and 180 days postirradiation, two irradiated pups and one unexposed animal were sacrificed. At 270 days postirradiation, the remaining animals were sacrificed.

The brains of all thirteen pups were extracted. Two samples from each brain were analyzed, one from the cerebrum, and one from the pons. The brain lipids were extracted by the method of Folch et al. The extracts were analyzed on thin layer chromatograms, the results of which were quantitized by densitometry.

The analog output was digitized and the areas under each lipid peak were computed using the trapezoidal rule by electronic computer. The fraction of the total area that each lipid constituted was computed. A postirradiation time analysis and a dose analysis were carried out on the resulting fractions of lipids.

The time analysis showed the same relationships in time between various lipid fractions in both the irradiated and the control animals. These data indicate that 500 R produces no major effect on myelination over time.

The dose analysis was completed on the following four lipid classes: (1) Lysolecithin, sphyngomyelin, sulfatides; (2) lecithin; (3) cholesterol; and (4) phosphatidyl ethanolamine, cerebrosides.

The lipid fractions in two portions of the brain, the cerebrum and the pons, were analyzed separately. As indicated in Table 12 an exposure of 500 R to the head produces various responses in lipid formation in the beagle. The formation of class (1) in the cerebrum was enhanced by irradiation, but in the pons it was retarded. Irradiation enhanced the formation of lecithin in the cerebrum, but produced no significant change in the pons. The levels of cholesterol were not changed by irradiation in either the cerebrum or the pons. The formation of class (4) lipids was unaffected by irradiation in the cerebrum, but was enhanced by the treatment in the pons.

TABLE 12. SIGNIFICANCE OF LIPID FORMATION IN IRRADIATED AND UNIRRADIATED DOG BRAIN

Lipid Class	Treatment	Mean	95% Confidence Limit		Significance Level
			Lower	Upper	
		Cerebrum			
Lysolecithin Sphyngomyelin Sulfatides	Control	0.1801	0.1746	0.1856	0.01
	Irradiated	0.1963	0.1919	0.2007	
Lecithin	Control	0.1793	0.1727	0.1859	0.01
	Irradiated	0.1912	0.1859	0.1965	
Cholesterol	Control	0.2378	0.2287	0.2469	not significant
	Irradiated	0.2313	0.2241	0.2385	
	Overall	0.2338	0.2282	0.2394	
Phosphatidyl ethanolamine Cerebrosides	Control	0.3046	0.2956	0.3136	not significant
	Irradiated	0.2995	0.2924	0.3066	
	Overall	0.3015	0.2959	0.3071	
		Pons			
Lysolecithin Sphyngomyelin Sulfatides	Control	0.2322	0.2252	0.2392	0.01
	Irradiated	0.2138	0.2048	0.2228	
Lecithin	Control	0.1516	0.1481	0.1551	not significant
	Irradiated	0.1509	0.1482	0.1536	
	Overall	0.1512	0.1491	0.1533	
Cholesterol	Control	0.2128	0.2043	0.2213	not significant
	Irradiated	0.2236	0.2170	0.2302	
	Overall	0.2196	0.2144	0.2248	
Phosphatidyl ethanolamine Cerebrosides	Control	0.3250	0.3166	0.3334	0.05
	Irradiated	0.3425	0.3316	0.3534	

RADIATION ONCOLOGY AND PATHOLOGY LABORATORY
Dr. Norman C. Telles, Chief

The primary research of the Radiation Oncology and Pathology Laboratory has focused on the pathogenetic mechanisms involved in radiation-induced tumors. The approaches continue to be largely morphological and biochemical, with great emphasis being given to studies of host-virus relationships, the importance of the immune response to carcinogenesis, and the effect of co-insultive agents on radiation induction of tumors. Recently nonionizing radiation effects have been included as part of the Radiation Oncology and Pathology Program, but these efforts are still too preliminary to be reported at this time. Several studies that have been completed in sufficient detail are reported further on in this section.

The study on radiation enhancement of SV40 transformation in 3T3 and human cells is particularly significant because it opens a new approach to assessing radiation effects on cells and tissues which should be of interest to radiobiologists, virologists, radiotherapists, and those concerned with the epidemiological and clinical aspects of radiation-induced disease.

Thus, an effort to obtain lung tissue from former uranium miners, and others exposed to ionizing radiation has already been started in this laboratory. Using the approach outlined in the report by Pollock and Todaro (Nature 219:520-521, 1968) we plan to explore the possibility that cells derived from cultures of these tissues may be more readily transformed by virus than non-exposed cells derived from similar tissues.

A. THYROID AGE SENSITIVITY STUDY IN YOUNG RATS
J. R. Childress, W. Lee, T. R. Horton

As a result of a nuclear test in the Pacific in 1954, 19 children on the island of Rongelap under 10 years of age were exposed to about 170 roentgens of external γ rays and an estimated 700 to 1,400 rads from ingested radioactive iodine. In this young Rongelap Island group an incidence of 78% thyroid nodularity developed within 12 years after exposure. The incidence of abnormalities in older age groups was only slightly higher than that in nonradiated individuals.[1] Epidemiologic investigation indicates a risk on the order of one case of thyroid abnormality per million children per rad per year for thyroid doses over 100 rads.[2] Hempelmann estimates an incidence of palpable thyroid nodularity for nonradiated control populations of 0.36 to 1.7%.[3] It appears that in a given irradiated population, children develop more thyroid tumors than other members of the group.

---

[1] Conrad et al. 1966. New Engl. J. Med. 274:1392.

Considerable investigation has been given to the effect of radiation on the rat thyroid. Lindsay, et al reported a 54% incidence of thyroid adenomas and a 31% incidence of alveolar carcinomas in Long-Evans rats two years after treatment with 1,000 R to the thyroid gland.[4] However, the incidence of thyroid adenomas and alveolar carcinomas was based on only 24.4% of the original experimental group of animals. Doniach found no gross difference in sensitivity between weanling and adult rats as measured by a thyroid weight response to a goitrogenic challenge four months after injecting a 0.5 - 5.75 μCi range of ^{131}I. Doniach has indicated that radiation acts to initiate, and cellular proliferation acts to promote, carcinogenesis of the thyroid in rats.[5]

The present thyroid age sensitivity study allows animals of different age groups to experience a common post-exposure risk period over which tumors might develop. Particular attention has been given to preventing death of the animals in the age sensitivity study for more accurate statistical evaluation of thyroid tumor incidence.

Briefly, 960 female, random-bred, Long-Evans rats were placed on the study. The anesthetized animals were given a highly localized dose of 1,000 rads of X radiation (250 kVcp, 15 mA) to the thyroid (see page Radiation scatter was minimized with specially designed brass and lead collimators (Figure 23). The brass reduced the primary beam to 1/30 of the original 1,000 rads; the lead reduced the beam by another 1/16 for an approximate 2-rad whole-body dose to the rat. Doses were determined with plastic-coated lithium fluoride rods imbedded in various sizes of rat cadavers (see page

The thyroids were located by palpating the cricoid cartilage. Anesthetized rats were positioned on a wooden board and the center of the irradiation field was marked with a small piece of white paper tape (Figure 24). A thin paper pointer fastened to the center of the collimator hole was used to position the thyroid under the center of the irradiating beam and to mark the predetermined source-to-thyroid distance.

After the Long-Evans rats had been on the study about eight months, 82 animals had died. Pneumonia was responsible for 72% of all deaths. Other causes of death included pleuritis (10%) and malocclusion, leukemia, encephalitis, and urolithiosis (7%). Because of postmortem

---

[2] Conti et al. 1960. Radiology 74:386.
[3] Hempelmann. 1968. Science 160:159.
[4] Lindsay et al. 1961. Cancer Res. 21:9.
[5] Doniach. 1957. Brit. J. Cancer 11:253.

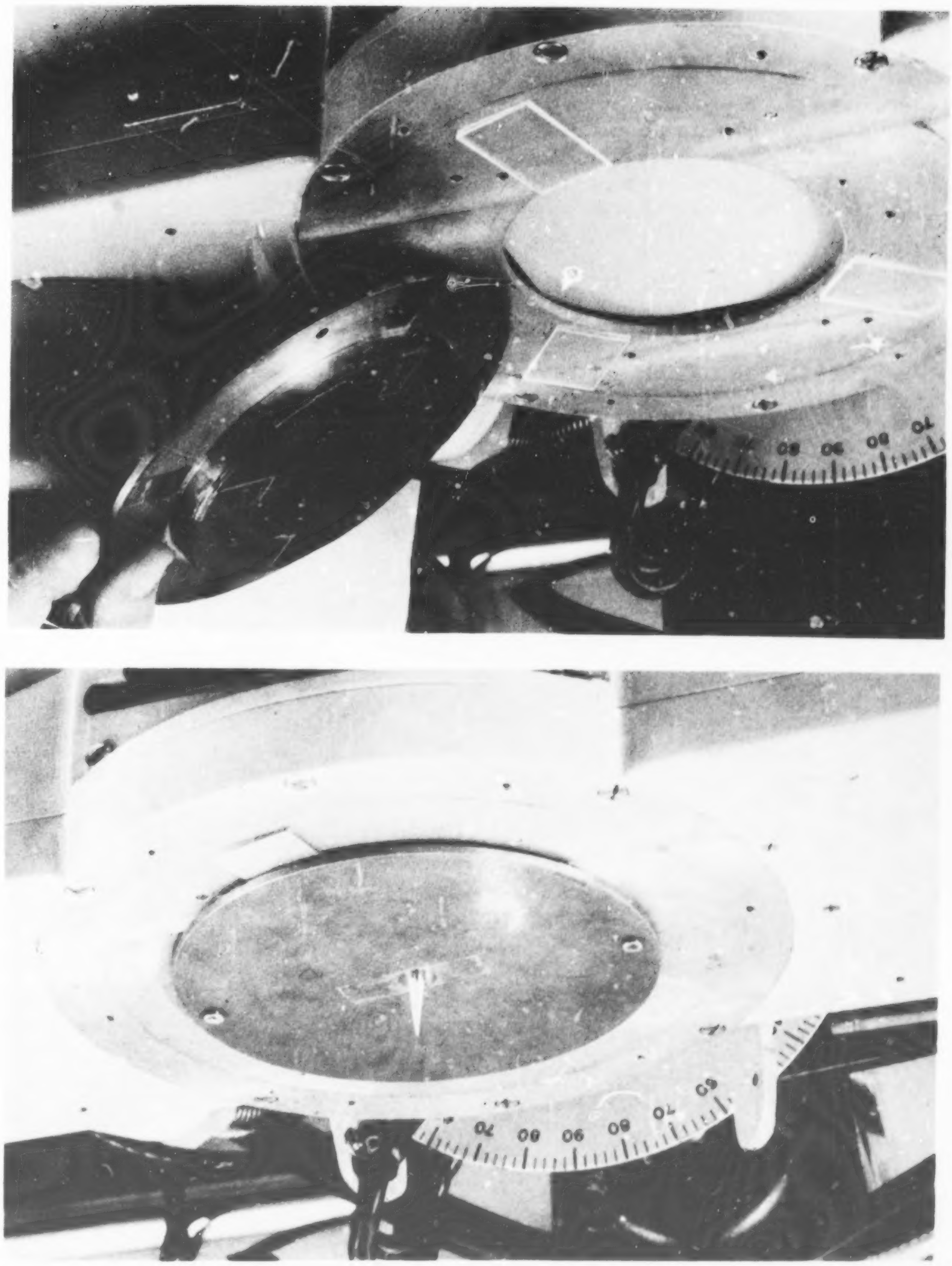

Figure 23. Brass and Lead Collimators Used in Narrow-Beam Irradiation of Rat Thyroid Glands. Bottom photo shows collimator in place with paper pointer used to align X-ray beam and thyroid.

autolysis, cause of death could not be established in 11% of the rats. No microscopic or gross thyroid irregularities have been found thus far. Table 13 shows percent deaths at each age. Owing to the high rate of mortality due to respiratory disease, tetracycline has now been added to the drinking water of the rats. This has reduced considerably the rate of death due to preliminary disease.

TABLE 13. DEATHS OF RATS IRRADIATED AT VARIOUS AGES

Age Group[a]	Deaths in Group (percent) Irradiated	Control
6 months	12.5	11.7
3 months	13.3	5.8
1 month	10.0	5.8
10 days	7.5	1.7

a. There were 240 animals in each age group, 120 per treatment.

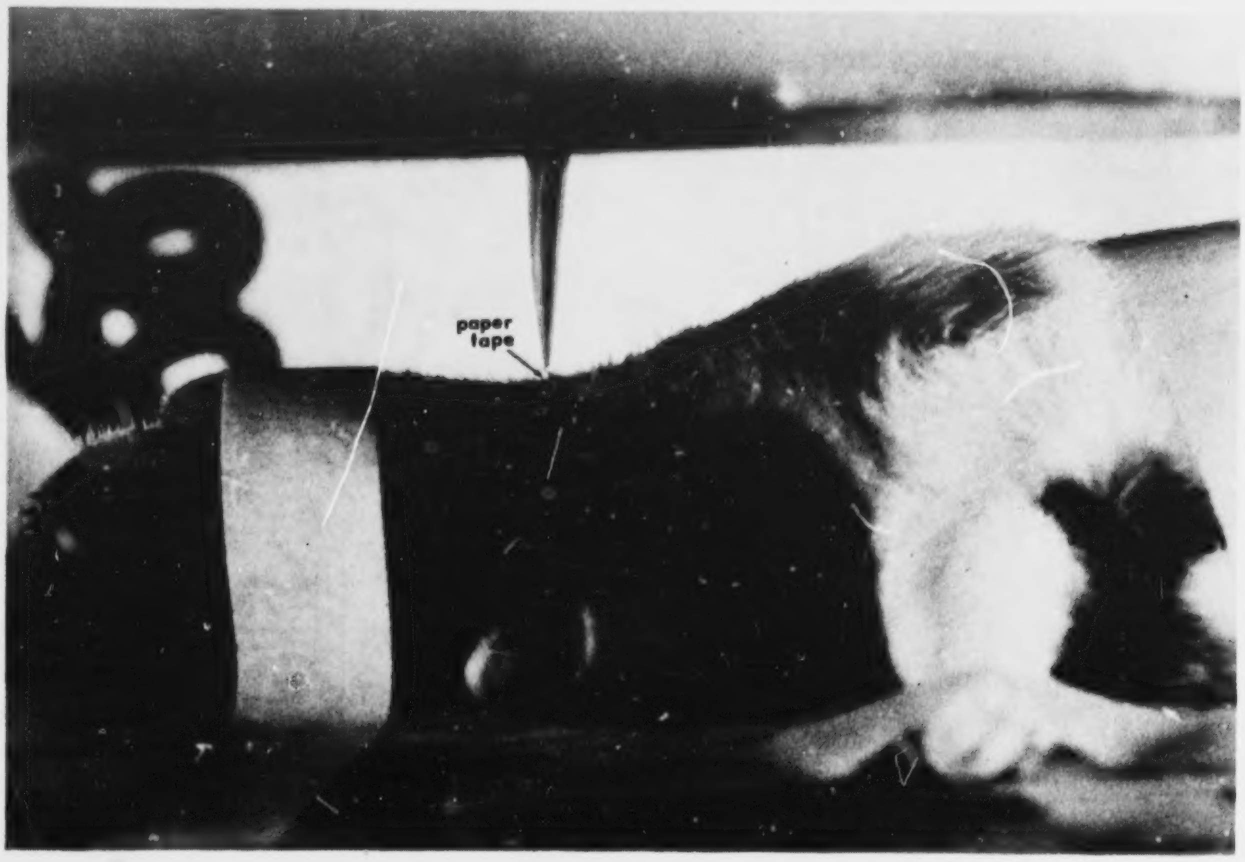

Figure 24. Position of Anesthetized Rat During Thyroid Irradiation.

B. SPONTANEOUS LESIONS IN A COLONY OF CHINESE HAMSTERS

B. C. Ward

In a study designed to determine the tumorigenic effects of ^{131}I on the thyroid gland in Chinese hamsters, a high incidence of hepatomas, uterine adenocarcinomas, and cerebrovascular lesions were found (Table 14). No statistical relationship between these lesions and treatment with ^{131}I could be shown.

Cerebral hemorrhage was observed in 20 percent of the hamsters in the study. The hemorrhage was found, in every case, to be associated with inflammation and necrosis of the anterior cerebral artery (Figure 25).

More than 25 percent of the animals developed liver tumors which upon histologic examination were found to be benign hepatocellular tumors (Figure 26). The tumors sometimes were as large as 1.5 cm.

Uterine tumors were found in 30 of the 120 females examined. The tumors were usually found in the cervical area of the uterus and may have originated there; however, due to the large size of the tumors it was difficult to ascertain the point of origin. Histologic examination showed the tumors to be adenocarcinomas (Figure 27).

None of these lesions have previously been reported in other colonies of Chinese hamsters. Further work will be done to investigate the hamsters in the Bureau of Radiological Health colony.

TABLE 14. INCIDENCE OF LESIONS IN RELATION TO DOSE OF ^{131}I

Treatment μCi ^{131}I	No. of Animals Male	Female	Brain Lesions	Liver Tumors	Uterine Tumors
0.1	26	23	12	14	8
0.05	25	28	11	12	5
0.01	27	24	11	11	5
0.001	24	26	10	11	6
0	31	19	7	18	6
Total	133	120	51	66	30

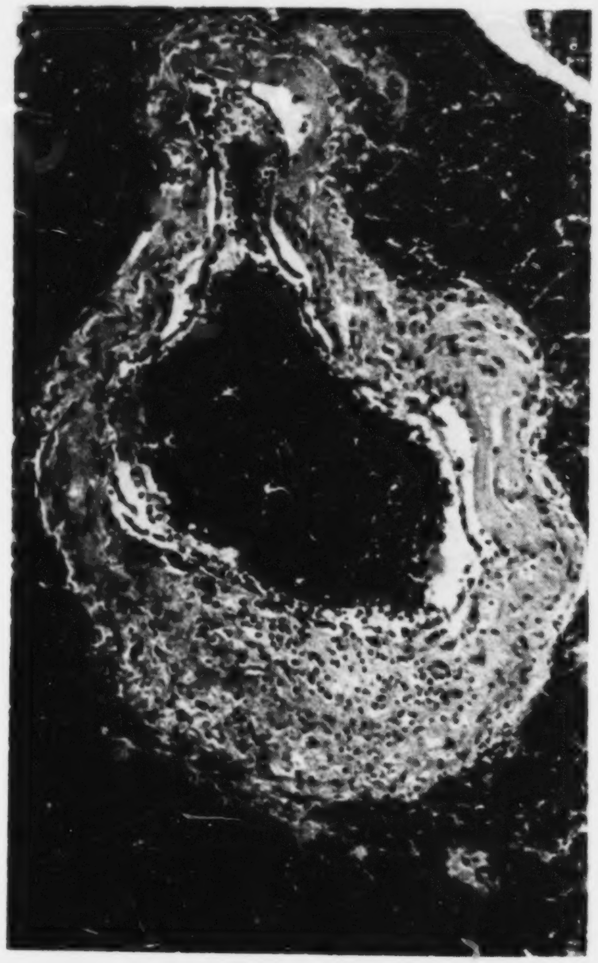

Figure 25. Microscopic View of Anterior Cerebral Artery in the Brain of a Hamster with Acute Massive Cerebral Hemorrhage. Inflammatory cells are present within the wall of the vessel. Hematoxylin and eosin. 125X.

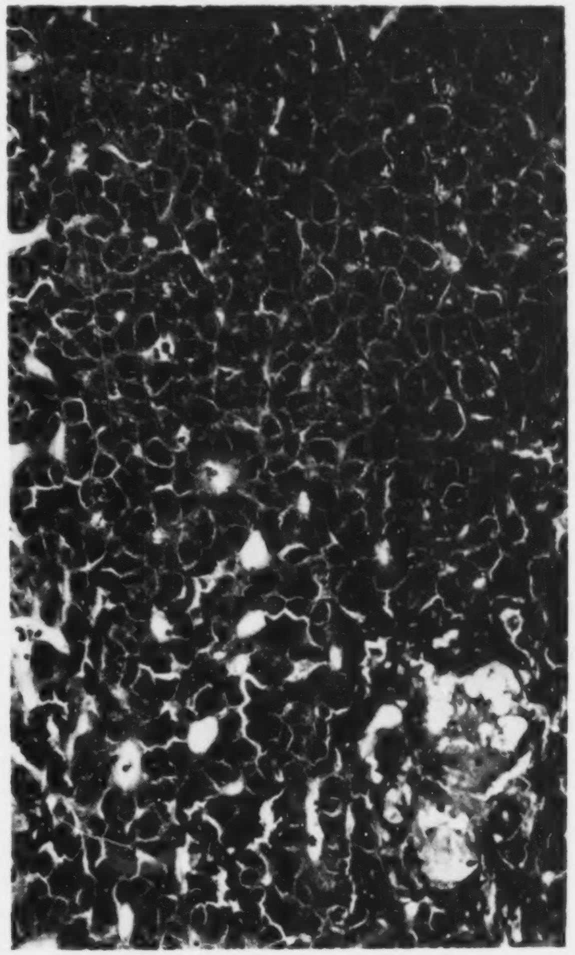

Figure 26. Liver. The liver tumors are composed of large hepatocytes growing in a disorganized manner. Hematoxylin and eosin. 40X.

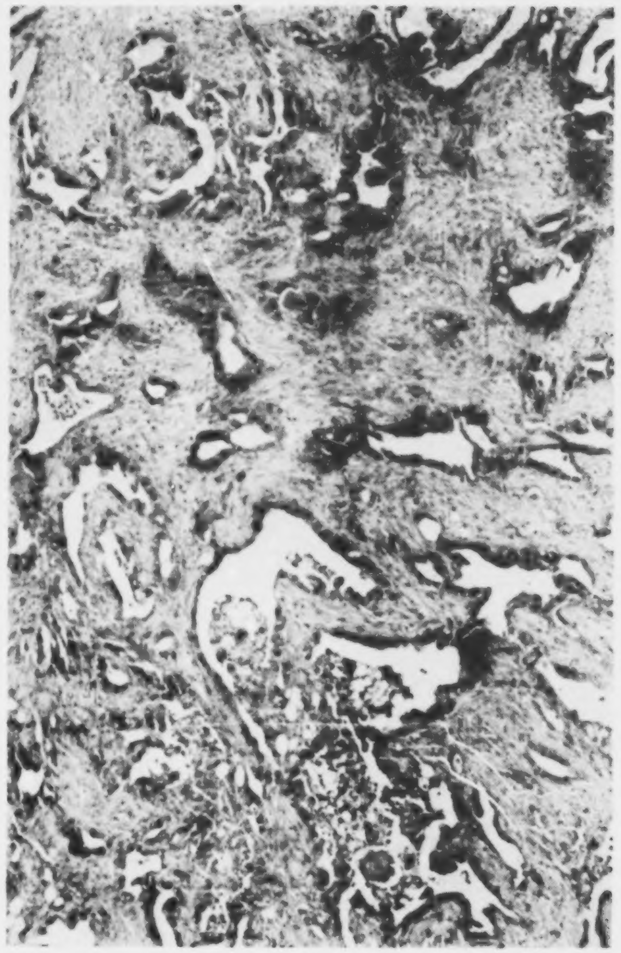

Figure 27. Uterus. Neoplastic glandular tissue amid abundant fibrous stroma characterized the uterine tumors.

C. STUDIES OF RADIATION - VIRUS INTERACTIONS

E. J. Pollock

Ionizing radiation produces both somatic and genetic effects. Carcinogenesis is one of the most perplexing and significant somatic effects. However, if cancer is regarded to be the result of a genetic change induced by radiation, then it can also be thought of as a non-heritable genetic effect. Our work has focused on the examination of genetic factors which could be altered by radiation and thereby lead to carcinogenic changes in cells or tissues.

We have considered the DNA strand-breaking effects of radiation. If cancer-inducing viruses are present in a cell when broken DNA strands are present or are being repaired, there is an increased probability that these cells will incorporate the viral DNA and presumably result in a transformed cell. This effect has recently been supported by studies in this laboratory in which irradiated cultured cells (3T3) were exposed to a transforming virus (SV40).

In another investigation, we have devised a method for studying both early and late viral functions in the same cell strain. Although it is well known that radiation can differentially inactivate various virus functions, transformation frequencies and infectivity have not been studied in the same cell strain. Studies are currently in progress to examine the inactivation of several tumor virus functions using the method.

There have been conflicting reports concerning the transformation of cultured cells by radiation. We have attempted to resolve some of the conflict areas in our own work. A line of contact-inhibited mouse fibroblast cells was developed from inbred BalbC mice. These cells were irradiated with 1,500 rads, and the surviving cells were subcultured. Colonies that did not appear to be contact inhibited were subcultured and grown in large numbers. Irradiated weanling BalbC mice were then inoculated with these cells. Four months have elapsed since the inoculation and no tumors have yet developed. No tumors have developed in control animals inoculated with the same but unirradiated cells. These animals are still under observation.

1. Radiation Enhancement of SV40 Transformation in 3T3 and Human Cells[6]

Radiation and viruses are implicated in carcinogenesis in man and animals. It has been shown that in C57Bl mice a virus present in the animal's tissues is the causative agent and has been implied that radiation increases an animal's susceptibility to tumor production by a virus. We have examined the direct effect of radiation on the susceptibility of individual cells to tumor viruses in tissue culture.

---

[6] The full article by Pollock and Todaro was published in Nature 219:520-521, 1968.

Human cells and mouse cells were grown in tissue culture. Cell monolayers were infected with an oncogenic virus, SV40, either prior to or after exposure to X rays. Radiation doses varied from 75 rads to 1,200 rads. The transformation frequencies of irradiated cultures were compared to those of unirradiated cultures. The relative increase in transformation frequency noted in the irradiated cultures was called the enhancement of transformation, which was found to be an exponential function of the radiation dose (Figure 28). Results were similar for mouse and for human cells.

This work contributes to the understanding of the mechanism of radiation carcinogenesis. Radiation increases the probability that an oncogenic virus will produce tumors in animals. Depression of immunological defenses plays a part in this process. The above experiments, however, show a direct effect of radiation on cellular susceptibility to transformation and suggest a second role of radiation in enhancing viral oncogenesis.

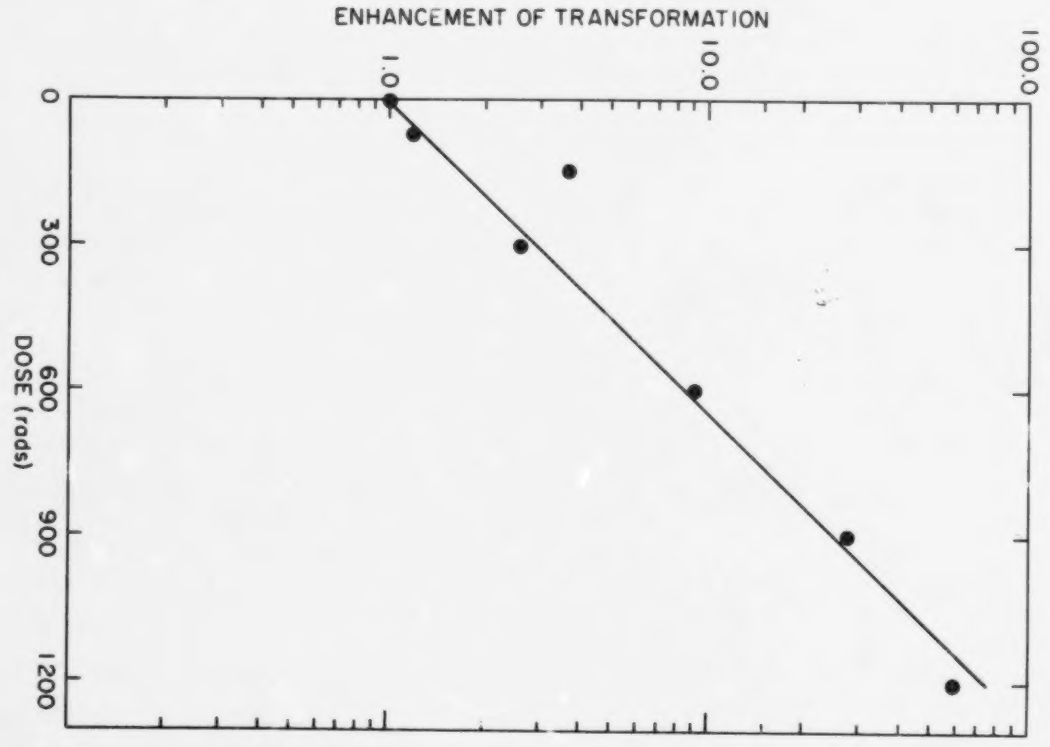

Figure 28. Data from Three Experiments Show the Enhancement of Cell Transformation after Irradiation and Infection with SV40.

2. Infectivity and Transformation Relationships of Ultraviolet-Irradiated SV40 Virus

Several genetic functions of tumor viruses are differentially inactivated by ultraviolet radiation. For example, transformation and oncogenecity are inactivated less rapidly by ionizing radiation than is infecting capacity. In these experiments, however, the transformation frequency in one cell strain was compared to the infectivity in a different cell strain, and different multiplicities of infection were used to determine each of the viral functions.

We have used several strains of cultured human cells and have devised methods where, in the same cell and at the same multiplicity, we can compare T-antigen inducing capacity, V-antigen inducing capacity, infectivity, and transformation. Irradiation with ultraviolet light differentially inactivates these functions. The rate of inactivation of V-antigen induction is 30 percent less than the rate of inactivation of infectivity.

The slopes of the inactivation curves for V-antigen are 5- to 6-fold greater than those for transformation. The curve for inactivation of T-antigen inducing capacity falls along a line with a slope midway between that for transformation and V-antigen induction.

The conclusions of previous studies of the differential inactivation of various genetic functions of tumor viruses have had to be interpreted in the light of comparing early and late functions in different cell strains and at different multiplicities of infection. Since the synthesis of coat protein is a late viral function, it is reasonable that this should be related to and necessary for the production of complete infectious virus, another late function. This has permitted us to compare early and late functions in the same cell line using the same multiplicity of infection.

Since ultraviolet radiation is used in sterilization procedures and in vaccine preparation, this work becomes significant because in a heavily irradiated virus a significant oncogenic potential may exist while infectivity may be undetectable. If infectivity is used to identify the virus, then its presence may go undetected.

D. RADIATION-ETHIONINE ULTRASTRUCTURE STUDIES - A SERIAL SECTION EVALUATION

N. C. Telles, D. W. Coble

We have previously reported some electron microscopic observations of a number of hepatomas developing in female Osborne-Mendel rats treated with radiation and ethionine. We concluded that a large number of the nuclei in the hepatomas contained cytoplasmic inclusion bodies and surmised that these were true inclusion bodies and not sectioning artifacts. We have modified this view based on the serial-sectioning work reported below.

The structure and configuration of intranuclear cytoplasmic inclusions occurring in rat hepatomas produced by X radiation and/or ethionine has now been studied by means of consecutive serial sections (Figure 29). Such intranuclear inclusion bodies have been described previously[7-11] but it has not always been clear whether the inclusions are true inclusions or simply psuedo-inclusions; i.e., simple invaginations of the nuclear membranes. Also, the manner of formation of such structures has not been determined.

Studies of serially sectioned hepatoma nuclei have shown that the greater proportion of intranuclear cytoplasmic inclusions are due to the invagination of the nuclear membranes, with continuity maintained between the cytoplasm and the invaginated cytoplasmic material (Figure 30). Rarely, an apparent break or discontinuity in the wall of the invaginated inclusion has been observed (Figure 31) leading to an admixture of cytoplasmic contents and nucleoplasmic material such as is illustrated in Figure 32.

Careful evaluation of serial sections of many nuclei containing these invaginations has revealed that the invaginatory pores tend to be fairly uniform in size. Furthermore, a single invagination may also give rise to one or more "satellite" invaginations (Figure 29). The nuclear membranes do not appear to be stretched or torn by the invagination. Also, the dimensions of the nuclear pores appear unaltered during the process of invagination.

Mechanical distortion of the nuclear membranes has been suggested as a possible mechanism of formation for intranuclear invaginations.[11] The uniformity of size of the invaginatory pores as well as their channel-like structure would seem to argue against this means of formation. Furthermore, extrinsic pressure on the nuclear wall would seem unlikely to give rise to satellite invaginations, even if intrinsic "weak" spots were to exist in the nuclear membranes. Traction forces appear equally

---

[7] Kleinfeld et al. 1956. J. Biophys. Biochem. Cytol. 2:435-439. Sup. 4.

[8] Leduc and Wilson. 1959. J. Biophys. Biochem. Cytol. 6:427-439.

[9] Brandes et al. 1965. Science 149:1373-1374.

[10] Mori and Onoe. 1967. J. Electronmicroscopy (Tokyo) 16:137-142.

[11] David, H. 1964. Submicroscopic Ortho- and Patho-Morphology of the Liver (Text Volume), Pergamon Press, Oxford, England. p. 234.

unlikely as an explanation for such invaginations.

We suggest that nuclear invaginations may result from a regional or localized increase in the total nuclear membranes. The enlarging membranes bulge in toward the nucleoplasm following a path of least resistance. Ultimately the invaginated wall may tear or open, discharging cytoplasmic contents into the nucleus.

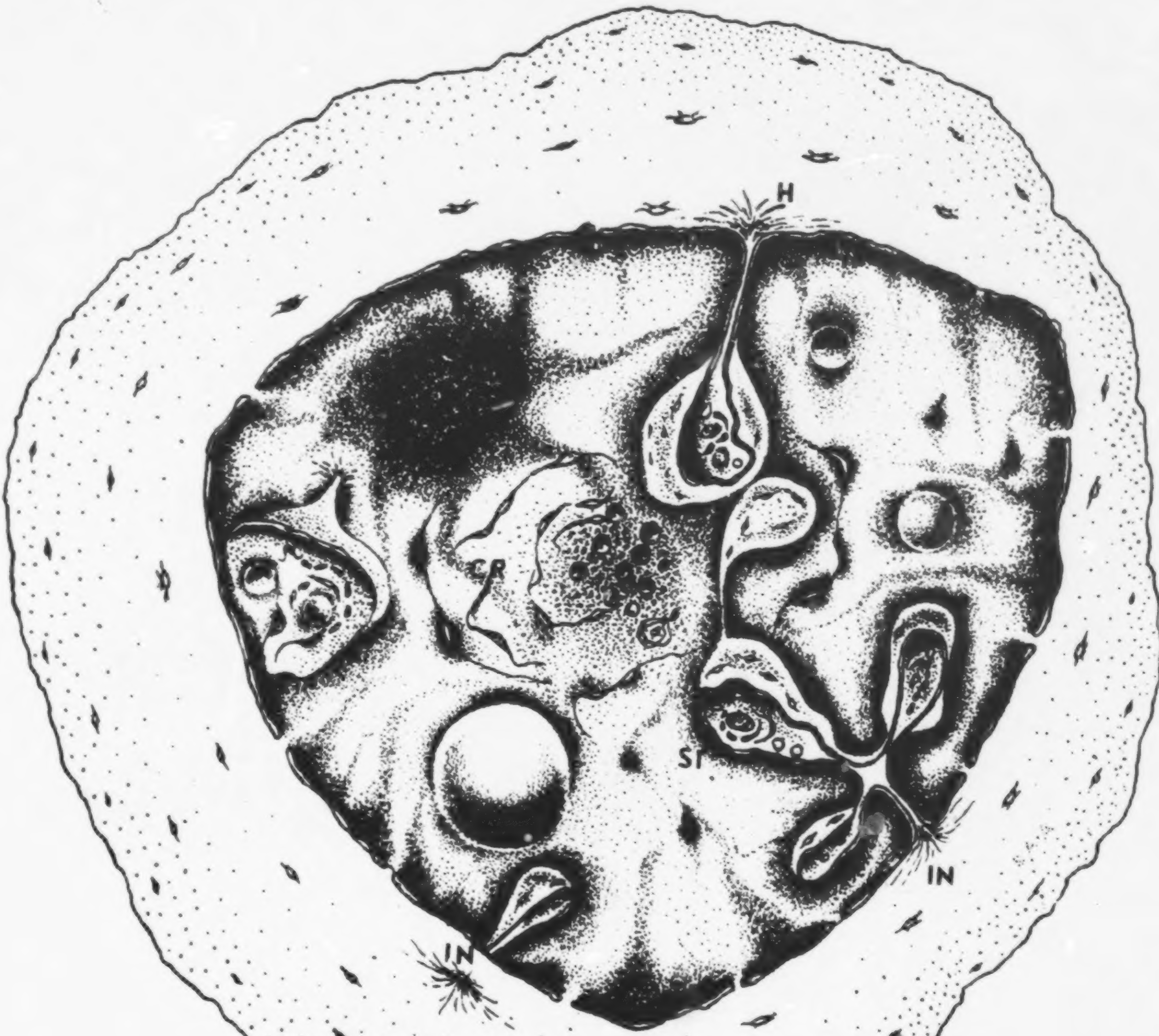

Figure 29. Artistic Representation of the Structure of Nuclear Cytoplasmic Invaginations. Note that the nuclear membranes have invaginated at several points (IN) and "satellite" invaginations (SI) are also present. Cytoplasmic remnants (CR) from a degraded cytoplasmic inclusion are present in the nucleoplasm. Regional increases in the nuclear membranes are represented by the stress lines in the nuclear surface (H).

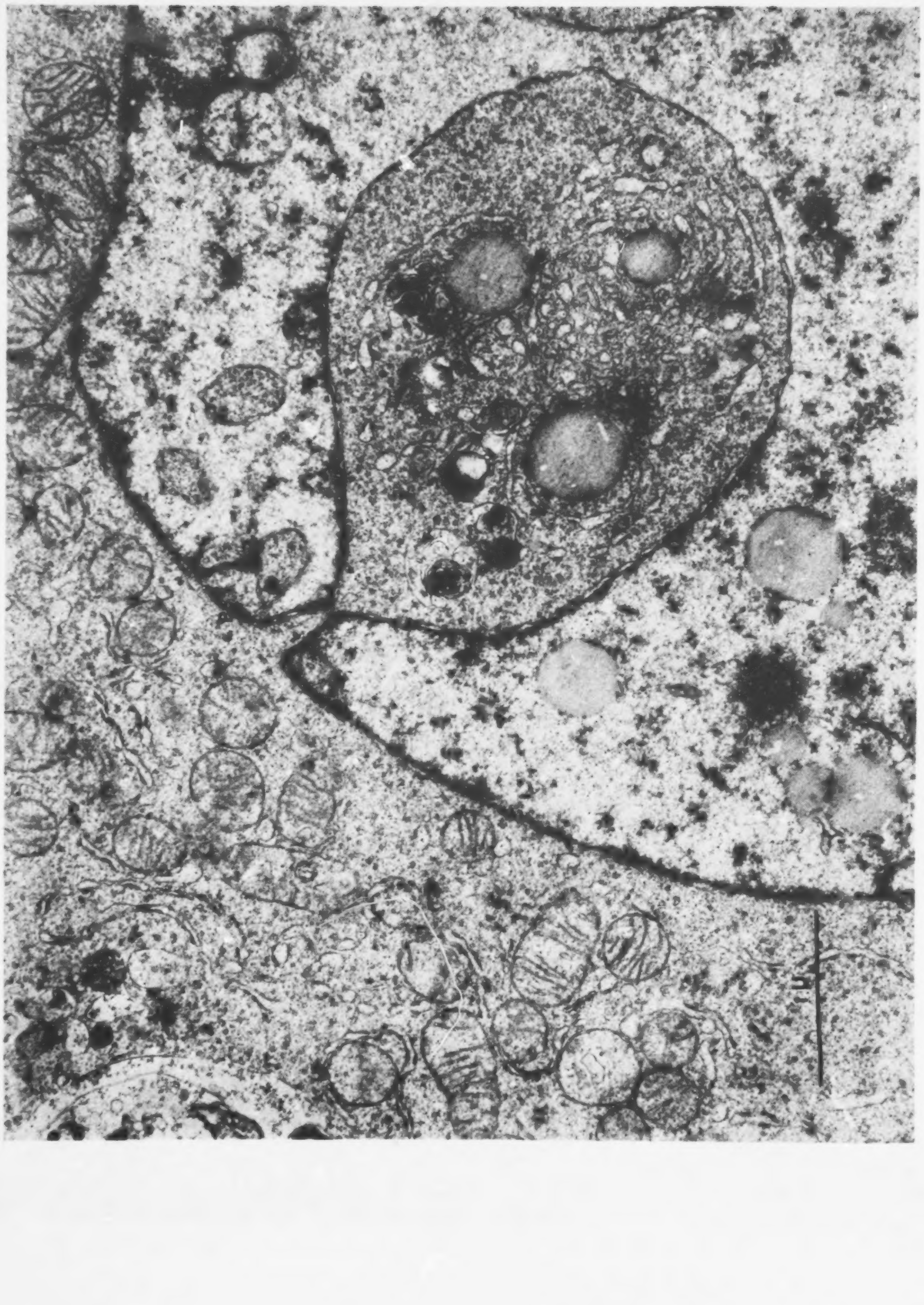

Figure 30. Invagination of Nuclear Membrane Showing Channel-Like Pore (P) which Provides Continuity Between the Cytoplasm and the Invaginated Material.

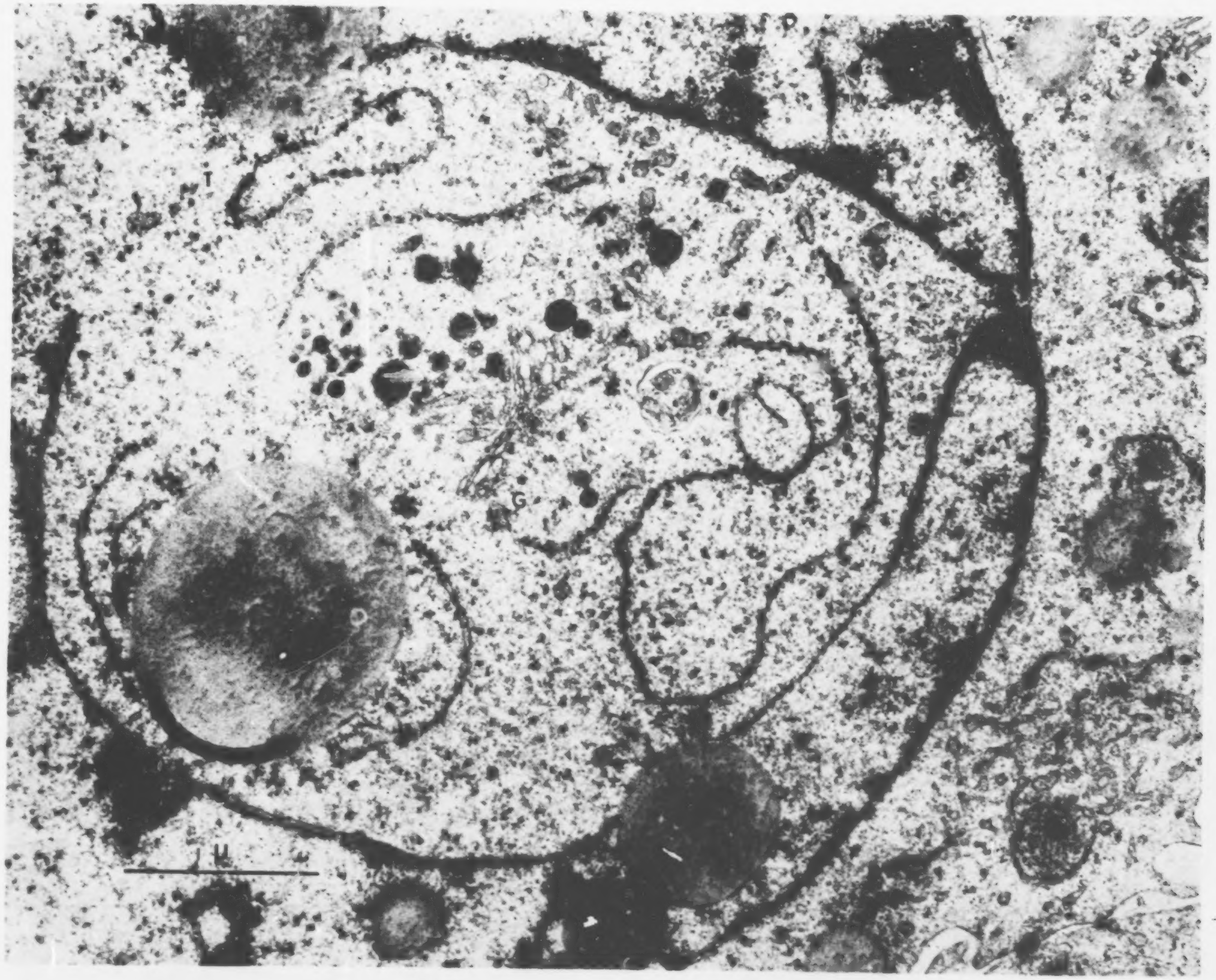

Figure 31. Apparent Opening or Break (T) in the Wall of the Invaginated Nuclear Membrane. Admixture of cytoplasmic and nuclear contents presumably occurs at this point. Note the Golgi apparatus (G) within the inclusion.

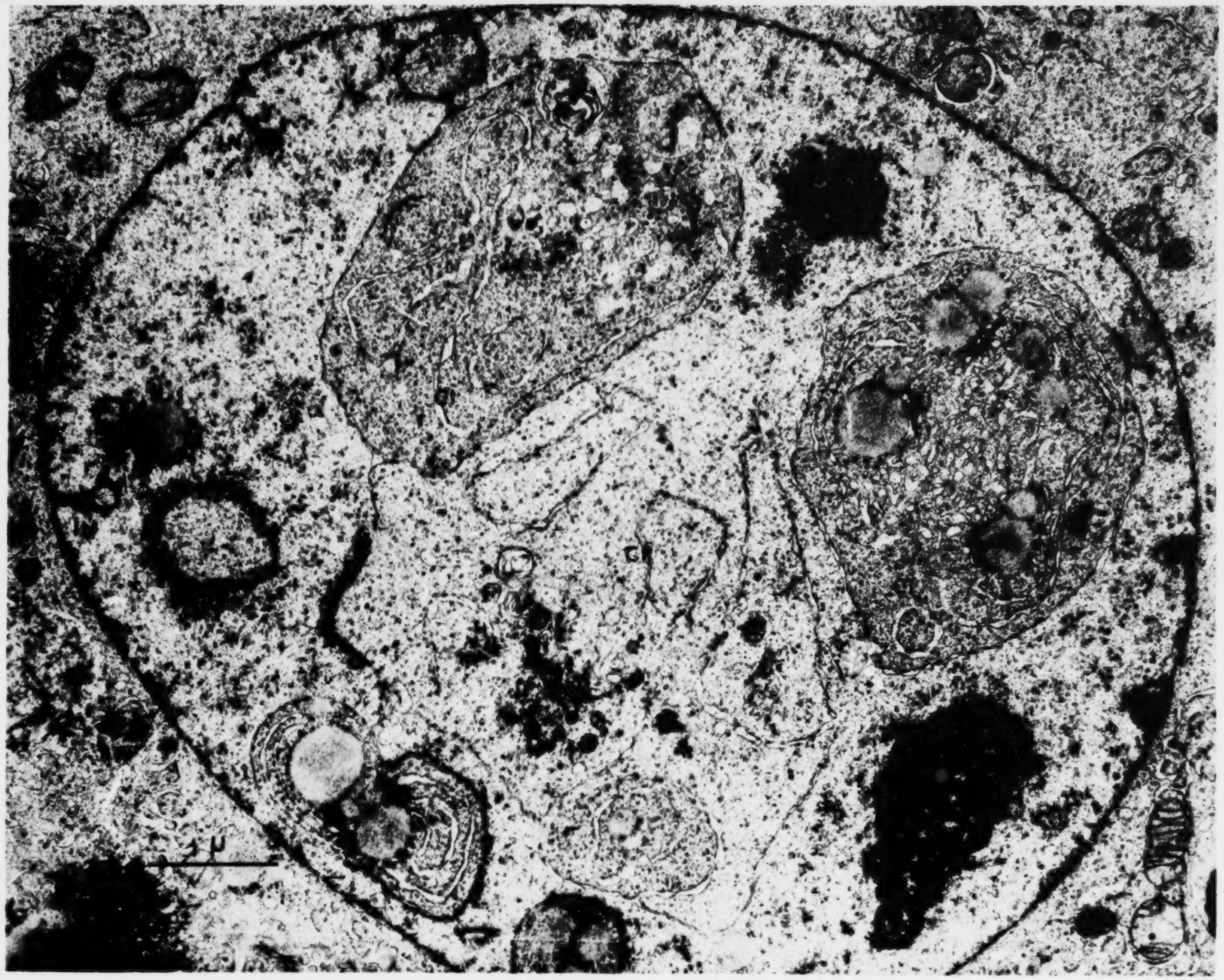

Figure 32. Hepatoma Nucleus Showing Nuclear Cytoplasmic Inclusions (CI) as Well as Cytoplasmic Remnants (CR). Invagination of the nuclear membrane is indicated at IN.

RADIONUCLIDE TOXICOLOGY LABORATORY
Dr. Jerry F. Stara, Chief

During 1968 the Radionuclide Toxicology Laboratory studied primarily the toxicity or other biological effects of specific hazardous radionuclides. The core project "The Effects of Strontium-89 on the Hematopoietic System of the Cat -- With Special Consideration to Leukemogenesis and Age Sensitivity," was given special emphasis. Its research objectives are to:

a) Determine and identify the time (or tissue) that may be uniquely sensitive to radiation-induced lymphoproliferative or myeloproliferative disorders associated with ^{89}Sr ingestion during development and growth of the cat;
b) Assess the radiation dose (rads) delivered to the bone marrow and other organs in several age groups of Felis domestica that have received dietary ^{89}Sr, and the relationship between the effective doses in cats and ^{90}Sr doses incriminated as leukemogenic in dogs and miniature swine;
c) Systematically investigate all leukemia cases for the presence of a viral agent, and study the transmissibility of such an agent in cats and possibly other mammalian species.

These efforts included several prerequisite and ancillary studies to obtain physiological, embryological, and radiological parameters for the core project, as well as initial experiments with cats subjected to high chronic dietary doses of ^{89}Sr.

A major change in the structure and planning of the Radionuclide Toxicology Laboratory was reflected in a decision to relocate the laboratory from Cincinnati, Ohio, to the Washington, D. C. area. The preparations for the transfer of the laboratory required much effort during the year to arrange suitable housing for the cat colony, and to provide for the transfer of the laboratory and its personnel with the least amount of interruption of the ongoing scientific endeavor.

Aside from the ^{89}Sr long-term project, the laboratory staff continued their investigations concerned with: (1) Evaluation of radiopharmaceuticals - specifically ^{131}I-tetracycline - as a promising aid in diagnosis of tumors, and sodium alginate as an agent for reducing strontium uptake and retention under chronic intake conditions; and (2) metabolism of heavy radionuclides, especially translocation studies following ingestion of chemical forms of ^{210}Po and ^{210}Pb found in the diets of guinea pigs and cats, in order to develop models related to ^{210}Po and ^{210}Pb exposure of selected populations, such as uranium miners or Alaskan Eskimos, from natural sources.

A. STATUS AND PRODUCTION OF THE CAT COLONY

J. F. Stara, N. S. Nelson, E. Berman, M. J. Replogle

The feline colony maintained by the Radionuclide Toxicology Laboratory consists of 235 male and female cats, a number lower than in normal times. The size of the colony was reduced to facilitate the transfer from the present location in Cincinnati to a location near the Rockville, Maryland, laboratory. A number of animals which had a poor reproductive record or unsatisfactory genetic traits were culled and used for short-term studies to provide required prerequisite or ancillary data for the long-term strontium-induced leukemia study.

Only 34 animals are presently on experimental status; the remainder are breeding animals. About 200 animals will be transferred. As a part of the preparation for transfer and initiation of a large cat colony, genetic and clinical histories for individual animals are being compiled to characterize the individual animals. Animals designated for transfer have been subjected to an extensive hematological examination; serum samples have been examined for specific diseases such as toxoplasmosis, with two positive cases yet unconfirmed.

The health of the colony during the past year was good. The 5% mortality rate was limited to young animals with few exceptions. During an extended period of cold damp weather, three cats developed pneumonia, which was caused by an erythromycin sensitive staphylococcus. The good health of the colony was primarily due to strenuous sanitary practices, effective prophylaxis, and personal dedication and careful handling.

The numbers of kittens produced, kittens per litter, and litters produced have been recorded for the past six years. During 1965-1968, 238 breedings were observed. Of these, 178 fertile breedings carried to term giving a 74.0 ± 5.5% conception rate in the colony for the four years.

Table 15 summarizes the production record of the colony. The data show that the greatest number of pregnancies produced four kittens (23.2% of the pregnancies). Except for litters of two kittens, the number of litters of various sizes born each year varied considerably. Most litters were biased in favor of males, but the sex was equally divided in the litters having one and six kittens. Overall, the colony produced 55% males and 45% females.

A large sample of the kittens (60%) were weighed at birth, either immediately after birth or within 8 hours of the time of birth. The mean weight distribution shows that individuals in litters of 1 to 4 kittens weigh approximately 100 grams. For litters of five kittens or more, the mean weight decreases somewhat as the litter size increases.

The weights at birth have not been adjusted for the length of gestation period. Since the duration of pregnancies in this colony varied between 62 and 68 days, with an average of approximately 65 days, it is possible that the rather large observed spread of weights reflects more the length of gestation period than the expected size of neonates. However, a sufficient number of litters of different gestation times were not available to demonstrate litter size vs. duration of pregnancy.

TABLE 15. KITTEN PRODUCTION DURING 1963-1968

Kittens/ Litter	No. of Litters	No. of Kittens Born			Birth Weight,[a] Grams	
		Male	Female	Total	Mean	Range
1	30	15	15	30	99.0	69.4-128.6
2	38	43	33	76	98.7	66.1-131.3
3	62	108	78	186	98.9	59.1-138.0
4	68	138	134	272	100.4	72.6-125.2
5	47	140	95	235	95.7	61.1-130.3
6	30	90	90	180	90.5	56.7-124.3
7	10	38	32	70	84.5	60.3-106.7
8[b]	-	-	-	-	-	-
9	1	4	5	9	85.6	75.8-95.4
Total	286	576	482	1058		

a. A sample of kittens from about 60% of the litters were weighed within 8 hours of birth.

b. No litters of eight kittens were born.

B. QUALITATIVE EVALUATION OF THE EMBRYONIC SKELETON IN CATS

E. Berman, J. F. Stara

In order to develop satisfactory estimates of skeletal dose in the embryo, accurate morphological data regarding time sequence of skeletal tissue formation throughout embryonic life is necessary. To study this problem, feline embryos are collected from normal pregnant dams by cesarotomy and treated with alizarin stain. This technique produces a fetal specimen whose soft tissues are almost completely transparent, while calcified tissues are stained red and purple, and are readily visible. The study was designed to determine the embryonic age at which bone tissue first appears in the fetus, the age at which calcium initially deposits in various areas of the body, and the relative rate at which each bone develops. This study will provide necessary information in investigations of bone-seeking radioisotope incorporation into feline embryos, as well as specific information in studies of mammalian development.

The embryos are collected at one-week intervals after confirmation of normal pregnancy, and from three weeks through nine weeks of life. Because of biological variation within a litter, at least three embryos each, from three different litters must be collected for each observation point. So far we have used 14 normal pregnant queens, considered as colony surplus, to produce the 26 embryos now in our collection. An additional eight embryonic litters must be collected at appropriate times to obtain a minimum set of samples.

Although this method of soft tissue clearing and bone staining is not completely quantitative as to the volume or the amount of calcified tissues, it allows gross measurement and morphological observation of the developing skeleton. After clearing and staining, the embryonic specimen is projected on a screen so that the embryos of various sizes are projected as equally sized images. Analysis of bone appearance and relative bone size is made from the tracings of these images. A special projector and tracing screen which will allow proper visualization of the entire embryo is being constructed. In small embryos, or for body areas which require greater magnification, camera lucida microscopic drawings will be made. Using a method of rotating the embryos along their mid-line axes, quantitative measurements of size and volume of selected bones can be made from the tracings.

C. PLACENTAL TRANSFER OF STRONTIUM AND CALCIUM IN THE FELIS DOMESTICA

N. W. Nelson, R. G. Wolfangel, J. F. Stara

The work involving placental transfer of strontium and calcium in the cat is part of a larger effort to elucidate the placental transfer of divalent cations in mammals. The results of this work also provide information that will be used in a study of radioactive strontium-induced leukemia in cats. Preliminary observations plotted in Figure 33 show weight and radioisotope content in embryos from two weeks of gestation to birth. The observed embryonic uptake curves were obtained from a group of embryos born of dams on ^{85}Sr chronic uptake regimen and a second group which received a mixed dose of ^{85}Sr and ^{45}Ca, intravenously 24 hours before removal of the embryos by cesarotomy. Predicted calculated values for chronic uptake using single dose data from another experiment were also plotted.

The ^{85}Sr chronic uptake curve shows values from 2 to 8 weeks of gestation, since embryos were not available from 8 weeks of gestation to birth. In animals given a single dose, the strontium curve roughly parallels the calculated curve. The calcium uptake was about 5 to 20 times greater during the first five weeks of gestation, but then leveled off more rapidly than the strontium values; at 8 weeks of gestation the calcium level is only about 50% higher than that of strontium. In addition, the strontium uptake in cronically dosed animals exhibited a much steeper slope than the curve for single-dosed animals, particularly during the last 9 days of pregnancy. Calculated values for chronic uptake were higher than the observed chronic uptake dose by a factor of two during the first 6 weeks of gestation, but were closely parallel during the last 2-1/2 weeks of pregnancy.

The data in Figure 34 indicate that for cats given a single dose, the strontium content of the placenta is proportional to its weight. The calcium content rises to a peak at about 5 weeks of gestation and then drops to a relatively constant level. The change in the radiocalcium uptake curves at 5 weeks of gestation (as demonstrated both in Figure 33 and Figure 34) suggests that there is either a change in the placental permeability or a total calcium pool at this time. Further investigation with particular reference to specific activity of maternal blood is necessary to evaluate these observations.

The curves for total strontium, calcium, and inorganic phosphorus (Pi) in the embryos are compared with weights in Figure 35. The phosphorus content seems to be directly related to embryonic weight; calcium and strontium content are more or less related to age (length of gestation). The high rate of deposition of the latter elements beginning at 5 weeks of gestation, indicates largely the increase of bone mineralization in the developing embryo. The data also point out that from 7 weeks of gestation to birth, the amount of phosphorus in the skeleton was between 60% and 75% of total body phosphorus; the skeletal strontium was between 70% and 85% of total body strontium; and the skeletal calcium was between 80% and 95% of total body calcium.

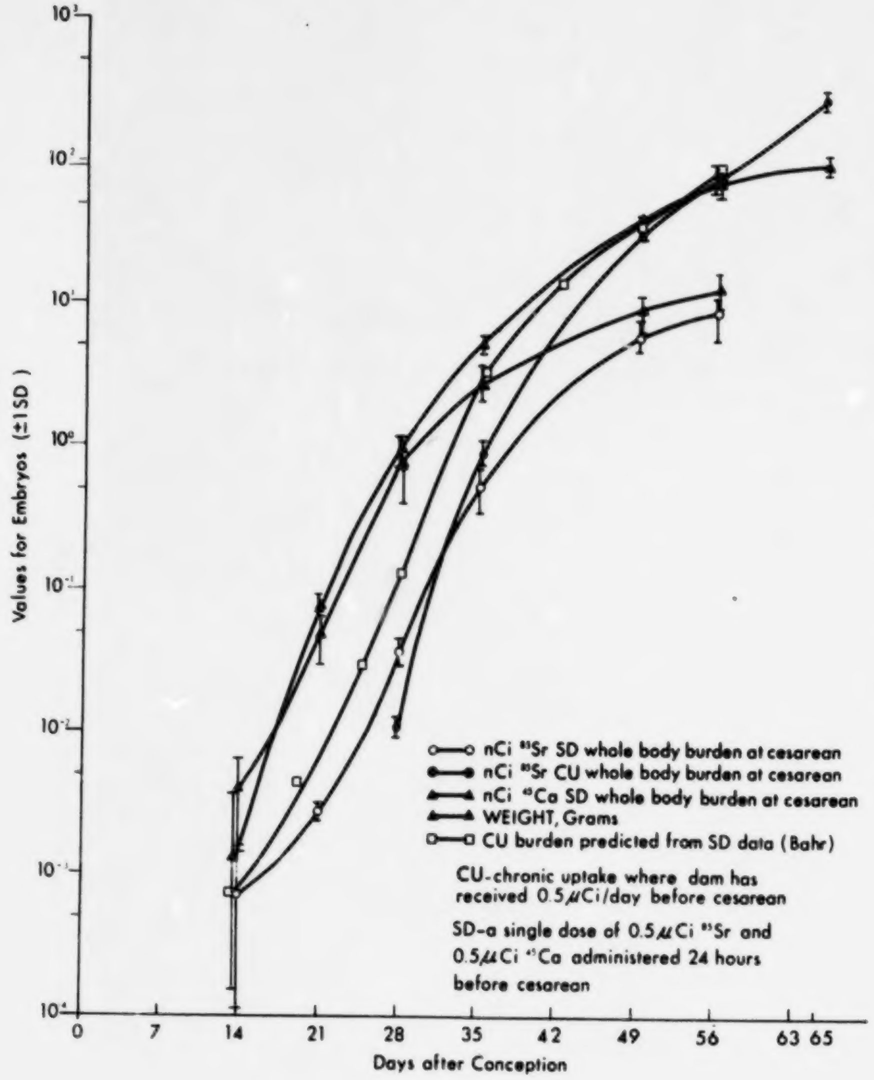

Figure 33. Weight and Radioisotope Content in Embryos.

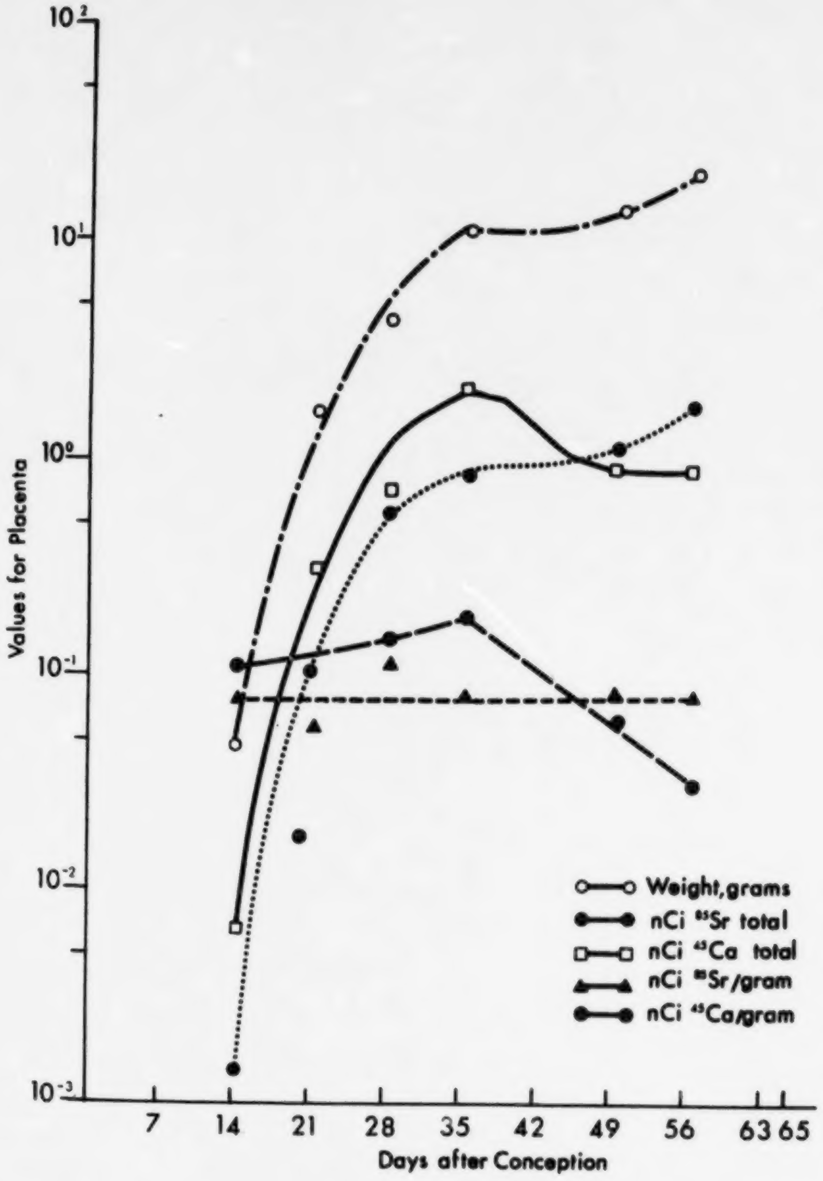

Figure 34. Weight and Radioisotope Content of Placenta.

These data and their interpretation are preliminary estimates, since they are based on single pregnancies at each observation point, even though two or more embryos were obtained from each pregnant dam. The minimum average values needed for each point are three pregnancies, representing nine embryos, before any statistically valid conclusions can be made.

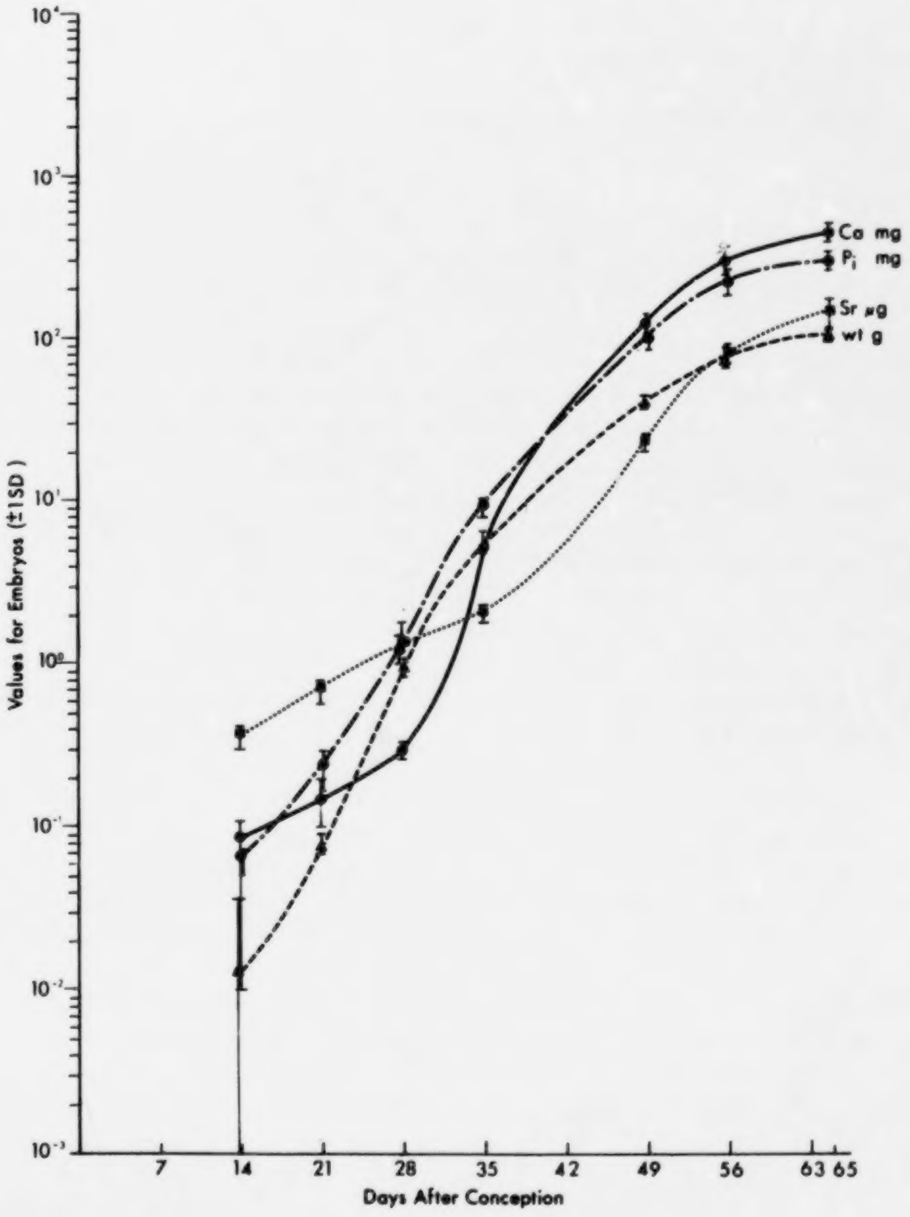

Figure 35. Radioisotope and Phosphorus Content and Weights of Embryos.

D. METABOLISM OF ^{85}Sr IN CATS

1. Methodology

J. F. Stara, R. G. Wolfangel

For the past four years, our laboratory has conducted an extensive investigation of ^{85}Sr metabolism in the cat. In order to "fill in the gap" which is present in much of the published literature regarding strontium metabolism, especially when acute single dose investigations are extrapolated to chronic intake situations, three experimental groups of animals were selected:

> Single dose: Each cat received a single oral dose of high specific activity ^{85}Sr as the chloride. The cats were subdivided according to age with at least three cats receiving the prescribed dose at 0, 1, 2, 4, 6, 8, 10, 12, 16, 20, 24, 32, 48, and 56 weeks of age. Cats older than 56 weeks were considered to be adults and were not used in this study.
>
> Chronic uptake dose: In this group, cats were divided similarly to the single-dose group, but were given daily ^{85}Sr oral doses. Under this regimen, the growing cats received ^{85}Sr radiation exposure prior to birth or weaning, via the maternal placenta and/or milk.
>
> Excretion following chronic uptake dose: This group of experimental cats is unique in that all of its members began receiving radiostrontium exposure from the time of conception. This group received ^{85}Sr as in the chronic group, but these animals were taken off the isotope at time intervals similar to those described previously and their excretion pattern followed for approximately a year.

Regardless of the study phase, each cat receiving radiostrontium was subjected to the following experimental observations at prescribed intervals: Whole-body radioactivity assay, excreta assay, blood analyses, and ^{85}Sr tissue distribution.

To supplement the ^{85}Sr metabolism data, various tissues--especially bone--were analyzed for stable strontium, calcium, and phosphorus. Ashed samples of the tissues were analyzed for strontium and calcium by atomic absorption spectrophotometry. Phosphorus was determined by ultraviolet spectrophotometry.

2. Whole-body Radioactivity Assay

J. F. Stara, R. G. Wolfangel, G. L. Jessup

For each experimental cat, the ^{85}Sr body burdens were analyzed in terms of initial experimental age. The tabular whole-body data were further treated and analyzed. The following equation adequately describes radiostrontium elimination from cats following both single oral dose and chronic uptake dose:

$$R(t) = A(t + d)^{-b}e^{-ct}$$

where R = whole body retention at Time = t

A and b and c = constants

The equations obtained for each cat were averaged for all members of a respective age group using appropriate computer subgroups. Since animal-to-animal variations were seen, it decreased the reliability of the single equation describing radiostrontium metabolism for the particular age group. However, the equation representing a particular age group should be considered the best estimate of ^{85}Sr metabolism in cats; treatment of the data is under way at the present time.

Figure 36 represents the excretion of ^{85}Sr in different age groups of cats which received a single oral dose. The older cats appeared to eliminate a significant quantity of the ^{85}Sr in a relatively brief period. Later, elimination of the remaining radiostrontium proceded at a rate nearly equal to the younger animals. In younger groups, the early rapid ^{85}Sr elimination pattern was nearly or completely absent.

Figure 37 shows the plots of ^{85}Sr retention values generated from the average group excretion equations of chronically-dosed cats. There appeared to be little or no rapid excretion of radiostrontium in any age group, demonstrating a significant difference from cats labeled with a single dose.

3. Excretion Data

R. G. Wolfangel, J. F. Stara

The quantity of ^{85}Sr appearing in 24-hour collections of urine and feces of the experimental cats has been computed from the available data. Figure 38 illustrates excreta values from cats on chronic uptake dosage versus cats on chronic excretion status. During the chronic dosage phase, the feces to urine ratio approached 100 and followed a stable trend. During the excretion phase, radioisotope levels were reduced significantly with the feces to urine ratio averaging about 10 during this phase. During the transition from the chronic uptake phase to chronic excretion phase, ^{85}Sr content in the feces decreased from approximately 1,000 nCi/day to 10 nCi/day, a factor of 100. In contrast, the amount of isotope in the urine decreased from 10 nCi/day to about 1 nCi/day during the same transition period.

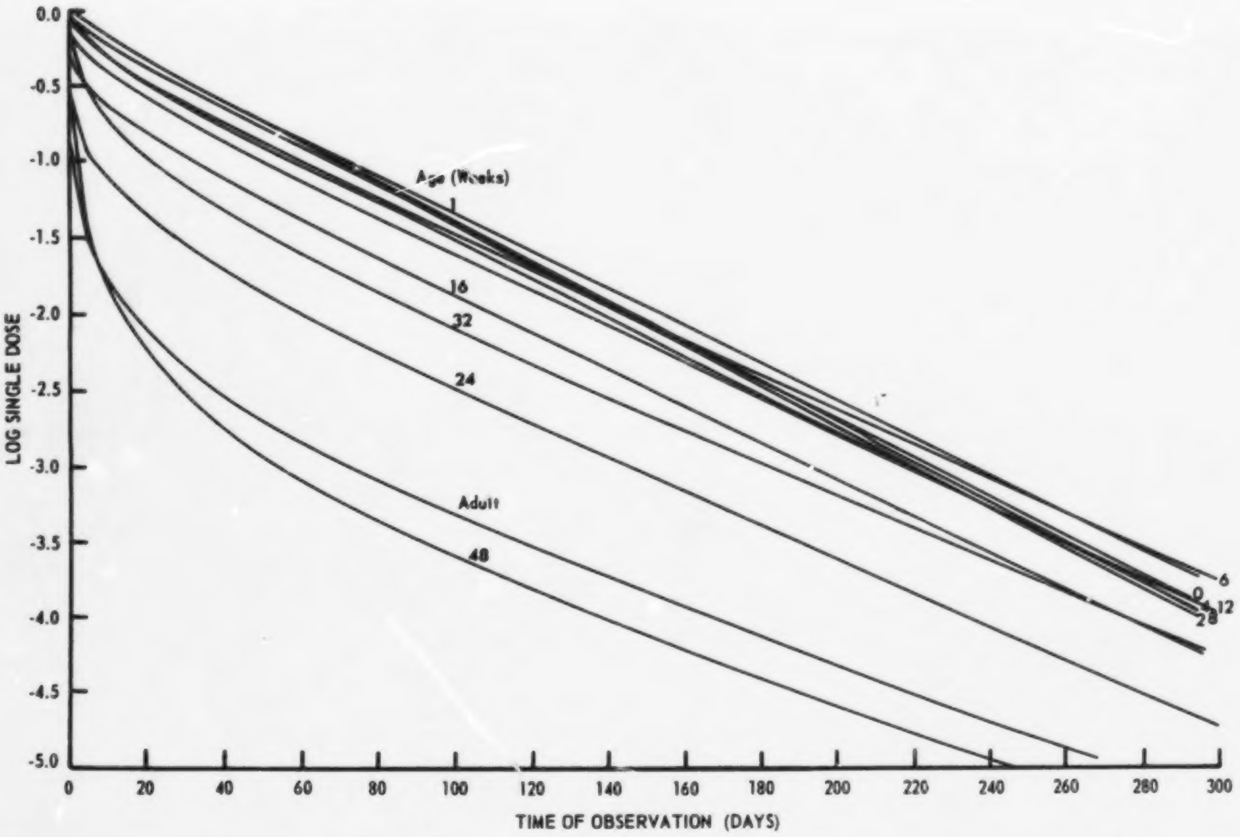

Figure 36. Excretion Curves of Cats Given a Single Oral Dose of ^{85}Sr.

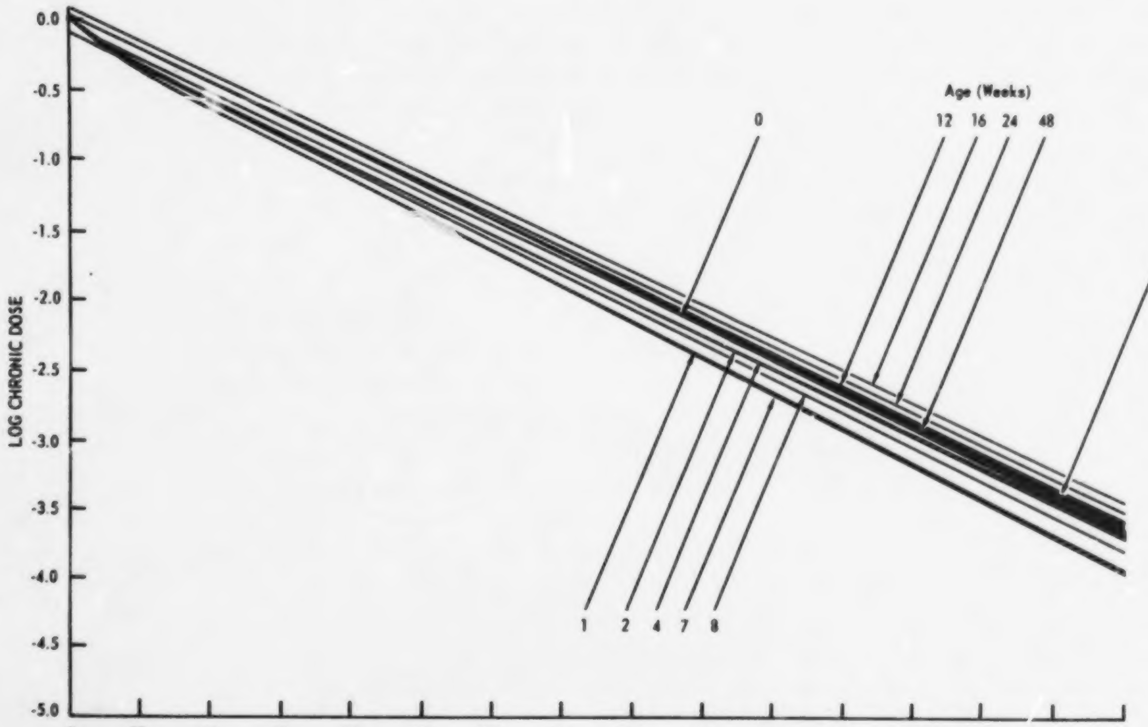

Figure 37. Retention Values Generated from Excretion Equations of Chronically Dosed Cats.

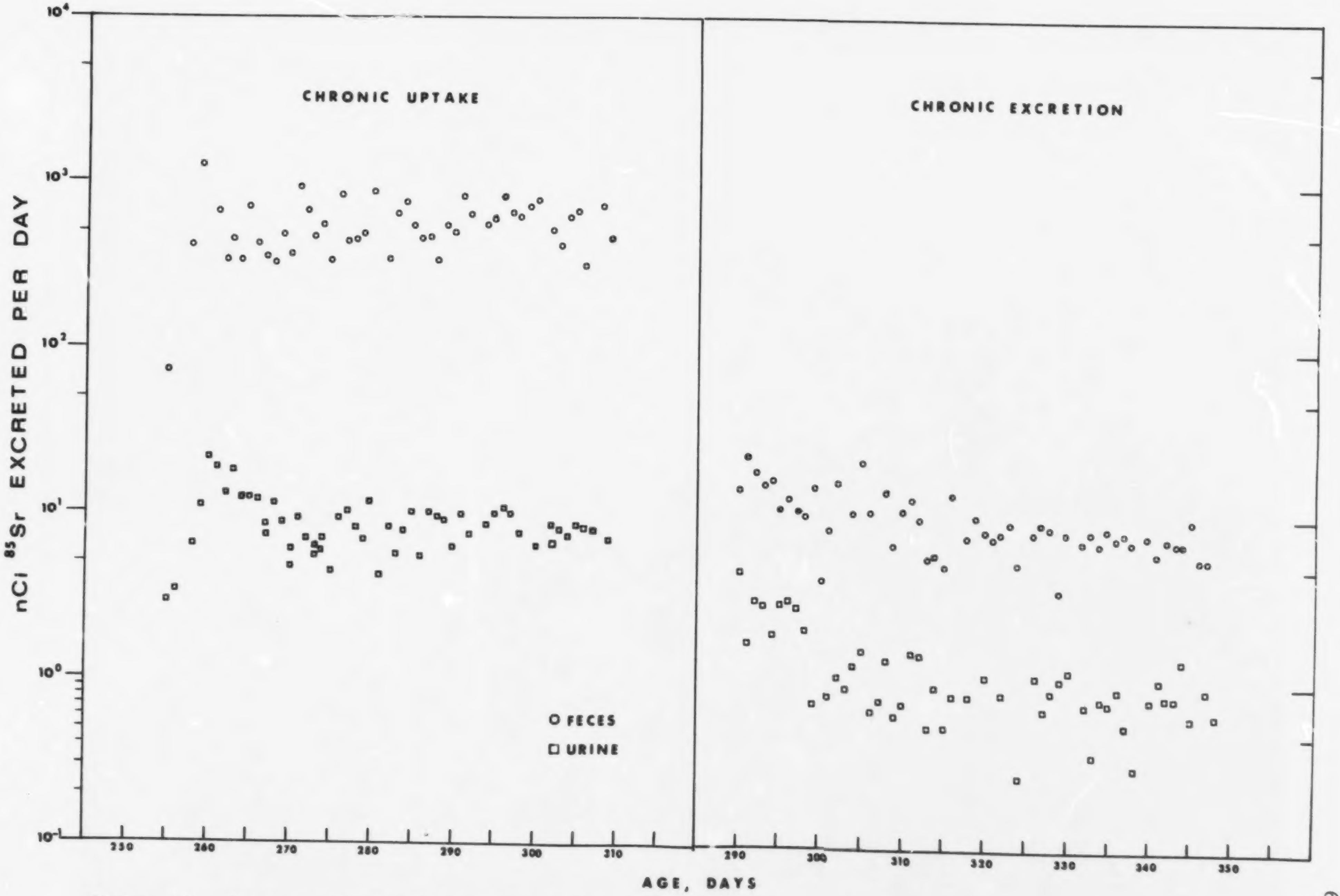

Figure 38. Feces and Urine Values for Cats on Chronic Uptake and on Chronic Excretion Regimens.

4. ^{85}Sr Distribution and Weights of Organ Systems in Chronically-Labeled Cats

N. S. Nelson, J. F. Stara, R. G. Wolfangel

Randomly selected, three adult female cats which had been on ^{85}Sr chronic uptake kinetic study (received an oral dose of 0.5 μCi ^{85}Sr/day for 365 days or more) were sacrificed and completely dissected. All organs and tissues, including individual bones, were immediately weighed and assayed for ^{85}Sr content. The average values and standard deviations for the different body systems are summarized in Table 16 by percent body weight and percent body burden at sacrifice. Although the skeletal system, for example, represented only 11% of the body weight, 91% of the ^{85}Sr was located there. As indicated in Table 17 individual bones vary greatly in their radiostrontium concentration and accordingly would deliver a wide range dose to the bone marrow. The hard tissues (skeletal system) contained about 100 times more ^{85}Sr per gram than soft tissues. Fatty tissues such as omentum and mesentery were lower by a factor of ten than other soft tissues.

The functions of the weights versus fractions of the burden contributed by each component of well-defined organ systems were compared. The values point out that the skull or mandible could be used to provide a good estimator of the total skeletal weight. The best estimate of strontium skeletal burden, however, could be obtained from the pelvis or the thoracic, lumbar, or sacral vertebrae.

These data are limited since they provide only observation for adult animals on chronic uptake of radiostrontium. Additional values for animals from birth to adulthood are necessary before growth and uptake curves for each organ in the feline body can be constructed.

TABLE 16. ^{85}SR DISTRIBUTION AND WEIGHTS OF ORGAN SYSTEMS OF ADULT CATS FOLLOWING CHRONIC DOSAGE

System	Percent of Body Weight	Percent of Sacrifice Body Burden
Integumentary	12.84 ± 0.90	3.42 ± 0.62
Respiratory	0.79 ± 0.17	0.15 ± 0.03
Gastrointestinal	3.48 ± 0.22	0.38 ± 0.08
Urogenital	0.78 ± 0.15	0.04 ± 0.01
Central Nervous	1.40 ± 0.19	0.06 ± 0.02
Skeletal	10.65 ± 1.43	91.05 ± 1.83
Internal Organ	3.68 ± 0.15	0.14 ± 0.02
Muscle and Connective Tissue	56.69 ± 2.24	3.69 ± 0.98
Mesentery and Omentum	3.20 ± 0.64	0.05 ± 0.01
Blood	4.75 ± 0.22	0.24 ± 0.06

TABLE 17. WEIGHT AND ^{85}SR DISTRIBUTION IN CAT SKELETON

Bone	Percent of Skeletal System Weight	Percent of Skeletal System Burden
Skull	12.45 ± 0.77	19.34 ± 3.46
Mandible	2.73 ± 0.04	3.50 ± 0.72
Vertebrae Cervical	5.53 ± 0.72	5.46 ± 0.77
Thoracic	8.59 ± 0.67	9.14 ± 0.51
Lumbar	10.06 ± 0.88	11.80 ± 1.20
Sacral	2.38 ± 0.67	2.68 ± 0.12
Coccygeal	3.98 ± 0.26	1.60 ± 0.50
Scapula	3.49 ± 0.12	6.15 ± 1.36
Humerus	6.05 ± 0.24	4.65 ± 0.74
Radius	1.92 ± 0.11	1.22 ± 0.53
Ulna	2.46 ± 0.14	1.95 ± 0.67
Carpals	0.533± 0.12	0.25 ± 0.09
Metacarpals	1.25 ± 0.30	0.51 ± 0.14
(F) Phalanges	1.54 ± 0.05	0.54 ± 0.01
Pelvis	4.72 ± 0.17	7.88 ± 0.74
Femur	7.42 ± 0.12	5.65 ± 2.65
Tibia	6.41 ± 0.13	4.87 ± 1.43
Fibula	0.805± 0.32	0.49 ± 0.25
Tarsals	2.91 ± 0.22	1.13 ± 0.23
Metatarsals	2.52 ± 0.22	1.05 ± 0.41
(R) Phalanges	2.14 ± 0.57	0.72 ± 0.34
Ribs	8.42 ± 0.24	7.67 ± 0.24
Sternum	1.53 ± 0.28	1.60 ± 0.32

5. Analysis of Stable Elements in Skeletal Tissues of Cats

R. G. Wolfangel, J. F. Stara, J. M. Cooper

Tissues of selected cats, which were sacrificed as a part of the radiostrontium metabolic studies, were analyzed for levels of Sr^{++}, Ca^{++} and Pi (inorganic phosphate). Ashed tissue samples were analyzed for Sr^{++} and Ca^{++} using an atomic absorption spectrophotometric technique. Phosphorus (Pi) was determined using an ultraviolet spectrophotometer. A high-speed digital computer was utilized to compute and sequentially arrange the data according to age groups.

The results (Figure 39) showed a gradual increase in the percent ash (ash weight/wet weight x 100) in skeletal tissues with increased animal age. The Ca^{++} and Pi levels in bone ash were virtually independent of age, ranging between 34-37% for Ca^{++} and 16-18% for phosphorus. The strontium to calcium ratios were low (0.5) in the neonates, but were elevated quickly to a maximum at about 10-15 weeks of age; thereafter the ratios gradually declined with increasing age. The percent strontium in ash generally followed the same trend. To date, nearly all stable chemistry data have been computed and summarized in the manner described; statistical evaluation of the data is in process.

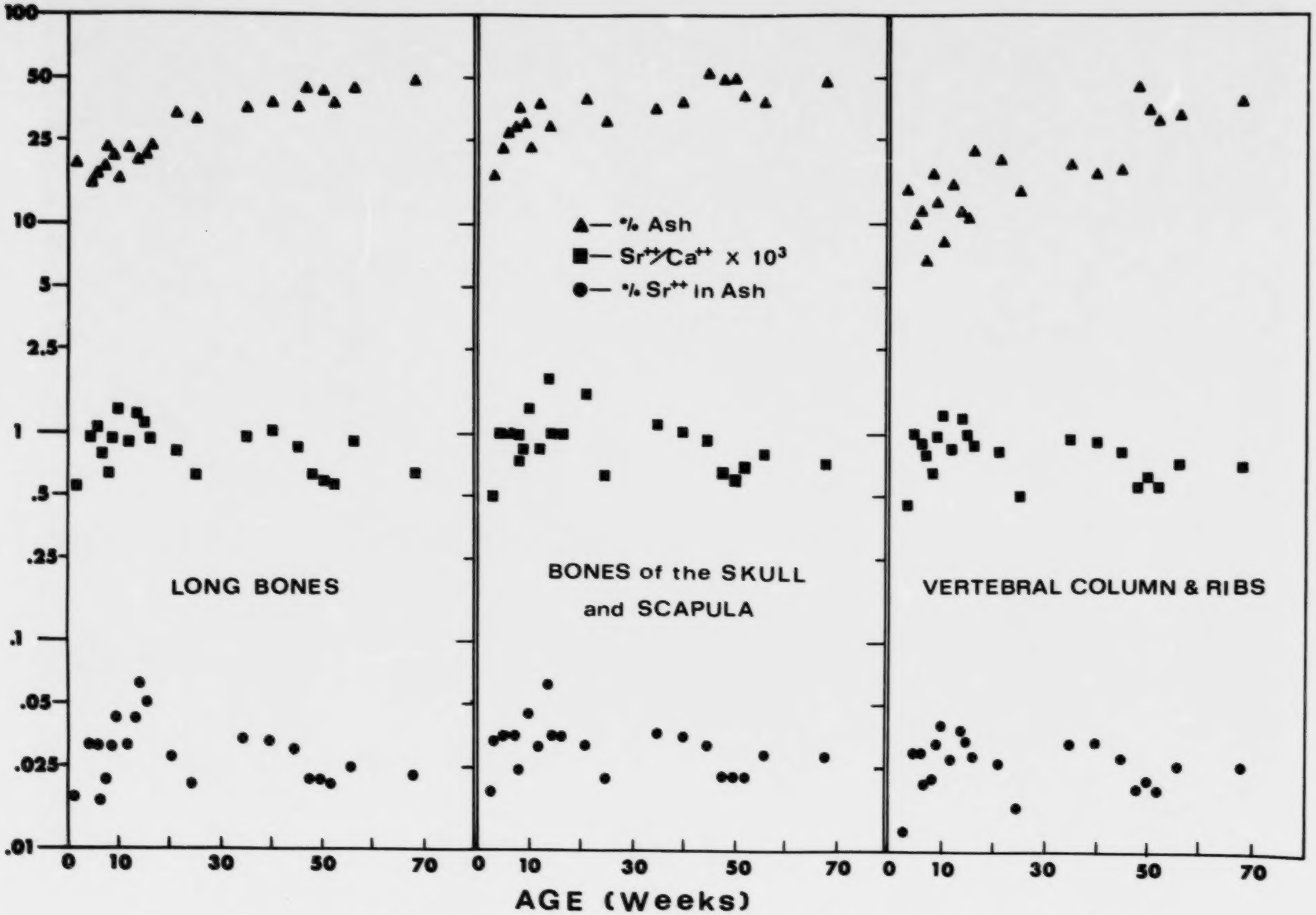

Figure 39. Strontium Levels in Three Types of Skeletal Tissue as a Function of Age.

E. DOSIMETRY OF RADIOSTRONTIUM IN SKELETAL TISSUES OF CATS

1. Nuclear Emulsion Characteristics and Calibration

L. S. Rosenstein, N. S. Nelson

In depth observations on Eastman Kodak Nuclear Tract plates were continued this year. Studies were restricted to those emulsions which could be of potential value for autoradiographic quantitation. These included Kodak NTB and NTB-2 emulsions both of which are extremely suitable for recording of charged particles. NTB-2 nuclear emulsions are the more sensitive of the two.

Fading and sensitivity tests were repeated to ascertain the effects of seasonal changes on the performance of nuclear emulsions. As expected, no difference could be detected in either NTB, or NTB-2 emulsions stored with dessicant at -10°C (freezer). For nuclear emulsions stored under ambient conditions with no dessicant, the image loss and sensitivity changes were far more critical in the early summer months (under high-humidity conditions) than under low conditions of saturation found in January and February. Batch differences were eliminated by using each nuclear tract plate as its own control.

The results of the above study indicate that exposure of quantitative autoradiograms can best be accomplished under deep-freeze conditions. It was concluded that, under conditions of prolonged exposure, NTB-2 presented the most stable reaction as far as minimal image fading and sensitivity changes are concerned. Its greater sensitivity allowed for reductions in exposure time by as much as a factor of two.

Work has been continuing on the calibration of nuclear emulsions for quantitative autoradiography. By employing the method of Marshall et al., standard sources of radiostrontium ($^{90}Sr + ^{90}Y$) have been used in conjunction with absorbers to derive calibration curves for less than thick sources. These calibrations have been applied to bone sections to determine bone concentration (μCi ^{90}Sr/gram) and further to describe the distribution of radioactivity within a bone sample.

2. Strontium-90 Dose Distribution in Chronically Labeled Cats of Different Ages

L. S. Rosenstein, J. F. Stara

Pregnant dams received daily doses of ^{90}Sr in their diet from conception. With this method the skeletal tissues of kittens were uniformly labeled at the time of sacrifice, whether the isotope was transferred to the developing offspring through the placenta, maternal milk, or in their own diet. Kittens were sacrificed at 0, 25, 50 and 200 days of age. The dams eventually were sacrificed and served as an adult subgroup. Selected bones were dissected, fixed, and embedded in bioplastic or methacrylate for sectioning, autoradiography, microradiography, and microdensitometry.

An example of autoradiographic quantitation is illustrated in Figure 40. The sample is an infinitely thick, cortical cross section taken from the femur of an adult cat (504 days of age), chronically labeled with strontium-90 via the diet. The autoradiogram showing evidence of short-term exchange on periosteal and endosteal surfaces, and the long-term diffuse exchange processes, is shown (40a). The resulting X-ray and Isodensitracer analog output are shown in b and c, respectively. An overlay reflecting the contours of absorbed dose rates have been included for a more adequate interpretation (40d). A photomicrograph of the identical femoral section of several magnifications is included in Figure 41 to illustrate the fine structure of adult feline bone. The dark circular bodies represent the osteons with Haversian Canals in the center. Evidence of accretion and resorption can be seen at the periosteal and endosteal surfaces, respectively.

In order to determine the distribution of absorbed dose rates in trabecular regions, an autoradiogram of an infinitely thick, longitudinal section of a young cat femur was scanned in the usual manner on the Isodensitracer (Figure 42). In addition, the analog output was not only graphically displayed 42b, c), but also digitized on magnetic tape. The area recorded has been outlined 42a). There were approximately 225,000 observations made on each plane 12.5 microns (abscissa) by 25 microns (ordinate). The data are being used to fit response surfaces and also to graphically display bone areas of interest to a much finer grid than could be obtained from the original response patterns 42b, c).

3. Development of Bone--A Review of Literature
L. S. Rosenstein

A very extensive literature search has been conducted into those areas that relate to isomorphic exchange and nucleation mechanisms at the level of the hydroxyapatite crystal. This review along with some aspects of calcium/strontium metabolism at the level of the crystal has been prompted by the demands of future investigations involving effects of localized deposition of ^{89}Sr, or ^{90}Sr occupying a lattice position.

Any mechanism resulting in the calcification of a mineralizable matrix obviously influences the building of a crystal structure in which calcium at its lattice position can be replaced by a radiotoxic element (any pertinent member of the alkaline earth series). Although the concept of crystal orientation (epitaxy) in most cases is rigid, there are some conflicting views as to how crystal growth initially begins.

Neuman and Neuman[1] first postulated nucleation mechanism in which crystallization occurs on sites to which minerals may be bound, thus forming nucleation centers. Later work showed that the site of calcium or phosphate binding may be in the collagenous fibrils in the ground substance. Furthermore, it was demonstrated that only collagen fibrils

---

[1] The Chemical Dynamics of Bone Mineral, Univ. of Chicago Press, Nature 218:1262.

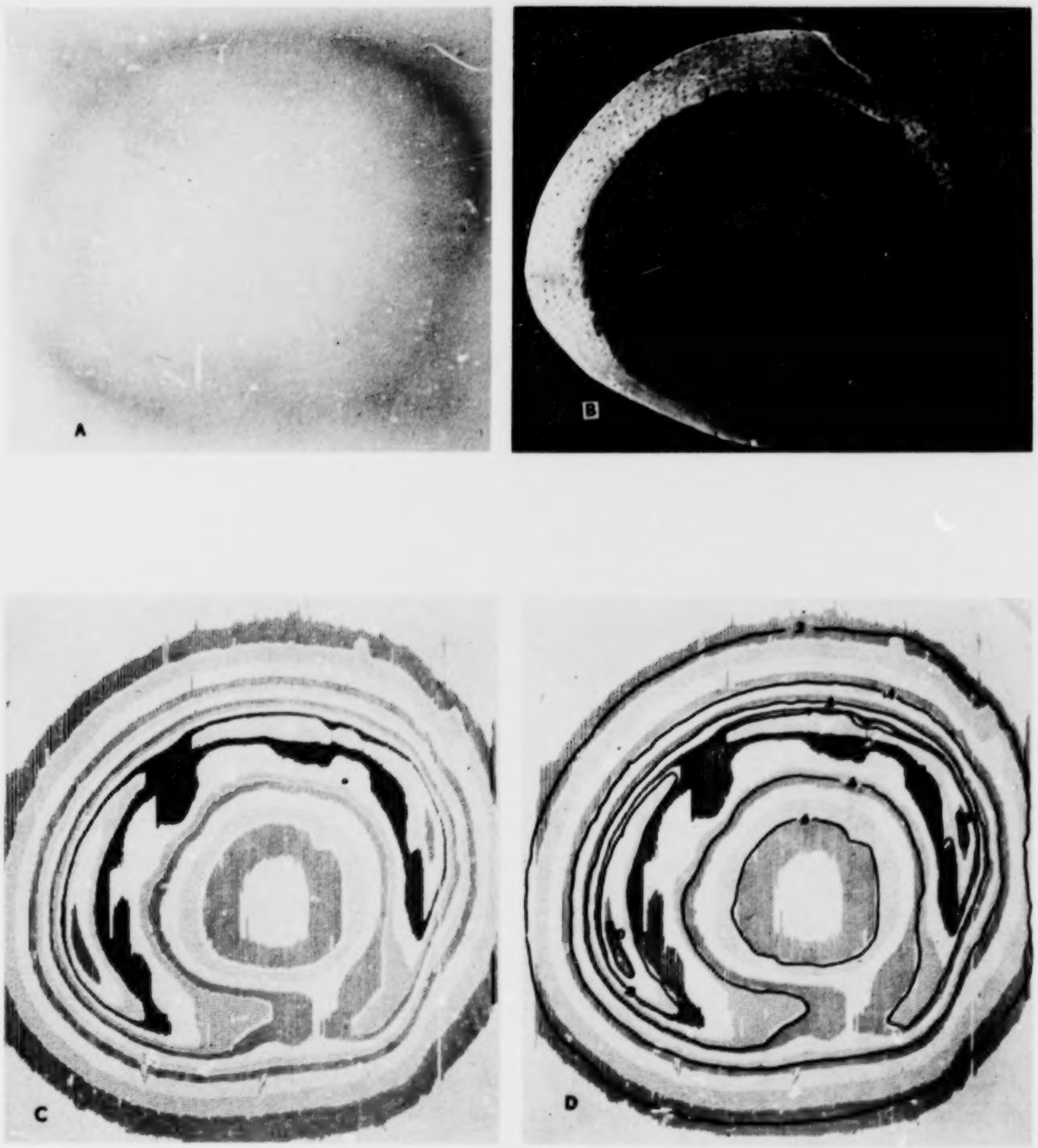

Figure 40. Cross Section of an Adult Cat Femur Showing Associated Autoradiograph (A), X Ray (B), and Absorbed Dose Rates in Rads per Day (C, D). The radionuclides are $^{90}Sr + ^{90}Y$.

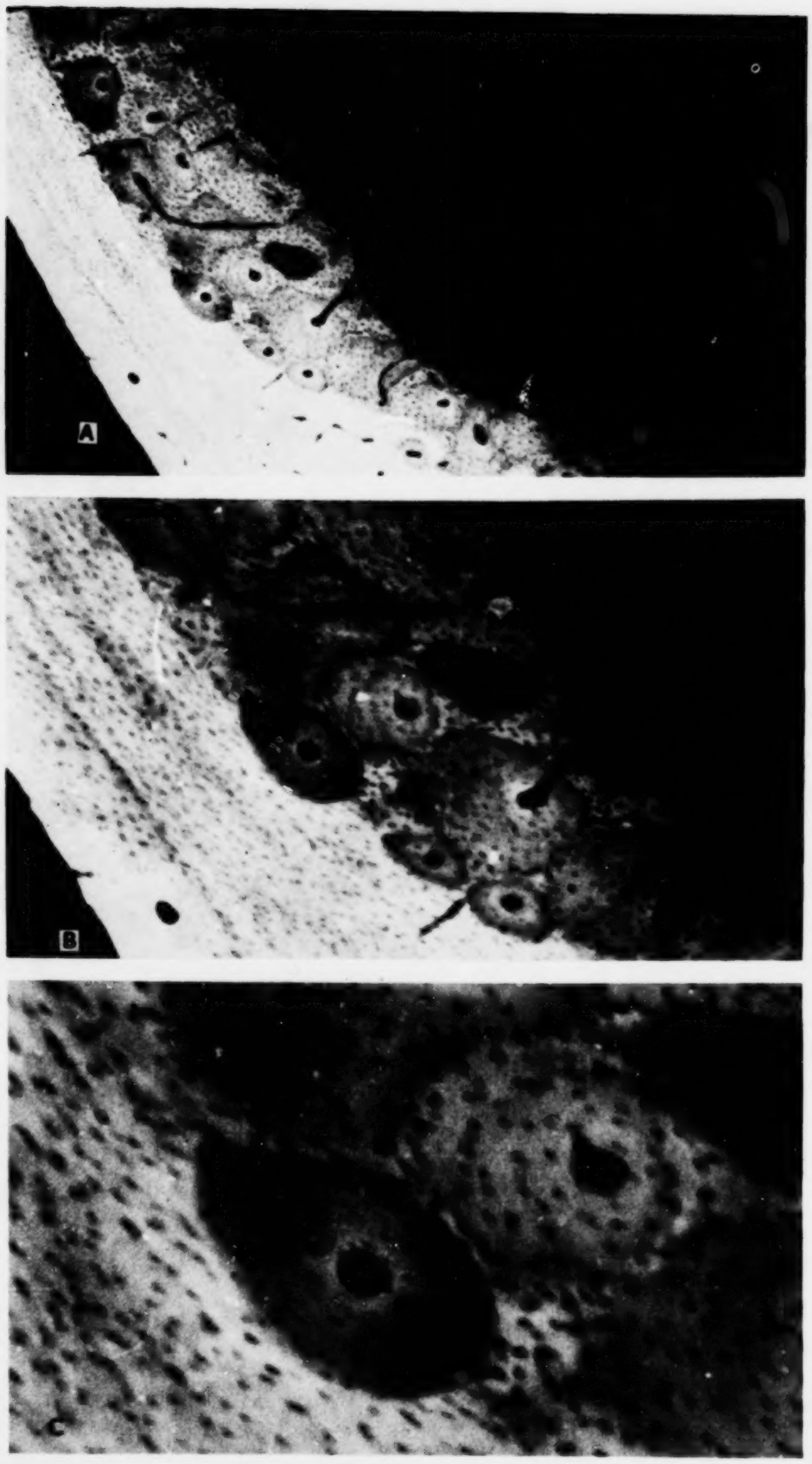

Figure 41. Photomicrographs Showing Cellular Detail of Adult Cat Femur Shown in Figure 40.

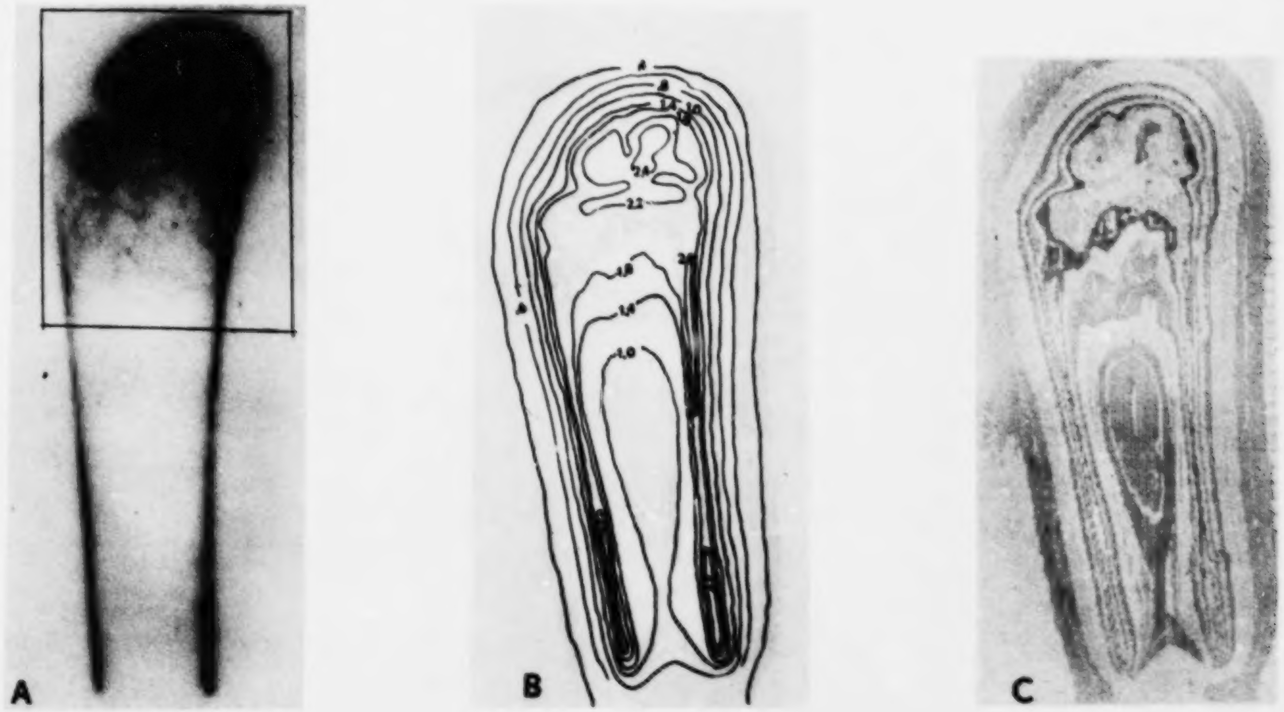

Figure 42. Longitudinal Section of Weanling Cat Femur Labeled with ^{90}Sr + ^{90}Y. The dose response surfaces (rads per day) were determined for the enclosed area in (A) and are shown in (B) and (C).

possessing certain periodic and stereochemical characteristics were able to mineralize. It was further suggested that ATP may provide the energy and phosphate groups (orthophosphate) necessary for nucleation. One other study stated that the ground substance (sulfated mucopolysaccharide) may interact with collagen fibrils and induce nucleation. In this instance, the binding of calcium was necessary for activation of the nucleation process. In pre-osseous tissue another study indicated that nucleation may occur by a reaction between calcium and tissue protein with the ground substance acting as an ion distributor.

In 1968, Samachson[2] proposed an alternative to nucleation and further growth called spinodal decomposition. It essentially reflects the views of those who contended that $CaHPO_4$ was formed first and later modified into hydroxyapatite (Ca_{10} $(PO_4)_6$ $(OH)_2$). This transformation involved the intermediate formation of an amorphous phase of calcium phosphate which was later redeposited in a form resembling hydroxyapatite. The initial formation of $CaHPO_4$, however, has no need for the collagenous template. Only where transformation to hydroxyapatite has occurred is the matrix necessary. Generally, Samachson's method involves the addition of Ca^{++} to the organic matrix followed by HPO_4^-. The removal of H^+ then follows allowing PO_4^- its proper position on the template. Ca^{++} or OH will be added until the hydroxyapatite is formed. Crystal growth will continue until an inhibitor is encountered (such as pyrophosphate) or the formation of an amorphous precipitate is incurred.

Within the past two years the cells themselves have been implicated as playing a much more active role in initiating calcification than formerly considered. In fact, the formation of an amorphous phase may well be intermediate between calcium incorporation in the cell and formation of hydroxyapatite.

---

[2] Nature 218:1262.

F. LETHAL EFFECTS OF ^{89}SR IN CATS

J. F. Stara, N. S. Nelson, R. G. Wolfangel

The original objective of this study was to assess the ^{89}Sr dose effect on feline embryos at five different chronic dose levels administered to the dams from day of breeding until deliveries. An attempt to obtain embryonic mortality probit curves from this pilot experiment was not entirely successful. Dams were fed ^{89}Sr in their diet at dose levels of 10, 62.5, 125, 250 and 500 μCi per day from conception to parturition. Levels producing over 50% mortality in embryos resulted in mortality rates of more than 50% in the dams prior to, or at the time of delivery. Several important observations were made, however, which will be of definite use in developing the long-term ^{89}Sr study.

At birth, the average weights of the kittens delivered of dams fed 10 μCi of ^{89}Sr per day were comparable to the average weights of controls in the same size litters. There was a slight downward trend in the average weights of offspring of cats receiving 62.5, 125 or 250 μCi/day. Offspring born from dams receiving 500 μCi/day showed a marked reduction (30%) in weight at birth. Most kittens born from radioactive mothers (in all dose groups) showed a slight retardation of growth during the first 4-7 weeks of life, but later caught up with the colony norms. Several resorptions and abortions occurred in the pregnant queens. Most pregnancies resulted in births with kittens alive and growing, but the general opinion of trained colony personnel was that the ^{89}Sr kittens were not "doing well." This observation was later borne out by a high death rate among the growing kittens. In dams on the highest level (500 μCi ^{89}Sr per day) a cannibalism occurred which is a well-known behavioral syndrome in cats, as well as certain other mammalian species, in cases when the mother delivers abnormal offspring.

The most severe effect seen in dams receiving ^{89}Sr was the depletion of the peripheral blood elements. The formed blood element responses are shown in Figure 43. The cause of death of the three queens which died at parturition, or shortly thereafter, was an uncontrollable hemorrhage, an apparent defect in the clotting mechanism. This hemorrhage could not be controlled by an injection of clotting agents such as adenochrome isonicotinic acid hydrazone nor by n-butyl alcohol. All queens receiving 250 or 500 μCi of ^{89}Sr per day exhibited a generalized anemia with PCV greatly reduced, as well as general cachexia. Only one queen (915) survived for 140 days post conception from the group receiving 500 μCi per day. Her blood count was precipitously dropping and her condition progressively worsened until she was sacrificed at 170 days after conception. At this time the RBC was 480,000 with a PCV of 6, and WBC of 2,500. In all adult females on high dose levels the adverse response was observable primarily in the hematopoietic system and the general body condition (cachexia).

The ^{89}Sr body burden, specific activity, and rad dose were calculated for selected dams and their offspring. In Table 18, the observed body burden of ^{89}Sr was compared with values predicted from pregnant animals

TABLE 18. PREDICTED AND OBSERVED ^{89}SR IN KITTENS FROM CONCEPTION TO 1 YEAR

Dose,	nCi/g At Birth		Rad Dose from Birth to 1 Year		Rad Dose from Conception to 1 Year	
μCi/d	Predicted[a]	Assayed[b]	Predicted	Assayed	Predicted	Assayed
10	58.80	8.08	30.01	4.20	44.57	6.24
62.5	361.25	33.03	187.70	16.89	287.70	25.08
125.0	722.50	177.18	375.15	93.99	557.15	139.29
250	1445.0	866.53	750.55	450.33	1114.55	668.73
500	2890.0	1546.37	1501.09	810.59	2283.09	1203.71

a. Predicted from pregnant animals which received daily dose of 0.5 μCi of ^{85}Sr for 1-3 years.

b. Average for all kittens assayed.

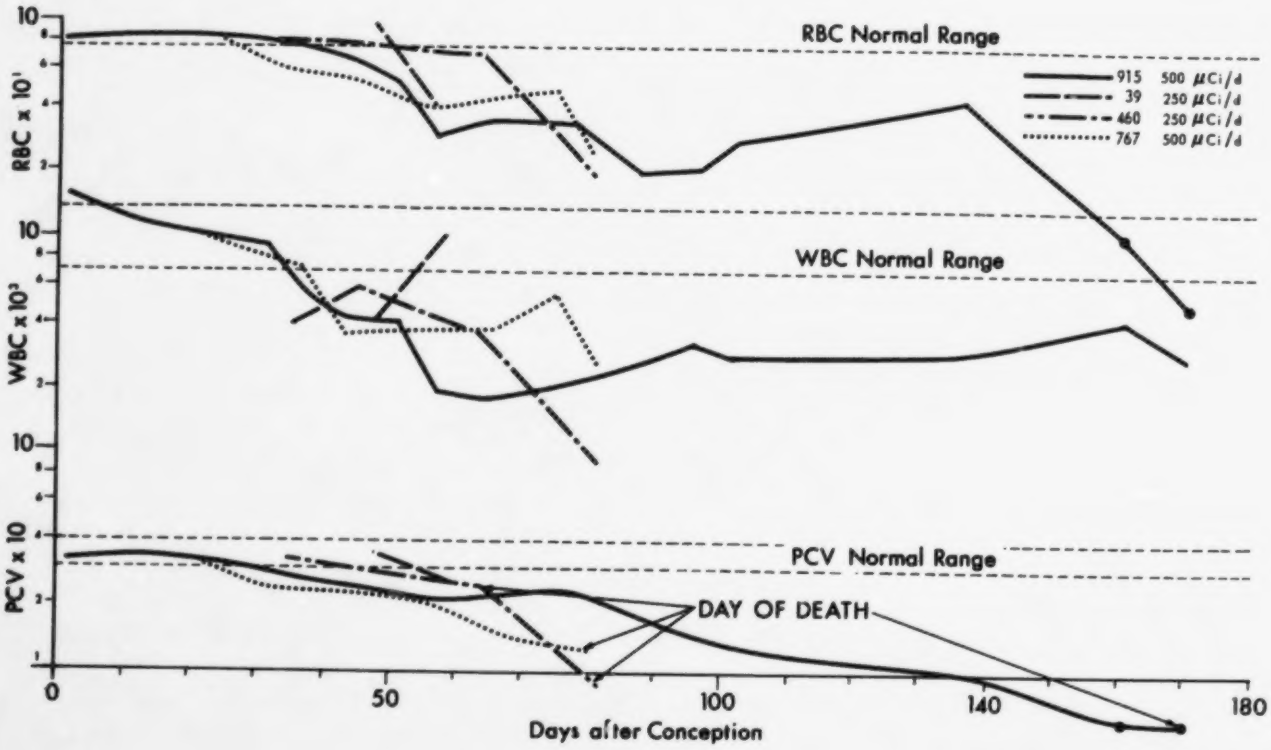

Figure 43. Blood Element Responses of Four Animals That Received ^{89}Sr Doses at Rates of 250 and 50 μCi per Day.

that received a daily dose of 0.5 μCi of ^{85}Sr for a 1-3 year period. The average body burden in the kittens labeled with ^{89}Sr differed from the predicted dose by a wide margin at the lower levels, and by about 50% at the higher dose levels.

Cat embryos were obtained by cesareotomy from dams receiving 0.5 μCi ^{85}Sr per day by pill prior to and during pregnancy. For the five different dose levels, the integrated dose from conception to birth was calculated. The calculated data from 14 to 35 days of gestation included the rad dose from the placenta. During this period of development the fetus is within the range of ionizing radiation originating in the placenta. At that time the placenta exhibits a higher concentration of radiostrontium than the fetus.

The observed and predicted integrated body burdens for each dose level of ^{89}Sr fed, appropriately corrected, are also given in Table 18. These data suggest that about 40% of the total predicted rad dose will be received by the embryo during gestation, and that the remainder will be received from birth to one year of age.

G. LOCALIZATION OF ^{131}I-LABELED TETRACYCLINE IN TUMORS USING SCINTI-SCANNING

R. G. Wolfangel, J. F. Stara

Various investigators have implicated tetracycline to be a potentially reliable agent for diagnosing neoplasms. In most cases this conclusion was based upon observation of yellow fluorescence arising from excised tumor tissue when irradiated with ultraviolet light. To evaluate and extend the use of tetracycline in diagnosis of tumors in vivo, radioiodinated tetracycline was synthesized and injected into cats and dogs which showed clinical symptoms of neoplasia; subsequently, scans of the affected animals were obtained using the scintillation camera.

Radioiodine-labeled tetracycline was produced in our laboratory by reacting ^{131}I-labeled N-iodosuccinimide with a deoxytetracycline in concentrated acid. Results of chromatographic, ultraviolet spectral absorbance, and optical rotation determinations on the final product were compared with published values. The analytical data indicated that small amounts of unreacted deoxytetracycline were present. However, 99% of the ^{131}I residing in the final product was found to be present as ^{131}I-tetracycline. These results were obtained by autoradiography of finished chromatograms and secondly by sectioning the chromatograms and counting each section. The specific activity of the tetracycline was assayed and found to be 1 μCi/mg of tetracycline.

Labeled tetracycline for animal injection was prepared by dissolving the antibiotic in sterile balanced electrolyte solution at a level of 20-25 mg/ml and filtering the preparation through a Millipore filter (0.22 micron using a "swinny" adapter).

Three experimental animals showing clinical symptoms of neoplasia were used in this experiment: A male Siamese cat (Kit) with a tumor in the submandibular area; a female dog - terrier (Petunia) - with a breast tumor; and a female dog - a red-bone hound (Lady) - also with a tumor of the breast. Both Kit and Petunia were injected with 5 mg of iodine, as potassium iodide, one hour prior to tetracycline administration because previous investigations in other species have shown slight thyroid uptake of ^{131}I activity; this is probably unbound radioiodine stemming from the 1% radiochemical impurity in our reaction products. Lady did not receive this treatment.

The prepared solution of tetracycline was in all cases injected intravenously, with Kit and Petunia receiving 80 mg and Lady receiving 12 mg. Since Lady weighed approximately 90 pounds, she was not subjected to scanning and was used only for tetracycline tissue concentration study; i.e., distribution analysis of dissected tissue. For the scinti-scanning procedure, both animals were anesthetized and the radiotetracycline injected immediately before the first scan. Each animal was scanned in several positions and at various times during three days following tetracycline administration. Polaroid photographs of the scintillation scans were taken each time. The serial determinations over the three-day period were to investigate the optimal time distribution relationship and body position which would be most beneficial for the tumor diagnosis.

After scanning was completed, each animal was sacrificed by exsanguination, dissected, and samples of major organs and neoplastic tissues were collected for radioassay. The levels of tetracycline in the various tissues were normalized and corrected for physical decay. In the case of Kit, high tetracycline levels were found in the tumor tissue, the spleen, and the liver; in the case of the two dogs, the level of tetracycline in mammary tumors did not surpass that in normal healthy tissues.

On the scinti-scans, Kit showed similar accumulations of high level radioactivity in the area of the neck, liver, spleen, and urinary bladder, demonstrating a good agreement with the distribution analysis. Pathological examination confirmed the diagnosis of lymphosarcoma in a submandibular region which had metastasized and produced visible neoplastic nodules in the spleen and the lymph nodes.

Scinti-scans of Petunia showed ^{131}I tetracycline penetration into the mammary tumor, but not in a greater concentration than normal health tissue such as liver. In all cases distribution data corroborated the scans. Pathological findings diagnosed a squamous-type tumor in the mammary gland which was well circumscribed and localized. Results obtained from Lady were essentially the same.

The small number of animals studied presents obvious difficulties in interpretation of the results. Diagnosis of the type of tumors present in the two dogs does not appear possible using tetracycline administration and scintillation methods. The fact that the tetracycline scanning procedure did provide excellent interpretative illustrations of lymphocytic neoplasm in the affected cat warrants further evaluation of this agent as a potential cancer diagnostic aid in vivo.

H. EXPERIMENTAL MYXEDEMA IN CATS PRODUCED BY ^{131}I

J. F. Stara, N. S. Nelson

A cooperative study was initiated with the National Heart Institute to investigate the effects of myxedema on heart musculature in the cat. Fifty-three adult felines (25 males and 28 females) were dosed with high levels of ^{131}I to produce partial ablation of the thyroid with resulting myxedema. Prior studies of iodine retention in felines indicated that a single dose of 500 μCi of ^{131}I/kg would produce a hypothyroid state.

Serum samples were initially obtained from all animals to provide baseline protein bound iodine (PBI) values. Normal PBI values averaged 5.0 μg percent with a range of 1.8 to 8.9. The I.V. dose of 500 μCi/kg depressed the PBI values by approximately 50% at 90 days. However, the NHI laboratory assayed six animals at 120 days post-dose and found no myxedematous conditions and subsequent changes in heart muscle.

Based on this finding, a second dose of ^{131}I at an increased level of 1 mCi/kg was administered to all remaining animals. Serum samples obtained at 30 days and 60 days after dosing demonstrated PBI values below 2.0 μg percent, a reduction from normal values by 60%. There was a severe change in the behavior and daily activity of the cats. The majority gained weight, exhibited lethargy, stiffness, and awkward movements, and displayed changes or complete elimination of voice signals.

To confirm reduced thyroid function, ^{123}I was administered to six of the experimental animals. The ratio of thyroid uptake values was 20:1 in the control vs. experimental animals.

The clinical findings combined with the ^{123}I thyroid uptake values and the PBI values produced sufficient evidence of severe hypothyroidism and myxedematous conditions in these animals. Investigators at the NHI confirmed these results and found altered conditions in cardiac musculature. Testes, ovaries, thyroid, adrenal, and heart muscle from selected animals are presently undergoing histopathological examination.

I. MATERNAL-FETAL ^{131}I RELATIONSHIPS IN THE GUINEA PIG

N. S. Nelson, J. F. Stara

Investigations of maternal-fetal relationships of ^{131}I metabolism in the guinea pig have shown that the pattern of iodine deposition in the thyroids of 26 and 30 day embryos resembles that of mature animals in that follicular deposition has occurred. Iodine deposition in thyroids of 21 day embryos was somewhat more diffused. Apparent deposition of iodine in tissues of the embryonic eye was observed in 21, 25, and 30 day embryos. This deposition occurred apparently in the tissue which would become, in the adult, tapetum lucidum. Although some deposition of iodine occurred in other tissues, its magnitude was greatest in the tapetum lucidum and in the thyroid.

J. DISTRIBUTION OF CARRIER FREE AND ^{99}MO-LABELED MILK IN CATS

R. G. Wolfangel, J. F. Stara

Because of recent interest in ^{99}Mo, the Environmental Surveillance group asked this laboratory to conduct a pilot study of the metabolic behavior of this radionuclide. They supplied ^{99}Mo as an aqueous molybdate solution ($^{99}MoO_4^{=}$), and in labeled milk; the milk was obtained from a dairy cow which had ingested a dose of the $^{99}MoO_4^{=}$. The ^{99}Mo in the milk was non-ionic or protein bound as indicated by passing the milk through anionic and cationic ion exchange columns. Three cats were administered the aqueous solution by intravenous injection, and three others were fed 60 ml of the labeled milk. Whole body measurements were obtained on all animals for 36 hours; at the end of this period, the animals were sacrificed and dissected. The mineralized tissues of animals that received the labeled milk contained 7 or more times the amount of ^{99}Mo than the aqueous solution-dosed cats. The soft tissues showed the same trend, although the ratio was somewhat lower. The preliminary data strongly suggest major differences in the metabolism of the aqueous ^{99}Mo versus the ^{99}Mo biologically labeled in milk not withstanding the fact that different routes of administration were utilized.

After 36 hours, the milk-fed cats retained nearly 90% of the administered ^{99}Mo; cats given aqueous ^{99}Mo by capsule retained less than 20% of the initial dose. The milk-fed cats displayed a urine to feces ratio of 0.40; those given the capsule showed a value of 2.5.

The results of the pilot study indicate that ^{99}Mo ingested in the form of labeled milk is metabolized differently than aqueous molybdate solution. The internal radiation exposure resulting from ingestion of contaminated dairy products would therefore be appreciably greater than that resulting from administration of an aqueous solution where molybdenum is in the ionic state.

K. CARCINOGENIC EFFECTS OF DEPOSITED RADIOACTIVE PARTICLES IN THE LUNG[3]

R. E. Stanley, H. J. Monie

The study to assess the potential human health hazard associated with the inhalation of respirable, highly radioactive particles emitted in the effluent from reactor engines began at the Southwestern Radiological Health Laboratory (SWRHL) in 1967. The project was designed to be conducted in three phases. The expected results from the first phase, production of primary lung cancer in the rat, would serve as an indication of the existence of potential hazard and of the need for proceeding with the second phase projected for the dog. Failure to produce primary carcinoma in the rat with exposure levels likely to be encountered in the environment would terminate the project at the conclusion of the first phase.

Progress to date has been limited to the completion of an extensive survey of the literature on inhalation toxicology and to three preliminary studies. The third preliminary study was started in July. In this study, field-collected radioactive particles from reactor effluent were injected via the trachea into the lungs of five rats. We have found, as in the two previous preliminary studies, that the clearance of radioactive particles from the rat lung is best described by a two-phase curve. The first phase represents the initial clearance and varies with the individual animal. It is probably dependent upon the dispersion of the particles in the lung and the individual efficiency of the ciliary escalator. The clearance half time for this phase is from 1 to 5 days. The second part of the curve apparently is primarily influenced by physical decay of the retained isotopes and varies with the age of the particles injected. In a previous study, fresh particles containing both short- and long-lived isotopes were used and a 7-day half time was observed in the second phase of the clearance curve. The present study uses particles 3 weeks old, the clearance half time is 11 days indicating a predominance of long-lived components. Gross and microscopic effects data for the limited studies are not yet available.

---

[3] This study conducted at the Southwestern Radiological Health Laboratory, Las Vegas, Nevada.

L. INVESTIGATION OF ALPHA PARTICLE AND TOBACCO SMOKE SYNERGISM[3]

S. C. Black, E. W. Bretthauer

This investigation was conducted in two distinct phases. Phase I consisted of the quantification of not only ^{210}Po but also ^{210}Pb and ^{226}Ra in tobacco and mainstream smoke over a wide range of parameters, i.e., locale of tobacco growth, variability in smoking patterns, effectiveness of commercial cigarette filters, etc. If the exposure due to smoking could not be easily eliminated or significantly reduced as suggested by such a parameter evaluation, then Phase II, animal studies to determine whether the amounts of radiation derived from Phase I actually produce lung carcinoma, was to proceed. The laboratory work on Phase I has been completed.

Phase II of the Project began in early January, 1967. A literature search revealed that an inhalation chamber for introducing cigarette smoke at comparable conditions (temperature, particle size, and concentration) to human smoking did not exist for small animals. A series of experiments was undertaken to provide data useful for the design of an inhalation chamber which would meet the above criteria. A prototype chamber was fabricated, tested and modified until it exhibited acceptable agreement with the desired criteria.

To successfully test this chamber several problems were solved which should enhance future progress: (1) a method for uniformly adding ^{210}Po to cigarettes to enhance concentration in smoke, (2) development of an animal restrainer to minimize trauma during exposure, and (3) a method of removing ^{210}Po from mainstream cigarette smoke. A large scale smoking device (exposure of 20 rats simultaneously) was completed in November. Experiments are now in progress to determine dose ranges to be used for the long-term experiments which will be designed to determine whether the quantities of alpha radiation present in cigarette smoke actually produce lung carcinoma.

PHYSIOLOGY AND BIOPHYSICS LABORATORY

Dr. Moris L. Shore, Chief

In evaluating the hazards of ionizing radiation, a number of approaches have been taken by the Physiology and Biophysics Laboratory. One approach is based on the hypothesis that ionizing radiation produces its most significant long-term effects through alterations in DNA, the structural integrity of which is essential to the maintenance of all normal cellular activity and thus the functional viability of any living organism. Any radiation-induced alteration, produced directly or indirectly in the normal base sequence of DNA, constitutes a mutation. Such mutations are generally considered to be deleterious, and even if not, constitute damage produced by ionizing radiation. Mutations may be expressed in such obvious ways as birth abnormalities, decreased lifespan, tumor induction, or cataract formation. Mutations may also find more subtle expression as decreased functional capacity of specific organ systems, alterations in immunological competency that may decrease resistance to bacterial or viral infection, or alterations in the synthesis of proteins whose synthesis is directly dependent on the integrity of DNA, Messenger RNA, and the translation process.

Other studies have examined the effects caused by radiation delivered in utero. These studies have dealt with protein synthesis in general, specific enzyme systems, possible effects on immunological processes, and effects on components of the peripheral blood.

This past year, the Physiology and Biophysics Laboratory integrated studies related to the effects of microwave radiation into many of its projects. The first study, summarized in the following section, relates to the biological effects of microwaves. Additional emphasis on nonionizing radiation studies and low-energy X-ray studies are planned for next year.

A. EFFECTS OF MICROWAVE RADIATION ON CHINESE HAMSTERS

D. E. Janes, W. M. Leach, W. A. Mills, R. T. Moore, M. L. Shore

Increased concern has developed recently over the possible biological hazard of electromagnetic radiation in the microwave frequencies. The scientific literature indicates that microwave radiation produces significant effects on a number of biological systems, including the nervous system, the eye, the circulatory system, and the reproductive system. At the cellular level, observations have shown that microwaves (1) produce lenticular opacities, (2) can arrest the process of differentiation in embryos without necessarily arresting cellular proliferation, (3) can produce testicular damage (even when such irradiation is effected below temperatures necessary to cause injury with infrared exposures), and (4) can produce irregularities in the mitotic process.

The present study, using Chinese hamsters, investigates the biological effects of microwaves on the mitotic process of bone marrow cells, and on the in vivo incorporation of ^{14}C-labeled phenylalanine into protein of liver and testis. The cytogenetic studies provided suggestive evidence for increased chromosomal stickiness after microwave radiation. However, no chromosomal or chromatid aberrations were observed. Studies on protein synthesis indicate that microwave radiation causes a marked decrease in the in vivo incorporation of labeled amino acid into protein both in liver and testis.

Unanesthetized Chinese hamsters weighing 25-35 grams were used in this study. Experimental animals were exposed to radiation produced by a microwave oven operating with the door open at a frequency of 2450 MHz (12.25 cm wavelength).

The irradiation was not performed under unequivocal far field conditions and the average power density of the microwave field at the point of exposure could not be effectively determined with instruments available for the measurement of average power density. Thus two approaches were employed for the relative characterization of the field; one, biological, employed lethality as an endpoint, the other, physical, employed calorimetry techniques using spherical water loads.

For the lethality studies, animals were irradiated for 3 minutes followed by no radiation for 1 minute until the time of expiration. The duration of microwave exposure which resulted in deaths of the hamsters ranged from 9 to 36 minutes. Rectal body temperatures in hamsters at the end of the irradiation period during which mortality occurred ranged from 37.9° C to 47° C with a mean of 43.6° C.

Data were obtained on the absorption of microwave energy in spherical phantoms filled with distilled water. The phantoms had volumes of 500 ml and 200 ml and radii of 4.92 and 3.63 cm respectively. The pyrex containers used for the phantoms were assumed to be in thermal equilibrium with the water mass of the phantom. The calorimetric technique showed an average temperature rise per minute in the 500 ml water phantom (4.92 cm radius) to be 0.178 ± 0.002° C per minute; in the similar 200 ml (3.63 cm radius) phantom, 0.198 ± 0.001° C per minute. The average rates of energy absorption, expressed per unit of cross sectional area of the phantom were 87.1×10^{-3} (500 ml) and 71.3×10^{-3} (200 ml) joules sec^{-1} cm^{-2}. These values are useful as a point of reference, but cannot readily be extrapolated to measures of the average power density of the microwave field since the absorption cross section for these phantoms is not known.

1. Chromosomal Effects

Cytogenetic studies were performed in animals exposed to the microwave field for a total of 12 minutes. Two chromatid breaks were observed in a total of 50 analyzable cells. In the control animals, one chromatid break was observed in 100 cells that were examined. Five of the 100 control cells were aneuploid; four had a small acrocentric chromosome missing, the other cell contained two extra submetacentric chromosomes. Aneuploidy was not observed in the irradiated cells.

A substantial proportion of metaphase cells from irradiated animals showed gross chromosomal anomalies, similar in appearance to the "early physiological" or "stickiness" effects observed in dividing cells after X irradiation. Because of the complexity in stickiness effects after X radiation, it may be of questionable value to attempt, at the present, a quantitation of stickiness in cells exposed to microwaves. Stickiness phenomena may be observed either between parts of one chromosome (chromatid stickiness) or between two or more chromosomes (chromosome stickiness). In the present study only metaphase cells were evaluated for chromosome stickiness and chromosomal aberrations. In the controls up to 20 percent of the metaphase spreads contained what appeared to be chromatid stickiness, but no chromosome stickiness. In the cells from animals irradiated two hours after Colcemid injection, over half of the metaphases showed chromatid stickiness. Chromosome stickiness varied from preparation to preparation in a range from about 25 percent to 67 percent of the metaphase cells. The cells from animals injected after irradiation were essentially similar to control cells. Almost 50 percent of cells from animals injected just prior to irradiation showed chromatid stickiness, but chromosome stickiness was not observed.

In preparations obtained from animals irradiated two hours after injection, we found evidence that cells were escaping from the Colcemid block, and attempting to complete mitosis and cytokinesis. Detectable cytokinesing cells were those in which stickiness interfered with daughter chromosome separation. Long chromosomal bridges connected the daughter nuclei in about 10-15 percent of the dividing cell population. Similar bridging was observed in cells from animals exposed immediately after injection (4-5 percent), as well as cells from animals injected after exposure or control cells (less than 1 percent in either case). It is apparent that stickiness may interfere with the completion of cytokinesis. Since chromosomal material is in the bridge between the daughter nuclei, it is possible that chromosome rearrangements may be detected in subsequent cell divisions. Experiments to examine this possibility are in progress.

2. Effects on Amino Acid Incorporation

The in vivo incorporation of ^{14}C-labeled phenylalanine (^{14}C Phe) into liver and testis protein was examined in Chinese hamsters after microwave irradiation. Since animals were injected with ^{14}C Phe intraperitoneally, variable amounts of the labeled amino acid may have been available within the tissues of interest for incorporation into protein. Thus both acid soluble ^{14}C Phe in liver and testis as well as acid insoluble ^{14}C Phe were determined. The data on incorporation are expressed as relative activity -- % injected dose ^{14}C Phe in tissue protein/% injected dose ^{14}C Phe in tissue acid soluble fraction.

Animals received a total microwave exposure of 12 minutes as previously described. Controls were sham irradiated. Rectal temperature was obtained with a thermistor probe on completion of exposure or sham exposure. The mean increase in rectal temperature as a result of microwave irradiation was 4.2 ± 0.6° C.

Table 19 presents the average relative activity in liver and testis at 80 minutes and 20 hours after the midpoint of exposure. Since liver value for irradiated animals is not significantly different from zero at 80 minutes, it appears that labeled amino acid incorporation into liver protein was essentially abolished by 80 minutes after microwave exposure. A similar effect, though not as pronounced was seen in testis 80 minutes after exposure. The value of relative activity in testis of irradiated vs. control animals was decreased by approximately 45 percent. The difference between sham controls and irradiated animals was significant ($P < .05$).

TABLE 19. RELATIVE ACTIVITY[a] OF AMINO ACID INCORPORATION AT VARIOUS TIMES AFTER MICROWAVE IRRADIATION

Time After	Liver		Testis	
Irradiation	Irradiated	Control	Irradiated	Control
80 minutes[b]	0.564 ± 0.334	4.73 ± 0.328	0.331 ± 0.065	0.609 ± 0.093
20 hours[c]	5.368 ± 0.603	5.689 ± 0.455	0.539 ± 0.082	1.092 ± 0.231

a. $\frac{\text{\% injected dose } ^{14}C \text{ Phe in tissue acid insoluble fraction}}{\text{\% injected dose } ^{14}C \text{ Phe in tissue acid soluble fraction}}$

b. Average of 11 animals.

c. Average of 12 animals.

Table 19 also shows that incorporation of amino acid into protein, which was essentially abolished 80 minutes after exposure was restored to normal values 20 hours later. The relative activity of sham irradiated controls was not significantly different in either the liver or the testis group although a tendency toward lower values is suggested 80 minutes after sham irradiation relative to the 20 hour controls.

In contrast to the recovery of amino acid incorporation into liver, the value for testis remained depressed relative to sham controls 20 hours after exposure to microwaves. The factors underlying this difference are not readily apparent, but hormonal stresses associated with the sham irradiation may be involved. It is apparent, however, that in all cases exposure to microwave radiation did decrease the incorporation of labeled amino acid into testicular protein. This effect was apparent as early as 80 minutes after irradiation and lasted at least through the 20th hour after exposure.

The finding of decreased amino acid incorporation into protein in liver and testis after microwave exposure cannot be equated to decreased protein synthesis without qualification. For instance, if microwave radiation causes an increase in the amino acid pool in tissue, then the specific activity of the amino acid precursor (labelled Phe/total Phe) will be lower in irradiated relative to sham control animals. Under this condition the incorporation of equivalent amounts of phenylalanine in both groups of animals will lead to a decreased incorporation of ^{14}C Phe in the irradiated animals. The degree to which incorporation of label was reduced in liver 80 minutes after irradiation, as well as the persistent effect in testis 20 hours after irradiation, however, suggest that increase in the size of the precursor amino acid pool may not be the mechanism underlying this effect. Further experiments will have to be performed to establish the mechanisms underlying altered amino acid incorporation into proteins in tissues of microwave irradiated animals. The mechanism may be either thermal or nonthermal. If thermal, however, it is probably an indirect rather than a direct effect, since temperature rises such as those observed in this study are not normally associated with protein denaturation. Thus, a molecular effect is implied which may be mediated by hormonal or other factors.

B. HEMATOPOIETIC CHANGES ASSOCIATED WITH IN UTERO IRRADIATION

D. G. Hazzard, R. A. Budd

Small amounts of irradiation to blood forming organs cause arrest of hematopoiesis and changes to the peripheral blood. Most sensitive of all blood cells are the lymphocytes and their precursors. We are studying the changes produced by irradiation at various embryonic stages of development, at various total exposures, and from energy sources in the 250 keV and 25 keV regions on total white cell count, total red cell count, nucleated red cell count, hematocrit, and body weight of the offspring of irradiated rats.

Figure 44 shows the results of irradiating pregnant rats with 180 rad from a 250 keV source days 13 through 21 of gestation on the total white counts of pups 24 hours after birth. Figure 45 shows the effects of similar irradiation on day 15 of gestation on the recovery of the white cell counts of the pups from birth to 10 days of age. It appears that there are marked decreases in the WBC of those irradiated *in utero* for the first 2-3 days after birth, but that by the fourth day the WBC of the survivors recovers to approximately normal levels. Effects on survival are shown in Table 20.

Figure 46 shows the effect of various doses on the white count of 24-hour-old pups when they were irradiated *in utero* on day 15 of gestation. Because of the wide variance in counts, statistically significant difference as measured by "Student's t test" were noted at only the 180 and 240 rad dose levels, both being different from the control ($P < 0.01$). The intraperitoneal injection of 40 μg of endotoxin per 100 g of body weight 24 hours prior to irradiation resulted in a significant increase in white cell count ($P < 0.01$).

Figure 47 shows the dose effect of irradiation at 15 days gestation on total red cells and nucleated red cells; Figure 48 similarly shows the response on hematocrit and body weight. All these criteria except hematocrit show marked effects in the pups 24 hours after birth as a result of *in utero* irradiation of the mother at 15 days gestation.

TABLE 20. EFFECT OF IRRADIATION DOSE AT 15 DAYS GESTATION ON LITTER SIZE AND SURVIVAL OF PUPS BORN

	Average Litter Size	% Survival 24 hr.	% Survival 2 wk.	% Survival 30 days
No Irradiation	10	100	100	100
60 rad	9.5	100	100	100
120 rad	10	100	100	100
180 rad	12	97.2	86.1	86.1
180 rad + endotoxin	8	100	81.2	81.2
240 rad	9.3	39.3	28.6	0
240 rad + endotoxin	9.6	44.8	27.6	27.6

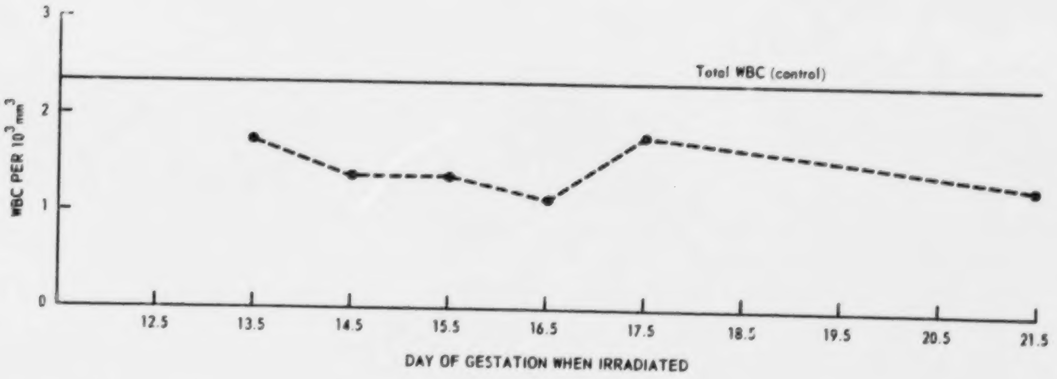

Figure 44. Effect of X Rays at Various Gestation Times on White Cell Count Taken at 24 Hours of Age.

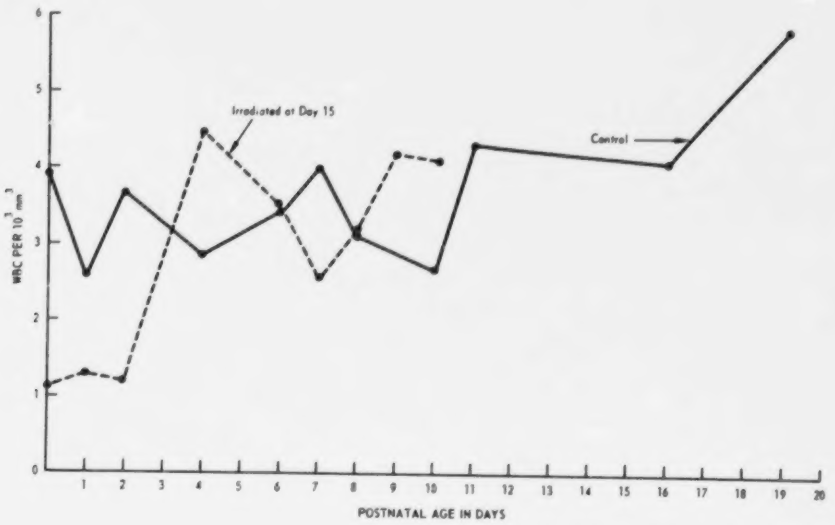

Figure 45. Effect of Irradiation at Day 15 of Gestation on White Cell Count at Various Ages After Birth.

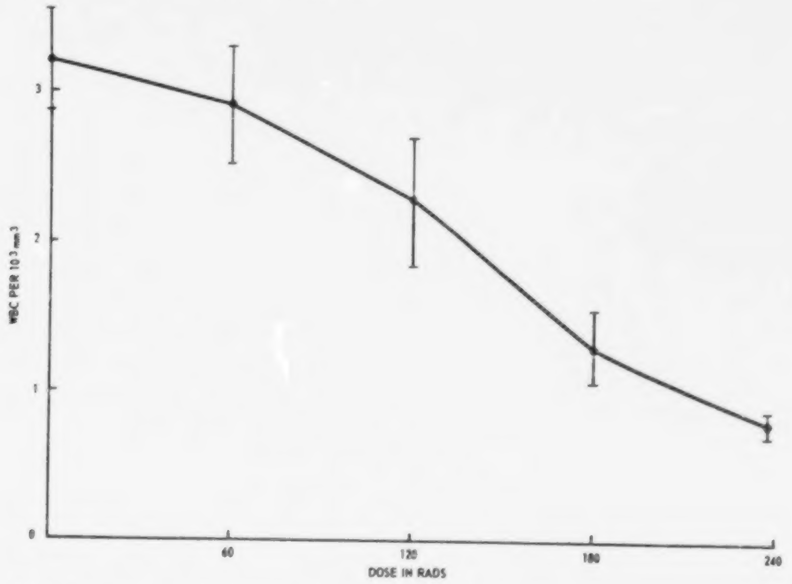

Figure 46. Effect of Various Doses Given at Day 15 of Gestation on the White Cell Count Taken at 24 Hours.

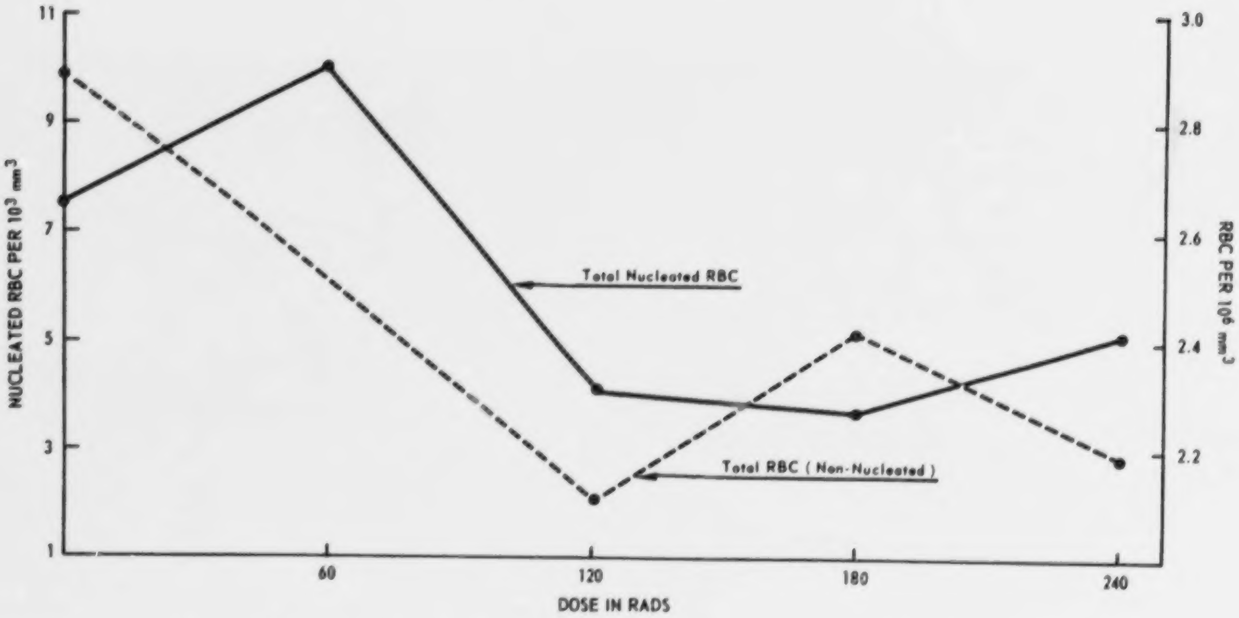

Figure 47. Effect of Various Doses Given at Day 15 of Gestation on Total Red Blood Cells (Non-nucleated) and Nucleated RBC at 24 Hours.

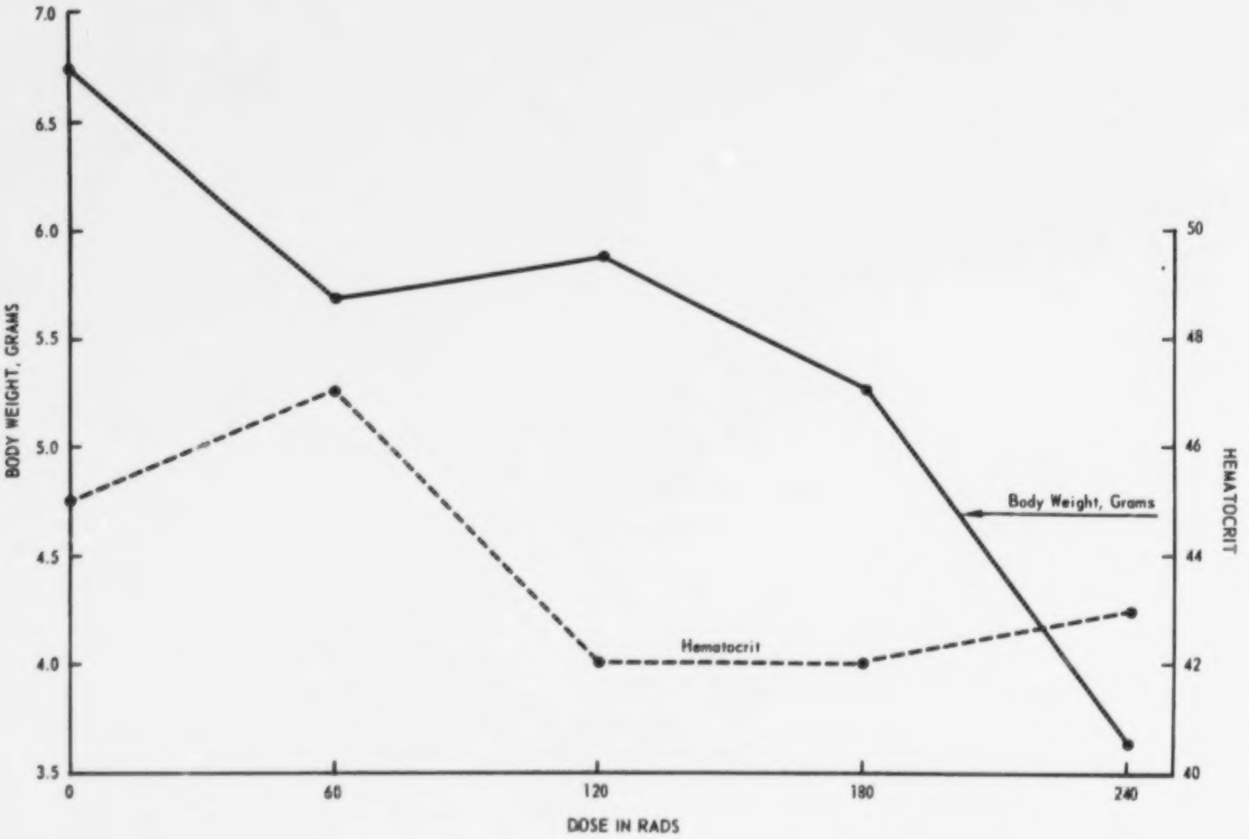

Figure 48. Effect of Various Doses Given at Day 15 of Gestation on Body Weight and Hematocrit at 24 Hours.

C. IN UTERO IRRADIATION WITH HIGH AND LOW ENERGY X-RAYS AT VARIOUS DOSE RATES

D. G. Hazzard, R. A. Budd, T. J. Withrow, C. Ronayne

This study examines the dose effects of irradiation at varying embryonic development stages to find: (1) if biochemical effects of irradiation are more pronounced when irradiation occurs very early in embryonic development, (2) to find the developmental stage-dose relationship exhibiting the most sensitive period for in utero irradiation, and (3) to compare the relative effects of radiation obtained from low energy source to that from high energy source.

Rats at varying stages of gestation received 180 rads of 250 keV X rays to study the effects on lactic dehydrogenase (LDH) and total protein. In one series of studies representing 186 animals, no differences were observable in liver LDH levels of pups 24 hours or 6 days after birth when their dams had been irradiated on the 15th day of gestation. Neither were any differences found at 24 hours after birth when irradiation occurred on day 5 or 10 of gestation. The corresponding total protein values for these animals did show a 7% increase ($P < 0.02$) at 24 hours after birth, but no differences at 6 days or when irradiation occurred on day 5 or 10 of gestation.

Studies involving 180 rad exposures to the pregnant females on day 13, 14, 15, 16, 17, and 21 of gestation have shown considerable variation in LDH and total protein levels. However, the variation about each point was so great that none of these values was statistically significant ($P < 0.05$) from the control value.

D. EFFECT OF X-RAY RADIATION AND MICROWAVE RADIATION IN VITRO AND IN VIVO ON HUMAN AND RAT GAMMA GLOBULINS

G. P. Kamat

Pregnant rats were X irradiated on day 13 of gestation with a dose of 180 rads and killed 24 hours later. Serum was separated from each rat. Gamma globulins were precipitated with 18%, 14% and 12% sodium sulphate. The same procedure was repeated with non-irradiated control rats.

The serum of the offspring of X irradiated pregnant rats was individually collected and gamma globulins were precipitated with 18%, 14%, and 12% sodium sulphate. Gamma globulins were also prepared from rats after exposure to microwave irradiation for 9 minutes and 15 minutes. High-titre antisera were prepared in rabbits against human gamma globulin (Cohn Fraction II) and normal rat gamma globulins using Freund's complete adjuvant.

The various gamma globulins of rats exposed to X and microwave radiation will be tested for the changes in their antigenic structures by using acrylamide gel electrophoresis, Ouchterlony's gel diffusion technique, immunoelectrophoresis as well as the other chemical methods to study properties after denaturation such as release of sulphydryl groups, increase in optical levo rotation, and precipitation with the homologous antisera.

Human gamma globulin (Cohn Fraction II) was fractionated on Sephadex-G-200 using 0.01 M phosphate buffer pH 7.6 containing 0.15 M NaCl. The first peak of IgM gamma globulin was separated and recycled on the same column using the same buffer. A single peak of IgM was obtained. Similarly the peak containing the IgG human gamma globulin was fractionated on DEAE cellulose column using 0.0175 M phosphate buffer pH 6.3. A single peak of IgG was obtained. The results showed that human gamma globulin (Cohn Fraction II) from Pentex Corporation contains 91.9% IgG and 8.1% IgM.

Optical rotation of human gamma globulin in H_2O and 0.9% NaCl was determined at specific wavelengths (365 mμ, 405 mμ, 436 mμ, 546 mμ, and 578 mμ). Lambert-Beer plots for human gamma globulin (Cohn Fraction II) from Pentex Corporation were determined for four wavelengths, 260 mμ, 278 mμ (peak), 280 mμ and 290 mμ. The spectra for human gamma globulin at a concentration of 0.1 mg/ml in 0.15 M NaCl were determined for wavelength range 200 mμ-310 mμ. The nature of aggregation of human gamma globulin (Cohn Fraction II) for native form and heat denatured form in 0.9% NaCl solution were determined with modified Coulter Counter apparatus.

The method for the quantitative determination of sulphydryl groups using 5,5'-dithiobis (2-nitrobenzoic acid) was standardized for human gamma globulins. Pure samples of IgG and IgM human gamma globulins will be irradiated with X-rays and microwaves in vitro. The configurational changes occurring in IgG and IgM after X-ray irradiation and microwave irradiation will be studied by determining the four parameters of optical rotation:

1) (α) specific rotation
2) a_o, constant for helical and intrinsic residue contributions
3) b_o, constant characteristics of helix and
4) λ_c, optical rotatory dispersion constant.

The changes in the functional properties of IgG and IgM human gamma globulins such as precipitation with the homologous antiserum, and complement fixation will be studied. The mechanism of denaturation of IgG and IgM human gamma globulins after exposure to X-ray radiation and microwave radiation will be studied by separating the aggregates on Sephadex G-200, determining their sedimentation constants, and their amino acid composition. These studies should help in explaining the following question: Can radiation cause human auto-immune diseases and if so, how?

E. THE ISOLATION OF KUPFFER CELLS FROM RAT LIVER AND STUDIES OF CELLULAR RESPIRATION DURING PHAGOCYTOSIS

R. K. Fred, T. G. Zaremba

Previous studies in this laboratory have indicated that sublethal irradiation of mice causes a decrease in the phagocytic capacity of the reticuloendothelial system. To determine the site of radiation damage, it is necessary to study the effect of radiation on phagocytosis at the cellular level. This may be accomplished by isolating the phagocytic cells of the liver (Kupffer cells), determining the biochemical pathways during phagocytosis, and studying the effect of radiation on the pathways.

We have developed a method for isolating Kupffer cells from rat liver which, unlike previous methods, yields sufficient material to study cellular respiration using the Warburg apparatus. Briefly, a suspension of intact liver cells is prepared using a modification of the method of St. George; the suspension is incubated in dilute trypsin at 37° C, and finally the cells are purified by centrifugation of the trypsinized suspension in a density gradient and washing. This method yields approximately 150-200 mg of Kupffer cells from each 10 grams of rat liver. Figure 49 is a typical phase micrograph of cells obtained in this manner.

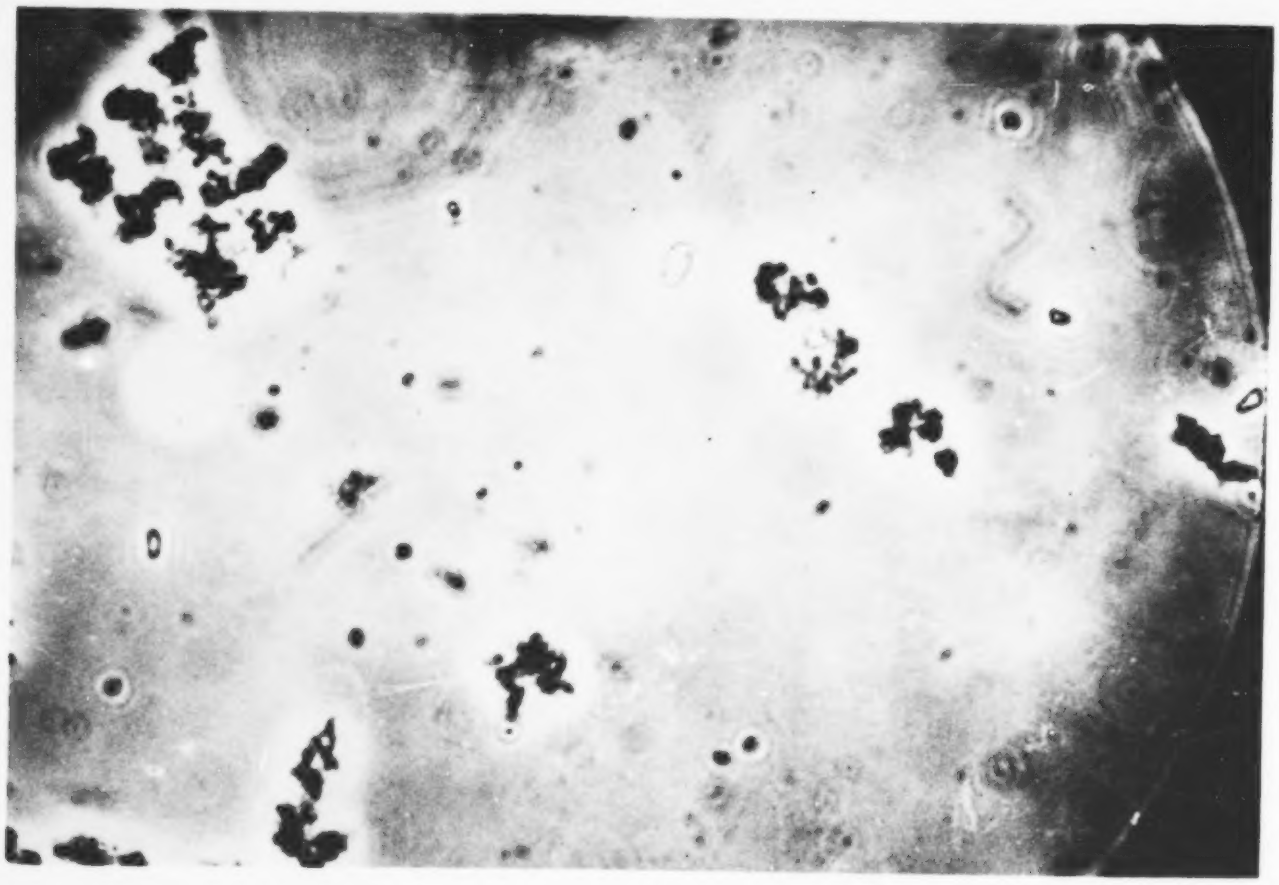

Figure 49. Phase Photomicrograph of Unstained Kupffer Cells.

To determine if these small irregularly shaped cells were Kupffer cells, rats were injected with carbon and the Kupffer cells were later isolated at various times. If the cells were isolated a few hours following the carbon injection, small irregularly shaped cells, which appeared to have carbon uniformly dispersed in the cytoplasm, were obtained. If the cells were isolated several weeks following the injection, they appeared to be the same size and shape, but the carbon was noted to be distributed into aggregates.

Respiration studies were performed using four different types of liver cell preparations: (1) A liver mince, prepared by chopping the liver with a razor blade to a fine mince; (2) whole liver cells prepared by passing the liver through a tissue press, suspending in tissue culture media and passing this suspension through a 100 mesh filter to remove large clumps of cells; (3) "washed liver cells" prepared simply by washing the whole liver cell suspension with tissue culture media; (4) Kupffer cells, isolated as previously described. The oxygen uptake of each of these four liver preparations was measured over a 2-hour period at 37° C on a Warburg apparatus. The results, presented in Figure 50 are typical oxygen uptake curves and show that duplicate values agree well for the first 60 minutes. However, the slopes tend to decrease by variable amounts after 60 minutes, so only the first 60 minutes were used in the calculations. The rate of oxygen uptake of washed liver cells is approximately 60% lower than that of the whole liver cells. Recent experiments have indicated that debris associated with the whole liver cell suspension is responsible for a large portion of the oxygen uptake. Therefore, of the values obtained for unwashed and washed liver cells, the values for the washed cells are probably a better indication of the rate of oxygen uptake of liver cells. The QO_2 of the Kupffer cells was not significantly different from that of the washed liver cells. Approximately 7×10^9 polystyrene particles were added to the Kupffer cell suspension; although the rate of oxygen uptake was 29% higher than that of the Kupffer cells without particles, this difference was not found to be statistically significant.

To determine if the Kupffer cells had ingested the polystyrene spheres the suspension was washed several times and viewed with phase and electron microscopy. Figure 51 is a phase micrograph showing the Kupffer cells with polystyrene particles. It is difficult to determine if the particles are inside of the cells or only attached to the outer surface. Figure 52 an electron micrograph of a section from the same suspension, shows that the polystyrene particles are associated with cytoplasmic constituents such as mitochondria and endoplasmic reticulum. These microscopic observations strongly suggest that the polystyrene spheres had been ingested by the in vitro suspension of Kupffer cells.

Since there was no significant increase in oxygen uptake by Kupffer cells during in vitro phagocytosis, it was of interest to determine the rate of oxygen uptake by Kupffer cells which already contained particles. Therefore, rats were injected with 72 mg of a carbon suspension and

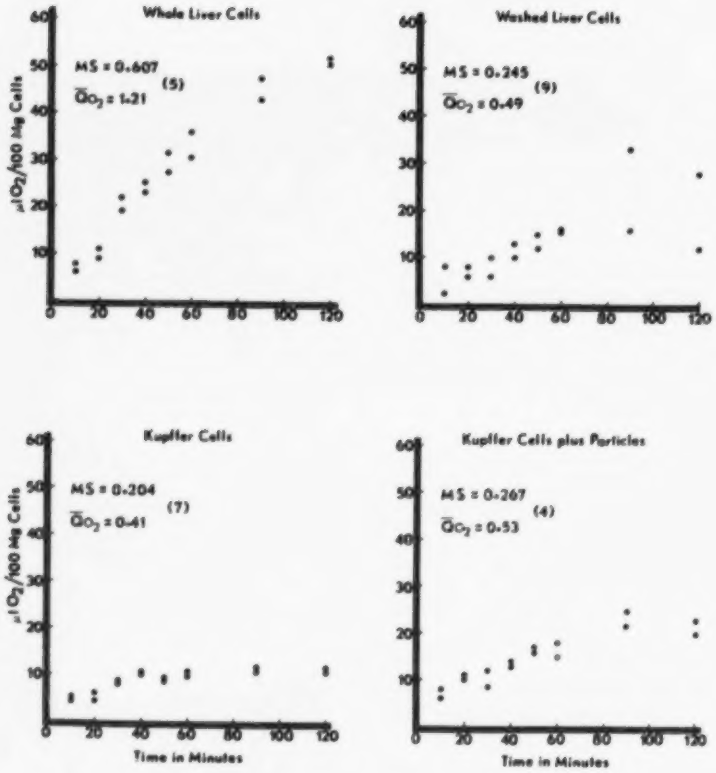

Figure 50. Oxygen Uptake Curves for Various Types of Liver Cell Preparations. MS = mean slope in μl 0_2/100 mg wet tissue per minute; $Q0_2$ in μl 0_2mg dry tissue / hour; numbers in parentheses refer to the numbers of duplicate experiments.

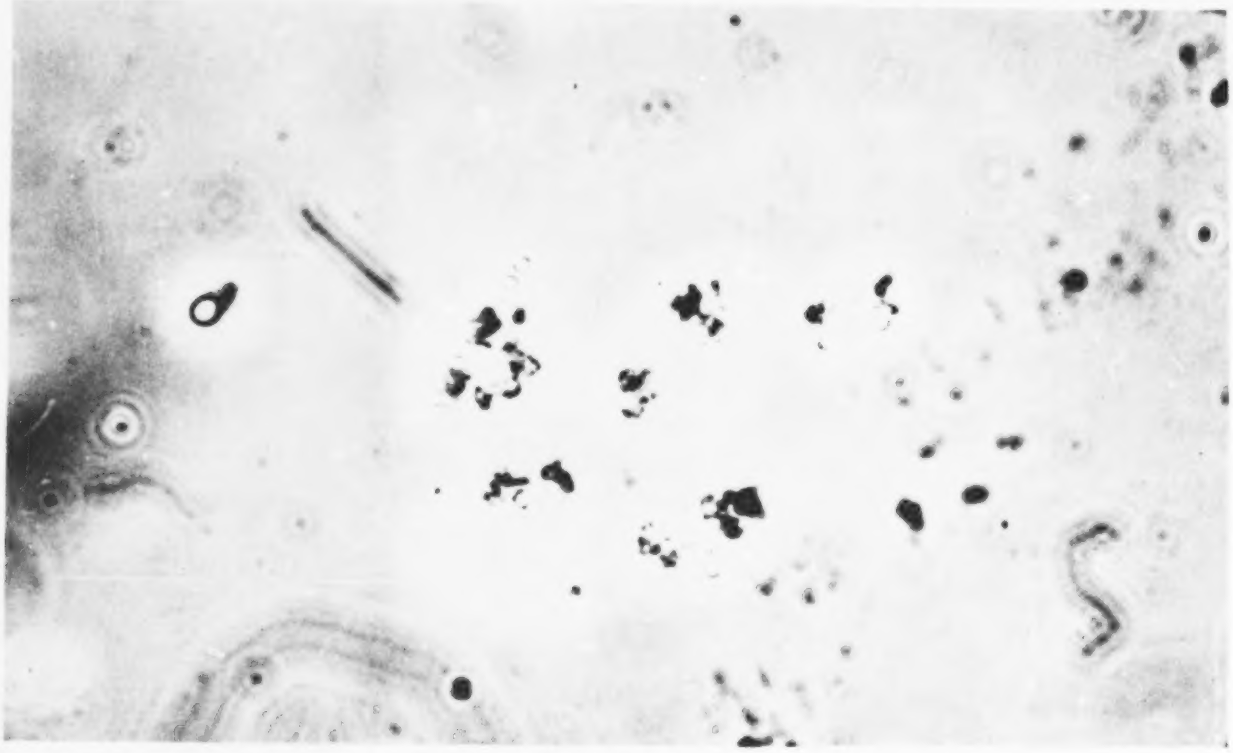

Figure 51. Phase Photomicrograph of Unstained Kupffer Cells that Had Been Incubated with Polystyrene Particles In Vitro.

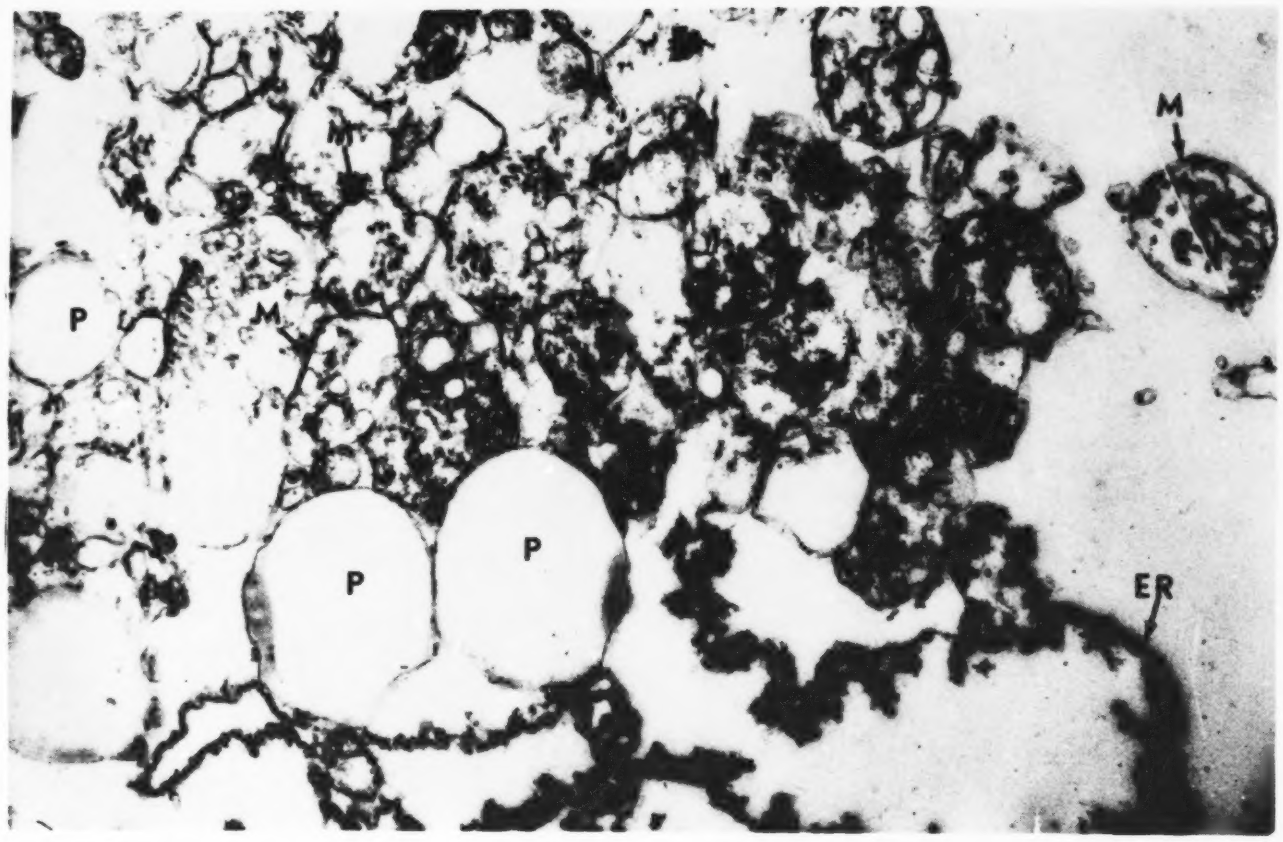

Figure 52. Electron Photomicrograph of Kupffer Cells That Had Been Incubated with Polystyrene Particles In Vitro. P = polystyrene particles; M = mitochondria; ER = endoplasmic reticulum.

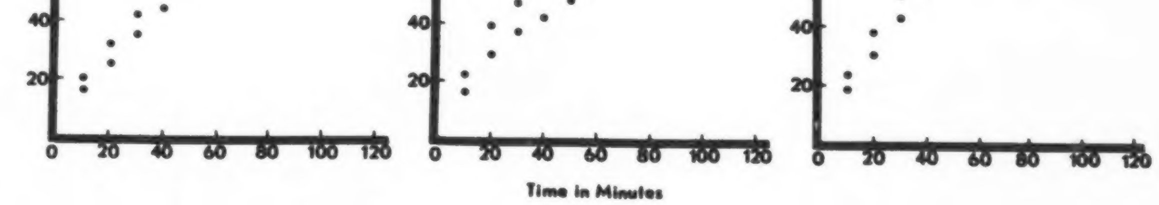

Figure 53. Oxygen Uptake Curves for Liver Mince. MS = mean slope in μl O_2/100 mg wet tissue / minute; QO_2 in μl O_2/mg dry tissue / hour; numbers in parentheses refer to the number of duplicate experiments.

sacrificed 15 minutes later. Initially, the respiration studies were performed using liver mince; the results are shown in Figure 53. These graphs, as those in Figure 50, are typical oxygen uptake curves with the duplicates closely agreeing for the first 60 minutes. Twenty milligrams of carbon were added to the liver mince (this is approximately equal to the concentration of carbon initially present in the blood of rats injected with 72 mg of carbon). There was no significant difference in the rate of oxygen uptake between the liver mince with particles and that without particles. However, the liver mince from rats injected with carbon exhibited a 40% increase in the rate of oxygen uptake compared with controls. In order to determine whether the large increase in oxygen uptake exhibited by the liver mince from carbon-injected rats was attributable to the Kupffer cells, the experiment was repeated using isolated Kupffer cells instead of liver mince. The results of these studies are shown in Table 21. The oxygen uptake of Kupffer cells from control rats and from carbon-injected rats were compared on a daily basis because of a large day-to-day variation. The Kupffer cells which had previously ingested carbon particles exhibited a 120% increase in the rate of oxygen uptake compared with controls.

TABLE 21. RATE OF OXYGEN UPTAKE OF KUPFFER CELLS[a]

Experiment	Kupffer Cells from Control Rats	Kupffer Cells from Rats Injected with Particles	Increment
1	0.1722	0.2484	0.0762
2	0.0865	0.1910	0.1045
3	0.0	0.1281	0.1281
Mean	0.0862	0.1892	0.1029

a. The numbers refer to the slope for 0 - 60 min (expressed as $\mu l\ O_2/100$ mg wet tissue/min).

The results of these studies suggest that an increase in oxygen uptake by Kupffer cells during phagocytosis most likely occurs after the particles are ingested. These results are in direct agreement with those of Selvaraj and Sbarra who reported similar results using polymorphonuclear leukocytes. This increased respiratory activity may represent changes in cellular metabolism which occur after the particles are within the cell. These changes may be related to such phenomena as the segregation of particles into phagosomes, enzyme activation, or membrane repair.

COLLABORATIVE RADIOLOGICAL HEALTH LABORATORY
Dr. R. John Garner, Director

A. THE BARRIER-MAINTAINED COLONY[1]

The cesarian-derived, barrier-maintained (CDBM) beagle colony provides the experimental material for the Collaborative Radiological Health Laboratory. The Colony is currently comprised of approximately 1,300 animals, a reduction of about 400 over the course of the year. This reduction has become possible following establishment of breeding programs appropriate to the needs of the long-term work. Culls were either absorbed by short-term studies in this laboratory or were used to fill requests from other laboratories.

The conception rate in the colony rose slightly during the course of the year but is still rather low, averaging 78%. Undetected infertility in the male is believed to be a primary factor. A program has therefore been introduced for selection of breeding males: preliminary results suggest that its adoption may help to raise the conception rate to approaching 90%.

In an attempt to meet budgetary stringencies, measures have been introduced to improve economy of routine operation without loss of efficiency. A drastic change has been made in the hitherto time-consuming process of disinfecting all bags of food entering the barrier-maintained area. Bacteriological tests reveal no significant increase in contamination of the feed as a result. Routine fecal examinations for parasite eggs have also been reduced in number by limiting individual sampling to pregnant females and otherwise using composite samples. There has been no change in the vaccination program.

Reduction in size of the colony presented an opportunity to examine apparently clinically normal mature dogs for pathological changes as well as animals culled because of clinical abnormalities. A finding of some significance was the high incidence of thyroiditis with or without clinical and pathological evidence of hypothyroidism. It is becoming evident that thyroid dysfunction may be a major problem in long-term studies.

---

[1] Current research conducted at the Collaborative Radiological Health Laboratory is reported in the Annual Report for 1968, Colorado State University - U.S. Public Health Service Collaborative Radiological Health Laboratory, Fort Collins, Colorado (Contract PH 86-62-135).

Spontaneous death or serious illness is relatively rare in mature dogs in the CDBM colony: it is therefore somewhat early to speak of "common" causes of death. However, it is possible to distinguish those conditions occurring with greatest frequency, and to associate these conditions with specific age groups. Most puppies dying at 7 weeks or a little older were cachectic and anemic. In slightly older animals, bronchopneumonia or right-sided heart failure predominated. Small groups of mature dogs died of uremia subsequent to chronic glomerulonephritis or nephrosclerosis or of anemia of undetermined origin. A point of some interest is that chronic diffuse interstitial nephritis, so common in street dogs, has not yet been encountered in dogs retained in the CDBM colony and that the "common" lesion in the colony, glomerulonephritis, is said to be extremely rare in dogs.

The spontaneous mineral deposition observed to occur in the soft tissues of puppies in the CDBM colony has continued to be investigated. It is characterized by deposition of calcium salts around proximal convoluted tubules in the kidneys and in subepithelial tissues of the lungs and upper respiratory passages. In these locations a peak incidence of about 90% is reached between 12 and 30 days of age, i.e. when puppies are nursing. The condition appears to be transient and does not resemble previously reported forms of spontaneous soft tissue mineralization. It does not produce clinical signs or prevent rapid growth; neither is it related to season, sex, litter size, or general health. The circumstances of its occurrence suggest that it may be an exaggerated physiological process.

One process which may be related is reabsorption of phosphate by the renal tubules. There appears to be an increase in the filtered load of phosphate during the period when calcium deposits are observed. Tubular reabsorption is high and conditions exist which would result in high phosphate concentrations in the tubules.

Subcapsular scarring and mineralization of the liver has been observed in about 8% of fetuses and very young puppies examined routinely. The lesion has no functional significance and its pathogenesis is not known.

B. THE LONG-TERM EXPERIMENT: CURRENT STATUS AND FEASIBILITY STUDIES

The raison d'etre of the Collaborative Radiological Health Laboratory is the experiment designed to examine the long-term effects in the beagle of a single whole-body exposure at different periods of development. Six periods of development have been chosen for study; 8, 28, and 55 days post-coitus and 2 days, 10 weeks and 1 year. Exposure levels are 0, 20, or 100 R over a constant exposure time of 10 minutes. A total of approximately 1,700 animals will be involved. The first pups were entered into the experiment in December, 1967; the total committed is now 122. Commitment of animals will continue over the next 4 to 5 years.

This experiment is expected to last for upwards of 20 years. In order to obtain a preview of events to be expected in animals reaching the end of their life-span, a pilot study has been initiated which will involve the intensive study for periods of up to 4 years of animals which have survived an exposure in the LD_{50} range at 8, 28, or 55 days post-coitus (dpc) or 2 days post-partum. This work is still in its initial stages.

Acute lethality studies are continuing using the 5,000 Ci cobalt-60 source and the constant exposure time of 10 minutes currently employed in the long-term experiments. Ages under consideration are 8, 28, and 55 dpc., 2 days, 2, 5, 9, and 10 weeks post-partum and young adult (1-2 years). The $LD_{50/60}$ in the young adult under these conditions has been established as 315 R (mid-line air dose), a value close to that observed in studies at Davis, California of which the long-term studies are regarded as an extension. Tentative values for the $LD_{50/60}$ at 10 weeks and $LD_{50/30}$ 9, 5, and 2 weeks are 270 and 270, 300, and 400 R, respectively.

A detailed analysis has been made of the results obtained from a comparison of $LD_{50/60}$ in young adults using the original (400 Ci) and the new (5,000 Ci) cobalt sources. "Days to death" was found to be marginally significantly dependent upon body weight and exposure level but not upon body width or age. The BEGA (beta-gamma) function was used in establishing an exposure-response curve; this approach offers theoretical advantages over the conventional probit analysis for estimating LD_{50}'s.

As the long-term experiment proceeds, methods will continue to be developed and refined to make the greatest possible use of the material and data available. Dental eruption may be of potential value as an indicator of effects upon growth and development, particularly of dogs irradiated _in utero_. The mean eruption times of the permanent teeth have been estimated and the minimum frequency with which examinations must be made to obtain adequate data has been established.

Electron microscopy is a powerful tool but has the disadvantage that only a very small volume of tissue can be examined. Staining procedures suitable for examination of plastic-embedded thin sections suitable for examination with the light microscope are currently being evaluated as an aid to fine-structure studies now proceeding on the kidney.

Restrictions imposed in relation to the degree of stress permissible in routine testing of long-term dogs have required the development of atraumatic procedures for assessing renal function. A simplified, rapid method of determining parameters of renal function (glomerular filtration rate, effective renal plasma flow, and maximum tubular secretory capacity) from analysis of plasma disappearance curves and bladder accumulation curves subsequent to a single intravenous injection of ^{125}I-labelled hippuran appears to have great potential. A disturbing feature, however, is the observation of glomerular and tubular lesions in dogs used for evaluating this technique against the traditional constant-infusion procedures. The origin of these lesions will need to be determined before the procedure can be adopted as standard practice.

A fruitful approach to the extraction of the maximum amount of information from physiological data appears to be the application of sophisticated methods of mathematical analysis. The electroencephalogram is particularly amenable to such treatment and the use of auto- and cross-correlation techniques is being investigated.

The maze is a common tool in psychological studies. Effort has been directed towards developing maze problems, initially using rats as experimental animals, which may be useful in assessing behavioral effects of biological insults. A linear, multiple-unit maze appears to be promising but both the apparatus and the testing procedure need to be simplified if they are to be developed for use on other than a very small sample of the long-term animals.

C. IRRADIATION OF THE EMBRYO, FETUS AND NEONATE

The phase of work in this laboratory which has taken second place only to the long-term experiment is definition of the acute injury following irradiation during early development. Prenatal canine development has been studied in unirradiated litters collected at daily intervals during the time of major organ formation and at weekly intervals before and after organogenesis to determine the extent of normal variations and to compare different methods of timing development. The short-term effects of a single exposure to 150 R cobalt 60 gamma radiation have been compared at five prenatal ages: 8, 15, 21, 28 and 35 days following breeding. Preliminary results indicate that 21 and 28 day concepti respond similarly in terms of lethal effects. However, animals exposed at 28 days lack the major malformations that characterize irradiation at 21 days.

An experiment has been initiated to investigate recovery in the embryo, fetus, and neonate following exposure at 8, 28, or 55 days post-coitus (dpc) or 2 days post-partum to 100 R cobalt-60 gamma radiation. A split-dose technique is being employed with determination of the $LD_{50/60}$ at 10 weeks after the conditioning exposure.

Development of renal function in the young beagle has been investigated during the first year of life. Parameters studied were ability to concentrate urine, urine pH, glomerular filtration rate (GFR), effective renal plasma flow, and maximum tubular secretory capacity for p-aminohippurate. The opportunity has also been taken to examine the effects of exposure to 290 R cobalt-60 gamma radiation at 8 or 28 dpc on these parameters. These pilot studies indicate possible early effects on urine osmolarity and GFR.

The developing mammalian eye appears to be peculiarly radiosensitive and considerable attention is thus being given to the visual system in both short- and long-term studies at this laboratory. A survey of survivors of LD_{50} studies in pre-, neo- and post-natally irradiated beagles in the CDBM colony has revealed an interesting variety of clinically observable eye lesions, particularly following exposure at 28 or 55 dpc or 2 days post-partum. The lowest exposure at which lesions which could be associated with irradiation were detected was 210 R (at 28 dpc). The results suggest that ocular lesions may well occur in some age groups receiving 100 R in the long-term experiment.

Another aspect of visual function currently being investigated is the average evoked visual potential (AVEP). Development of the AVEP in the beagle has been examined from birth to 6 months of age. It first appears at 5 days post-partum at which time it is the surface-negative immature type, but this is replaced by the surface-positive mature type by 30 days. Latency increases with age. Exposure to 300-500 R cobalt-60 gamma radiation at 57 dpc produces a significant change in initial peak latency and peak-to-peak amplitude of the primary response at 7-9 months of age. The irradiated animals had sustained extensive retinal damage; the results of this work indicate that cerebral damage was also present.

Exposure to 325 R at 2 days post-partum appears to have little effect upon visual discrimination learning in the dog as evaluated by tests of brightness discrimination, shape discrimination, and discrimination reversal; however, irradiated animals took longer to respond to the test problems than sham-irradiated dogs of the same age.

The effects have been examined of exposure to 150 R of the rat ovum, conceptus and neonate on post-natal activity of serine dehydratase in liver and glycerol phosphate dehydrogenase and non-specific esterase in liver and brain. Contrary to expectations, early irradiation may apparently have a stimulatory effect on post-natal enzyme activity.

D. DATA PROCESSING

Development of satisfactory systems for data acquisition, storage, and retrieval is an essential requirement in any study in which large volumes of data can be expected to accumulate over a number of years. The system currently in use at CRHL has been developed following the acquisition of a CDC-6400 computer by the Colorado State University Computing Center; it replaces the optical reader - IBM-1401 system previously described. The system is designed to facilitate daily updating and correcting of data files and to retrieve information in multiple output formats for generating listings and for performing data analyses.

The coding and retrieval of data collected from clinical examinations and autopsies poses a particular problem. The initial phase for the coding and retrieving of necropsy diagnoses by computer is nearly complete with the compilation and coding of a 4,700 word pathology dictionary. It is anticipated that the system can be readily extended to clinical data.

A new look has been taken at the analysis of life-death statistics. Some of the mathematical characteristics of the BEGA (beta-gamma) function, of promise in the analysis of LD_{50} studies, have been considered; a method for obtaining estimates of mathematical model parameters in terms of the type of data obtained in such studies has been developed.

BLANK PAGE

APPENDIX A

PUBLICATIONS JANUARY - DECEMBER 1968

Black, S.C., and E.W. Bretthauer. 1968. Polonium-210 in tobacco. Radiol. Health Data Rep. 9:145-152.

Campbell, S.D., and D.E. Body. 1968. An acclimation room for the detection of low radium 226 body burdens. U.S. Department of Health, Education, and Welfare, Public Health Service Publication No. 999-RH-31. 19p.

Fred, R.K. 1968. Effect of anticoagulant doses of heparin on the clearance of large doses of colloidal carbon in the mouse. J. Reticuloendothelial Soc. 5:589.

Harris, J.Y. 1968. Radioiodide clearance rates in lactating goats. Proceedings of the 24th International Congress of Physiological Sciences 7:181.

Kahn, B., C.P. Straub, P.J. Robbins, H.N. Wellman, R.A. Seltzer, and N.C. Telles. 1968. Retention of radiostrontium by infants. Health Phys. 15:203.

Lambert, P.D., A.C. Lee, J.A. Modrick, R.D. Phemister, and W.J. Tietz. 1968. Evaluation of eye defects in beagles by means of visual evoked responses. Proceedings of the 3rd Annual Joint Meeting of the Clinical Society and the Commissioned Officers Association. p. 28.

Lambert, P.D., R.D. Phemister, and W.J. Tietz. 1968. Visually evoked EEG potentials of beagles irradiated *in utero*. Electroencephalog. Clin. Neurophysiol. 25:278-281.

Leach, W.M. 1968. The thymidine pool in grasshopper neuroblasts during mitosis. J. Cell Biol. 36:282-286.

Mills, W.A., A.H. Wolff, and M.L. Shore. 1968. Biological considerations in measuring and evaluating X-ray exposures from color television receivers, p. 73-86. *In* Conference on detection and measurement of X-radiation from color television receivers, sponsored by U.S. Department of Health, Education, and Welfare, Public Health Service, in cooperation with Electronic Industries Association, Washington, D. C.

Mills, W.A. and H.D. Youmans, Jr. 1968. Population exposures from natural background radiation in Kerala, India. Health Phys. 15:188.

Mishkin, E.P., and M.L. Shore. 1968. Interference by X-irradiation with the induced synthesis of tryptophan pyrrolase. Radiation Res. 33:437-445.

Moore, W., Jr., and M. Colvin. 1968. Chromosomal changes in the Chinese hamster thyroid following X-irradiation *in vivo*. Intern. J. Radiation Biol. 14:161-167.

Moore, W., Jr., and M. Colvin. 1968. Persistence of chromosomal aberrations in Chinese hamster thyroid following administration of ^{131}I. J. Nucl. Med. 9:165-167.

Moore, W., Jr., and L.J. Gillespie. 1968. Hemogram of the rat kangaroo, *Potorous tridactylus*. Am. J. Vet. Res. 29:1073-1076.

Moore, W., Jr., and L.J. Gillespie. 1968. Cultivating leukaemic lymphocytes. Lancet 1:363-364.

Nankin, H.R., J. Sode, and M.F. Ball. 1968. Satellite association and trisomy in thyrotoxicosis. J. Med. Genet. 5:45-47.

Pollock, E.J., and G.J. Todaro. 1968. Radiation enhancement of SV40 transformation in 3T3 and human cells. Nature 219:520-521.

Pollock, E.J., and G.J. Todaro. 1968. Enhancement by irradiation of *in vitro* transformation by SV40 virus. Health Phys. 15:200.

Shively, J.N., and R.D. Phemister. 1968. Incomplete maturation of iridal pigment in heterochromia iridum. Proceedings of the 26th Annual Meeting of the Electron Microscopy Society of America.

Shively, J.N., and R.D. Phemister. 1968. Fine structure of the iris of dogs manifesting heterochromia iridis. Am. J. Ophthalmol. 66:1152-1162.

Shively, J.N., R.D. Phemister, and G.P. Epling. Demonstration of radiation induced changes in the fine structure of the canine retina. Proceedings of the Fourth European Regional Conference on Electron Microscopy, Rome, Italy, September 1968. p. 571-572.

Shore, M.L., and R.K. Fred. 1968. Calculation of specific activity - time curves in relatively inaccessible compartments of a three compartment kinetic steady state model. Proceedings of the First International Congress of Radiation Protection 1:769-774.

Shore, M.L., E.P. Sheppard, and A.K. Davis. 1968. Mechanisms underlying hormonal and substrate induction of tryptophan pyrrolase. Federation Proc. 27:514.

Telles, N.C., and D.W. Coble. 1968. The nucleolus - a morphological and possible functional relationship to the nuclear membrane. Federation Proc. 27:836.

Telles, N.C., and D.W. Coble. Intranuclear cytoplasmic inclusions - a serial section evaluation. Proceedings of the Fourth European Regional Conference on Electron Microscopy, Rome, Italy, September 1968. p. 183-184.

Youmans, H.D., G. E. Anderson, and W. Lee. 1968. Spectra and percentage depth dose of X-radiation emitted by a color television receiver, p. 31-51. In Conference on detection and measurement of X-radiation from color television receivers, sponsored by U.S. Department of Health, Education, and Welfare, Public Health Service, in cooperation with Electronic Industries Association, Washington, D. C.

Zaremba, T.G., and R.K. Fred. 1968. The isolation of Kupffer cells from rat liver and studies of cellular respiration during phagocytosis. J. Reticuloendothelial Soc. 5:583-584.

APPENDIX B

PRESENTATIONS JANUARY - DECEMBER 1968

Abuelo, J.G. Ultrastructural aspects of radiation-induced chromosome damage. Washington Area Radiobiology Association, Bethesda, Maryland, February 29, 1968.

Cisar, C.F. The rat kangaroo - handling and husbandry practices in a research facility. 19th Annual Meeting, American Association of Laboratory Animal Science, Las Vegas, Nevada, October 21-25, 1968.

Fred, R.K. The effect of anticoagulant doses of heparin on the clearance of large doses of colloidal carbon in the mouse. 5th Annual National Meeting of the Reticuloendothelial Society, New York, December 1-4, 1968.

Gillespie, L.J. Karyotypic and phenotypic observations on a mongoloid child. Hudson High School, Hudson, North Carolina, April 22, 1968.

Harris, J.Y. Radioiodide clearance rates in lactating goats. 24th International Congress of Physiological Sciences, Washington, D. C., August 25-31, 1968.

Kahn, B., C.P. Straub, P.J. Robbins, H.N. Wellman, R.A. Seltzer, and N.C. Telles. Retention of radiostrontium by infants. Health Physics Society, Denver, Colorado, June 16-20, 1968.

Lambert, P.D., A.C. Lee, J.A. Modrick, R.D. Phemister, and W.J. Tietz. Evaluation of eye defects in beagles by means of visual evoked responses. 3rd Annual Joint Meeting of the Clinical Society and the Commissioned Officers Association, San Francisco, California, March 26-29, 1968.

Leach, W.M. and J.G. Abuelo. Electron microscopy of chromosomes. Zoology Department, George Washington University Seminar, Washington, D. C., April 3, 1968.

Mills, W.A. and H.D. Youmans, Jr. Population exposures from natural background radiation in Kerala, India. Health Physics Society, Denver, Colorado, June 16-20, 1968.

Nankin, H.R. *In vitro* alterations of satellite association and nucleolar persistence in mitotic human lymphocytes. American Federation for Clinical Research, Atlantic City, New Jersey, May 5, 1968.

Phemister, R.D., B.P. Stuart, and R.W. Thomassen. Spontaneous soft tissue mineralization in young puppies. Annual Meeting of the American College of Veterinary Pathologists, Chicago, Illinois, December 1, 1968.

Pollock, E.J., and G.J. Todaro. Enhancement by irradiation of *in vitro* transformation by SV40 virus. Health Physics Society, Denver, Colorado, June 10-13, 1968.

Shively, J.N., and G.P. Epling. Demonstration of radiation induced changes in the fine structure of the canine retina. Rocky Mountain Society of Electronmicroscopists, Denver, Colorado, May 11, 1968.

Stara, J.F. The role of radioisotopes in veterinary public health. 72nd Annual Meeting of the U. S. Livestock Sanitary Association, New Orleans, Louisiana, October 8-11, 1968.

Stara, J.F. Radiation and man. Meeting of the Allis-Chalmers Management Club, Cincinnati, Ohio, January 20, 1968.

Stara, J.F., and S.C. Skoryna. The effects of alginate compounds on the reduction of radiostrontium in the body. 6th International Seaweed Symposium, Santiago de Compostela, Spain, September 9-13, 1968.

Telles, N.C. The program of the National Center for Radiological Health of the Public Health Service. The Medical Association of the Portuguese Language, Luanda, Angola, Africa, August 4-11, 1968.

Telles, N.C., and D.W. Coble. The nucleolus - a morphological and possible functional relationship to the nuclear membrane. Annual Meeting of the Federation of American Societies for Experimental Biology, Atlantic City, New Jersey, April 16-20, 1968.

Wagner, M.T., and R.J. Garner. The influence of prenatal gamma irradiation on postnatal enzyme patterns in the beagle. Radiation Research Society, Houston, Texas, April 21-25, 1968.

Ward, B.C., and W. Moore. Spontaneous lesions in Chinese hamsters. 19th Annual Meeting of the American Association of Laboratory Animal Science, Las Vegas, Nevada, October 21-25, 1968.

Ward, B.C., and N.C. Telles. Effects of radiation and ethionine on rat mammary tumor incidence. Washington Area Radiobiology Association, Bethesda, Maryland, February 29, 1968, and Armed Forces Radiobiology Research Institute, Washington, D. C., April 4, 1968, and 16th Annual Meeting of the Radiation Research Society, Houston, Texas, April 21-25, 1968.

Zaremba, T.G., and R.K. Fred. The isolation of Kupffer cells from rat liver and studies of cellular respiration during phagocytosis. 5th Annual National Meeting of the Reticuloendothelial Society, New York, December 1-4, 1968.

APPENDIX C
ADVISORY COMMITTEES

RADIATION BIO-EFFECTS AND EPIDEMIOLOGY ADVISORY COMMITTEE

Dr. Victor P. Bond, Chairman
Chairman, Medical Department
Brookhaven National Laboratory

Dr. Charles E. Dunlap
Professor and Head
Department of Pathology
Tulane University School of Medicine

Dr. Alan M. Gittelsohn
Department of Statistics
School of Hygiene and Public Health
Johns Hopkins University

Dr. Louis H. Hempelmann
Professor of Experimental Radiology
School of Medicine
University of Rochester

Dr. Edward B. Lewis
Professor of Biology
California Institute of Technology

Dr. Leonidas D. Marinelli
Director, Radiological Physics Division
Department of Radiological Physics
Argonne National Laboratory

Dr. Karl Z. Morgan
Director, Health Physics Division
Oak Ridge National Laboratory

Dr. Richard R. Overman
Associate Dean
College of Medicine
University of Tennessee

Dr. Leonard M. Schuman
Professor of Epidemiology
College of Medical Sciences
School of Public Health
University of Minnesota

Dr. M. Thomas Wagner, Jr., Executive Secretary
Assistant to the Chief
Radiation Bio-Effects Program
Bureau of Radiological Health

COLLABORATIVE RADIOLOGICAL HEALTH LABORATORY ADVISORY COMMITTEE

Dr. Edward Alpen
Head, Biology and Medical Sciences Division
U. S. Naval Radiation Defense Laboratory

Dr. Allen C. Anderson
Radiopathologist
Radiobiology Laboratory
School of Veterinary Medicine
University of California

Professor Ernest Furchtgott
Department of Psychology
University of Tennessee

Dr. Marvin A. Kastenbaum
Statistician
Oak Ridge National Laboratory

George A. Sacher, Jr., Chairman
Senior Biologist
Division of Biological and Medical Research
Argonne National Laboratory

Dr. Carl F. Tessmer
Chief, Experimental Pathology Section
M. D. Anderson Hospital and Tumor Institute
University of Texas

Dr. M. Thomas Wagner, Jr., Executive Secretary
Assistant to the Chief
Radiation Bio-Effects Program
Bureau of Radiological Health

Observers

Representing AEC:

Dr. William W. Burr
Chief, Medical Research Branch
Division of Biology and Medicine
Atomic Energy Commission

Representing AFWL:

Lt. Col. Milford D. Harris
Chief, Biophysics Division
Air Force Weapons Laboratory
(AFSC)
Kirtland Air Force Base

Representing NIH:

Dr. Nathan W. Shock
Chief, Gerontology Branch
Baltimore City Hospitals

APPENDIX D

RADIATION BIO-EFFECTS PROGRAM STAFF

Office of the Chief

Dr. William A. Mills, Chief
Dr. Norman C. Telles, Deputy Chief
Jayne Blanton
Leo C. Cox
Darla D. Davis
Valeria Dempsey
Ruth G. DePrenda
Linda G. Funk
Irene A. Hardman
Donald M. Hodge
William O. Holcombe
Linda F. Hutchison
Loretta G. Ilgenfritz
Joan L. King
Viola Schneider
Myrtle R. Smith
Evelyn B. Surles
Dr. M. Thomas Wagner, Jr.

Biometrics Support Unit

Dr. Gordon L. Jessup, Chief
Richard P. Chiacchierini
Louise A. French
Dr. Jesse Y. Harris

Animal Care Unit

Clayton F. Cisar, Chief
Flora S. Nicholson
Bernard L. Phelps
Warren L. Ridgely

Radiation Cytology Laboratory

Dr. William M. Leach, Chief
Dr. Emanuel C. Beyer
Steven Brecher
Darilyn Dolimpio
Dinniemaud J. Ellingson
Lillie J. Gillespie
Mayme M. Jiles
Susan A. Knadle
Nina D. Morris
Tim L. Pay
Dr. Kenneth T. S. Yao

Physiology and Biophysics Laboratory

Dr. Moris L. Shore, Chief
Thomas P. Abbott, II
Roger A. Budd
Rachel H. Draley
Richard P. Felten
Dr. Richard K. Fred
Dr. Dewitt G. Hazzard
Mary K. Howes
David E. Janes
Dr. Gopal A. Kamat
Anthony Lamanna
John W. Laskey
Katherine M. Selby
Lawrence R. Simmons
Sarah Jane Smith
Terrye M. Zaremba

Radiation Oncology and Pathology Laboratory

Dr. Norman C. Telles, Chief
Stephen A. Carr
Joe R. Childress
Don W. Coble
Dorothy R. Garcia
Kiki B. Hellman
Gwendolyn R. Johnson
Dr. Carl D. Lytle
Anthony N. Mikalis
Dr. Lawrence R. Muroff
Jean P. Nageli
Dr. Edward J. Pollock
George M. Samaras
Dr. James N. Shively
Judith O. Singley
Karen J. Sorkin
Alice G. Walters
Dr. Billy C. Ward
Elliot A. Willensky

Radiation Physics Laboratory
Harry D. Youmans, Chief
George F. Anderson
Ulrich H. Behling
Lynda Kramer
Wah Lee
Anne Marie G. Pakenas
Franklin C. Pendleton
Richard A. Tell
Victoria Yancik

Collaborative Radiological Health Laboratory
Dr. R. John Garner, Director
Dr. Dennis F. Cloud
Dr. A. K. Davis
Dr. Paul D. Lambert
Dr. Robert D. Phemister
Dr. Robert W. Thomassen
Thomas J. Withrow

Radionuclide Toxicology Laboratory
Dr. Jerry F. Stara, Chief
Helen H.Ball
Harold W. Barkhau
Dr. Ezra Berman
Arnold L. Cohen
Joan M. Cooper
Walden C. Crocker
Polly F. Geyer
Carol A. Haynes
Virginia W. Kincaid
Dr. Neal S. Nelson
Eugene S. Pinkston
Mary J. Replogle
Lawrence S. Rosenstein
Dr. Robert G. Wolfangel
Dr. James F. Wright

☆ U.S. GOVERNMENT PRINTING OFFICE : 1969—347-409/6